UC San Diego

UC San Diego Electronic Theses and Dissertations

Title

Developmental approaches to in vitro engineering of kidney -like tissues

Permalink

https://escholarship.org/uc/item/3xx7h06q

Author

Rosines, Eran

Publication Date

2008

Peer reviewed|Thesis/dissertation

eScholarship.org Powered by the California Digital Library
University of California

UNIVERSITY OF CALIFORNIA, SAN DIEGO

Developmental Approaches to *In Vitro* Engineering of Kidney-like Tissues

A dissertation submitted in partial satisfaction of the
requirements for the degree Doctor of Philosophy

in

Bioengineering

by

Eran Rosines

Committee in charge:

Professor Sanjay K. Nigam, Chair
Professor Robert L. Sah, Co-Chair
Professor Andrew D. McCulloch
Professor Bernhard Ø. Palsson
Professor Scott C. Thomson

2008

Copyright

Eran Rosines, 2008

All rights reserved.

The Dissertation of Eran Rosines is approved, and is acceptable in quality and in form for publication on microfilm:

_____

_____

_____

_____
Co-Chair

_____
Chair

University of California, San Diego

2008

For all the people in this world that provided true, unwavering support and complete belief in me… all four of you.

“You are almost there.”
-*Fortune Cookie, greatest ever*

“I'm Leonard Nimoy. The following tale of alien encounters is true. And by true, I mean false. It's all lies.
But they're entertaining lies, and, in the end, isn't that the real truth?
The answer is:
No.”
-*Leonard Nimoy, The Simpsons*

“It’s all just artifacts.”
-*Kevin T. Bush*

TABLE OF CONTENTS

LIST OF FIGURES

LIST OF TABLES

LIST OF ABBREVIATIONS

3D – Three dimensional

6-CF – 6-carboxyfluorescein

AQP – Aquaporin

CM – Conditioned medium

DB – *Dolichos biflorus*

ECM – Extracellular matrix

ESRD – End stage renal disease

FGF – Fibroblast growth factor

GAG - Glycosaminoglycan

GDNF – Glial derived neurotrophic factor

HA – Hyaluronic acid

HA-ase – Hyaluronidase

HPLC – High pressure liquid chromatography

IMCD – Inner medullary collecting duct

MALDI – Matrix assisted laser desorption/ionization

MDCK – Madin-Darby canine kidney

MEMS – Microelectromechanical systems

MET – Mesenchymal to epithelial transformation

MM – Metanephric mesenchyme

MMP – Matrix metalloprotease

MS – Mass spectrometry

MW – Molecular weight

NaP_i-2 – Sodium-phosphate 2 transporter

OAT – Organic anion transporter

PDMS - Polydimethylsiloxane

PNA – Peanut agglutinin

PTN – Pleiotrophin

RHAMM – Receptor for hyaluronic acid mediated motility

THP – Tamm-Horsfall protein

TOF – Time of flight

UB – Ureteric bud

VEGF – Vascular endothelial growth factor

WD – Wolffian duct

ACKNOWLEDGEMENTS

I'd like to start by thanking friends and family who have stood by me throughout all the challenges that I have faced in the past five and a half years. Next I'd like to acknowledge my advisor and committee chair, Dr. Sanjay K Nigam. Without him there would be no developmental approach to engineering kidney tissues. I'd also like to thank all my committee members for helping to keep things focused. I would like to acknowledge and thank the National Science Foundation for providing me financial support for three years of my research via their Graduate Research Fellowship program

I'd like to thank all those lab members directly involved in the research that led to my manuscripts, potential manuscripts, and chapters. Thanks to Hiro for general lab guidance and helping formulate a new tissue engineering role for previous growth factor research. Thanks to Mita for being my first official mentor in the lab. Thanks to Kohei for being a great neighbor and performing implantations that may have never happened otherwise. Also, thanks for helping with the MM cell line work. Thanks to Yohan for really promoting my natural inclination to finding deals and helping me step it up to a whole new level. That and some much needed Wolffian duct pictures. Thanks to Duke for being, hands down, the coolest lab member ever and being an incredible person to work with. Besides teaching me my dissecting techniques and helping start the tissue engineering project, you were an inspiration of how to go about living life. Thanks to Heidi for somehow finding joy in the most monotonous job ever (counting 100s of UB tips that is), and for being an additional engineering personality in the lab.

I'd like to thank all the members, past and present, of the Nigam lab that helped me out in everything from teaching me techniques to promoting a demented Futurama lust and everything in between. Thanks to Akito for being a great labmate and jumpstarting my independent work. Thanks to Wei for helping me with everything PCR related. Thanks to Kevin for repeatedly proofreading my manuscripts. Thanks to Derina for spending so many hours working with me on 3D reconstructions that, unfortunately, never came to be. Also, thanks for teaching me new meanings to old words. Thanks to Marvalyn for being a fellow J-O-O in the lab and being a fun person to work with. Thanks to James for getting me started with macro language programming, which directly led to being able to perform 3D reconstructions - that and the fun camping trip. Thanks to David for perhaps being the biggest musical influence in my life. At the Drive-in and The Mars Volta would have never been known to me without you and I think everyone knows where my musical tastes went after that. Your general prowess in the lab was also great; your lesson about the magical drawer was priceless. You also made an excellent disciple of mine continuing the tradition of great people attending the University of Texas at Austin – Go Longhorns! Thanks to Tom for being a great buddy in the lab and for being the biggest beer drinking influence ever – and I don't mean quantity. That together with your introducing me to whole leaf teas has drastically improved the quality of my liquid consumption in life-altering ways. Oh yeah, and most of all, thanks for all the truly priceless camping moments. Last, but certainly not least, and likely most, thanks to Pat for so much that listing it all would make for a thesis in and of itself.

Chapter 2, in full, is a reprint of the material as it appears in "Staged *in vitro* reconstitution and implantation of engineered rat kidney tissue" by Rosines E., Sampogna R.V., Johkura K., Vaughn D.A., Choi Y., Sakurai H., Shah M.M., Nigam S.K. in Proceedings of the National Academy of Sciences USA, 2007. 104(52): p. 20938-43. Reprinted with permission from the Proceedings of the National Academy of Sciences USA. The dissertation author was the primary investigator and author of this paper.

Chapter 4, in full, is a reprint of the material as it appears in The effect of hyaluronic acid size and concentration on branching morphogenesis and tubule differentiation in developing kidney culture systems: Potential applications to engineering of renal tissues" by Rosines E., Schmidt H.J., and S.K. Nigam in Biomaterials, 2007. 28(32): p. 4806-17. Reprinted with permission from the Elsevier publishing company. The dissertation author was the primary investigator and author of this paper.

VITA

2008	Ph.D., University of California, San Diego
2004	M.S., University of California, San Diego
2002	B.S. (Highest Honors), University of Texas at Austin

AWARDS

2003 National Science Foundation Graduate Research Fellowship
2001 John and Fanny Hertz Foundation Undergraduate Research Fellowship
2000 BP Amoco Engineering Excellence Scholarship

PUBLICATIONS

Rosines E, Johkura K, Nigam SK. "Creating renal progenitor tissues from cells and three-dimensional *in vitro* kidney culture: towards a broader method of *in vitro* engineering of kidney tissues" in preparation.

Rosines E, Sampogna RV, Johkura K, Vaughn DA, Choi Y, Sakurai H, Shah MM, Nigam SK. "Staged *in vitro* reconstitution and implantation of engineered rat kidney tissue" Proceedings of the National Academy of Sciences USA 2007. 104(52): p. 20938-43.

Rosines E, Schmidt HJ, Nigam SK. "The effect of hyaluronic acid size and concentration on branching morphogenesis and tubule differentiation in developing kidney culture systems: potential applications to engineering of renal tissues" Biomaterials 2007. 28(32): p. 4806-17.

Rosines E, Bersuker IB, Boggs JE. "Pharmacophore identification and bioactivity prediction for group I metabotropic glutamate receptor agonists by the electron-conformational QSAR method." Quantitative Structure-Activity Relationships 2001. 20(4): p. 327-334.

SELECTED ABSTRACTS AND PRESENTATIONS

Rosines E, Nigam SK. "Hyaluronic Acid Guides *In Vitro* Kidney Development Based on Size and Concentration" Biomedical Engineering Society National Meeting, September 2007.

Rosines E, Nigam SK. “Hyaluronic Acid in Renal Organogenesis”. Matrix Biology 2006 Nov;25:S31-S32.

Rosines E, Bersuker IB, Boggs JE. “Application of the Electron-Conformational Method of Pharmacophore Identification and Bioactivity Prediction to Group I Metabotropic Glutamate Receptors”. American Chemical Society National Meeting, Apr. 2001.

PATENTS

Rosines E, Nigam SK. “Formation and Use of Wolffian Duct-like, Ureteric Bud-like and Metanephric Mesenchyme-like Inductive Tissues from Cells for Tissue Engineering of Functional 3-dimensional Kidney Tissues in Stages”. UCSD Docket No. SD2007-300; July 2007.

ABSTRACT OF THE DISSERTATION

Developmental Approaches to *In Vitro* Engineering of Kidney-like Tissues

by

Eran Rosines

Doctor of Philosophy in Bioengineering

University of California, San Diego, 2008

Professor Sanjay K. Nigam, Chair
Professor Robert L. Sah, Co-Chair

Many tissue engineering strategies are being pursued to alleviate chronic kidney disease. This thesis presents two developmental approaches that aim to use progenitor tissues to engineer kidney-like tissues capable of providing significant renal functionality. If this can be done, and cells can be used to construct these progenitor tissues, then it may be possible to make kidney-like tissues from cells. In one approach, the Wolffian duct

(WD) is guided through the stages of kidney development, *in vitro*, and then recombined with metanephric mesenchyme (MM) to produce a kidney-like tissue. In the second approach, a small segment of WD is directly surrounded by MM recreating an embryonic kidney-like structure that may then be cultured in a three dimensional (3D) matrix to yield a kidney-like tissue. These strategies are advantageous because they; 1) potentially can begin with only two cell types; 2) require the construction of relatively small, simple tissues; 3) offer opportunities for tissue propagation; and 4) result in tissues with a 3D structure known to be important for kidney function. The objective of this dissertation is to examine the hypothesis that the developmental approaches to *in vitro* engineering of kidney tissues presented here are potentially feasible.

Using *in vitro* models of kidney development, it was demonstrated that a WD tissue could (in the context of appropriate growth factors and extracellular matrix molecules) be induced to recapitulate key stages of kidney development and ultimately be recombined with MM, resulting in a kidney-like tissue containing functional transporters and, following implantation into a host animal, markers of vascularization. Next, it was found that a homogenous cell line has the potential to be used in the construction of an epithelial tubule that can be used in the developmental strategies described; however, the MM may require an earlier cell lineage than currently available. Ideally, *in vitro*-formed kidney tissue would have a 3D structure comparable to the *in vivo* kidney. A type IV collagen suspension culture was shown to enable 3D embryonic kidney growth, resulting in a branching structure similar to *in vivo* ureteric bud branching morphogenesis. Differentiation factors may enhance the functionality of the *in vitro* engineered kidney-like tissue. A biocompatible polymer, hyaluronic acid, was found to be a potential

regulator of both UB and MM growth and differentiation, with the ability to strongly promote both branching morphogenesis and tubular differentiation of *in vitro* embryonic kidney cultures. This raises the possibility that HA can be used as a growth and differentiation enhancing scaffold material for *in vitro* kidney engineering. Together, these findings represent important advances towards engineering kidney tissues via developmental approaches.

CHAPTER 1:

Introduction

1.1 Kidney Function and Renal Disease

The kidney is a multifaceted organ responsible for numerous essential tasks, including drug handling, water homeostasis, pH control, salt balance and waste excretion. The kidney also is a key endocrine organ that secretes renin, erythropoietin, and calcitrol. Chronic kidney disease is a debilitating illness that can lead to premature death.

1.1.1 Kidney Function Depends on 3D Structure

The kidney accomplishes its multitude of tasks by employing complex three dimensional (3D) functional units known as nephrons. The adult human kidney is comprised of approximately one million nephrons, with each nephron containing 3D features vital to the proper function of the kidney (Fig. 1.1). The nephron is often divided into the glomerulus, the proximal convoluted tubule, the loop of Henle, the distal convoluted tubule, and the collecting duct. The glomerulus, the proximal convoluted tubule, and the distal convoluted tubule all reside in the outer portion of the kidney, or renal cortex, while the loop of Henle extends in to the inner portion of the kidney or renal medulla. The loop of Henle, which extends from the cortex towards the renal medulla, is in a countercurrent exchange with the vasa recta (capillaries that surround the loop of Henle). This architectural positioning results in the medullary gradient necessary for

urine concentration. In addition, the distal end of the loop of Henle (the thick ascending limb of the loop of Henle) and the beginning of the distal tubule are oriented in a fashion where by the tubule lies adjacent to the glomerulus. The cells of the thick ascending limb of the loop of Henle/early distal tubule closest to the glomerulus, known as the macula densa, together with the extraglomerular mesangial cells and juxtaglomerular cells of the afferent arteriole make up the juxtaglomerular apparatus (Fig. 1.1A). The juxtaglomerular apparatus functions in a feedback mechanism that responds to filtrate composition to release a vasoconstrictor that acts on the afferent arteriole to regulate both renal blood flow and glomerular filtration rate [15]. The collecting duct system employs an intricately branched 3D structure in order to connect every nephron to the ureter. The filtrate from the nephron flows into the initial collecting ducts that then connects to the cortical collecting ducts. The cortical collecting ducts merge in to the medullary ducts, followed by the papillary ducts. The papillary ducts empty in to the minor calyx, and multiple minor calyces converge to form the major calyx. The major calyces empty in to the renal pelvis that is connected to the ureter (Fig. 1.2) [15]. Without the 3D organization of the nephron components and the collecting duct system, the kidney would not be able to properly concentrate urine, regulate filtration rate and renal blood flow, or collect urine.

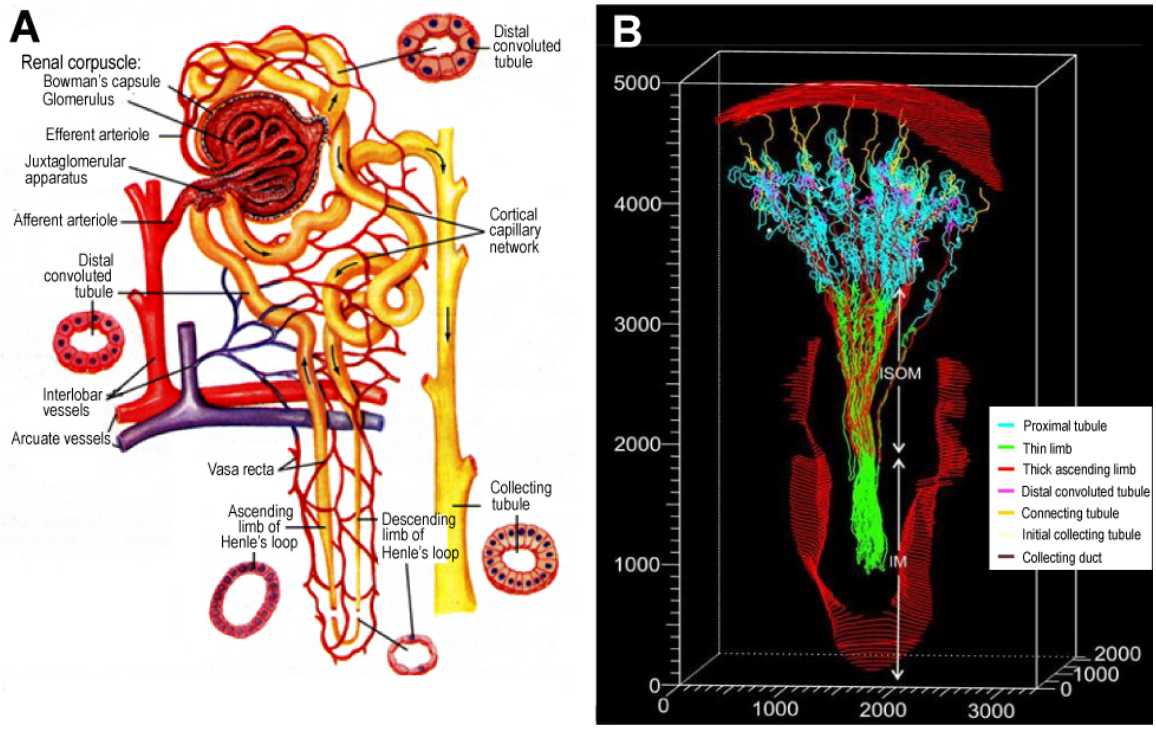

Figure 1.1: The nephron. The juxtaglomerular apparatus and loop of Henle pictured above are structures vital for kidney function (adapted from [175]) (A). A 3D reconstruction of murine long-looped nephrons illustrates the complex 3D organization (adapted from [198]) (B).

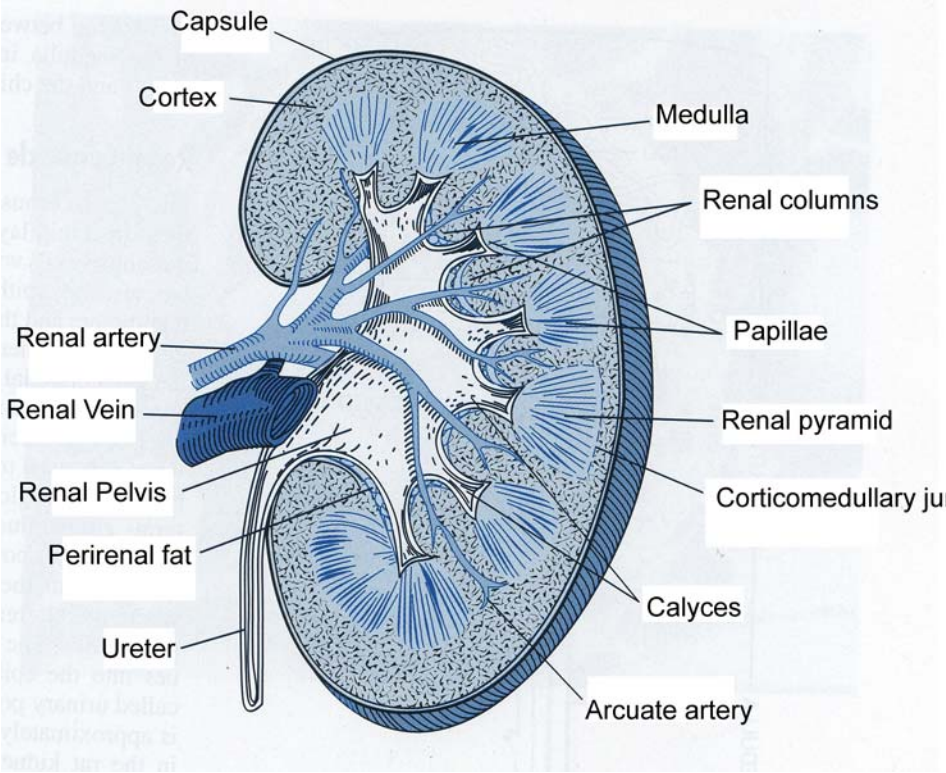

Figure 1.2: Diagram of a bisected adult kidney. The filtrate from each nephron is gathered by the collecting duct system into the renal pelvis before being expelled from the kidney via the ureter (adapted from [15]).

1.1.2 End Stage Renal Disease and Current Treatments

End stage renal disease (ESRD) is the condition in which the kidneys are no longer able to function at a level necessary for every day life. Without treatment, waste materials will accumulate in the blood and death will occur. Most cases of ESRD in the US are a secondary condition to diabetes or hypertension. In 2004, 472,099 US residents were being treated for ESRD, and 84,252 of these patients did not survive [3]. The current modality of treatment for ESRD is either dialysis or donor organ transplantation. Because of the shortage of donor organ availability, dialysis remains the primary treatment option for most patients. The 10 year survival rate for ESRD patients on

dialysis, 10.0%, is far less than that of a living donor transplant recipient, 75.6%, or deceased donor transplant recipient, 59.4% [3]. Furthermore, many studies show that the quality of life for patients receiving transplants is far better than that of patients undergoing dialysis [35, 115, 165, 184]. One possible reason for the inability of dialysis to be a viable long term treatment may be that dialysis is capable of replacing the waste filtering functions of the kidney, but generally cannot reproduce the reabsorption of important molecules or the endocrine and metabolic functions of the kidney leaving the patient at risk for additional problems. For instance, hemodialysis patients are at risk for developing severe osteomalacia, or "adult rickets", caused by the failure of the kidney to produce calcitrol [33]. With the kidney being responsible for 90-95% of erythropoietin release (the principal factor that stimulates red blood cell production), when the kidneys are being destroyed by renal disease, severe anemia results [116]. While there are drugs available to treat the conditions associated with chronic kidney disease managed by dialysis, these conditions and/or drugs can result in additional complications, increased expenses, and reduced quality of life.

The alternative to dialysis, and currently the best available ESRD treatment option, is renal transplantation. Although renal transplantation provides many advantages over dialysis (including complete renal function), problems still remain. Despite the large number of patients being treated for ESRD, only 16,905 kidney transplantations were performed in 2004 in the US, and there were still over 76,000 people on the transplantation waitlist as of December 2007 [2, 3]. The immunosuppressant drugs required to prevent rejection of the donor organ can have numerous adverse effects [196]. Ultimately, with a 10 year graft survival rate of only 54.7% for living donor transplants

and 39.2% for deceased donor transplants, organ transplantation remains a temporary solution [3].

1.2 Tissue Engineering Techniques

Dialysis and renal transplantation represent the best available ESRD treatments, but leave plenty of room for improvement. Tissue engineering is a discipline that aims to solve medical problems by creating biological-based therapies. Tissue engineering solutions range in complexity from single cell strategies to multicellular 3D constructs [77]. Various techniques in tissue engineering will be explored in this section followed by a review of which techniques are being used to pursue renal disease therapies in the next section.

1.2.1 Seeding Cells on a Scaffold

The traditional paradigm of tissue engineering has been to create a solid scaffold of the shape of a particular tissue and then seed cells of that particular tissue within the scaffold [77]. Scaffolding materials can generally be split in to two categories, synthetic or natural. Common synthetic scaffolding materials have included polymers such as poly lactic acid, poly glycolic acid, poly-coprolactone, amongst many others (reviewed in [67, 94, 194]). Natural polymers used for the purpose of creating scaffolds include included collagens, gelatins, chitosan, cellulose, and many others (reviewed in [67, 94, 194]). Scaffolding materials are often selected for their biocompatibility, ability to support cell adhesion and migration, pore size, degradation rate, and mechanical properties. These scaffold characteristics can be fine tuned by making composite scaffolds featuring

multiple natural and/or artificial components. This technique has been used to create an FDA-approved dermal substitute for venous or diabetic skin ulcers. The dermal substitute consists of a poly(lactide co-glycolide) scaffold seeded with dermal fibroblasts obtained from neonatal foreskin [101]. A canine bladder was similarly engineered by seeding urothelial and smooth muscle cells on a poly(glycolic acid) based scaffold in the shape of an adult bladder [125]. A scaffold composed of esterified hyaluronic acid polymers seeded with autologous chondrocytes obtained from a patient biopsy has been used in the construction of articular cartilage and is being used for treatment of articular cartilage defects [131]. Other tissues have been more difficult to engineer using solid scaffolding techniques due to the need for a vasculature and to increasingly complex architectures.

Hydrogels are a unique type of scaffold that traps large quantities of water between the polymers resulting in a scaffold with physical properties that more closely resemble natural soft tissues [12]. Hydrogel polymers also can be categorized as either natural or artificial. Some natural extracellular molecules like collagens and gelatins will solidify to form hydrogels at room temperatures while other natural polymers must be chemically crosslinked or altered to allow for gelation and hydrogel formation [12]. Alginate is a natural polysaccharide that can be crosslinked in the presence of calcium via ionic bonds to trap cells. Levesque *et al*., demonstrated that pancreatic islet cells trapped in alginate based hydrogels maintain secretory function in response to physiological cues. In addition, the microencapsulation protected the cells from immune responses [85]. Alginate has also been demonstrated to support chondrocyte proliferation resulting in cartilage-like tissues with higher levels of type II collagen and glycosaminoglycan expression (structural components of mature cartilage) [23, 56, 102]. A hydrogel

composed of a mouse-derived basement membrane solution known as Matrigel has demonstrated an ability to support the self organization of primary salivary gland cells into epithelial structures capable of branching morphogenesis and expressing markers of intact salivary glands [188].

The polymers used for both traditional scaffolds and hydrogels have been modified to be more cell compatible or provide biological cues. These modifications have included immobilizing amino acid sequences derived from natural extracellular matrix molecules or signaling molecules, such as growth factors [94 76]. Arg-Gly-Asp (RGD) is a fibronectin derived sequence known to promote cell adhesion [148], and Tyr-Ile-Gly-Ser-Arg (YIGSR) is a laminin derived sequence also known to promote cell adhesion [48]. RGD sequences covalently bonded to alginate polymers improved the adhesion and motility of mouse myoblasts [147]. YIGSR immobilized on a poly(ethylene glycol) based hydrogel promoted cell adhesion and proliferation of preadipocyte cells [130]. RGD and YIGSR sequences were used in combination to facilitate cellular adhesion of cardiac myocytes on a silicon substrate [14]. Growth factors have also been immobilized on scaffolds for promoting differentiation or other specific cellular response [94]. For example, vascular endothelial growth factor (VEGF) immobilized on a number of different types of scaffolds has been demonstrated to promote endothelial cell growth and proliferation within those scaffolds [37, 60, 162, 199]. This may represent a potential method of promoting vasculogenesis in tissue engineered constructs.

Another technique for generating scaffolds for cell seeding is the decellularization of existing tissues, either allogenic or xenogenic [47]. Multiple processing techniques exist for removing cells from existing tissues leaving behind the acellular structural

components of the tissue; the resulting scaffold can then be repopulated with cells so that seeded cells will adhere to the matrix in the same spatial organization as the natural tissue [47]. This technique has already been used clinically to create heart valve replacements from porcine tissues seeded with autologous cells [123]. Recently, Ott *et al.*, decllularized an adult rat heart and repopulated it with neonatal cardiac cells. After 8 days, the cells had populated much of the heart scaffold and the construct demonstrated an ability to beat in response to an electrical stimulus [128].

1.2.2 Microfabrication and Micropatterning

As researchers attempt to engineer more complex tissues, the techniques used to construct these tissues have also increased in complexity. Micropatterning refers to the ability to place cells or matrix in specific orientations on a microscale. Several micropatterning techniques have been developed to accomplish this task

The ability to print transparent sheets at very high resolutions using common inkjet printers has provided a simple means of creating inexpensive masks that can be used to expose only certain regions of photosensitive materials to light. Liu Tsang *et al*., developed a method whereby a photosensitive hydrogel containg cells was placed on a surface and covered by a sheet transparent only in certain shapes (Fig. 1.3A) [88]. When light was exposed to the hydrogel through the transparency, only the hydrogel under the transparent region was crosslinked leaving the rest of the hydrogel solution to be washed away. This process was repeated resulting in layers of pattered hydrogel [88].

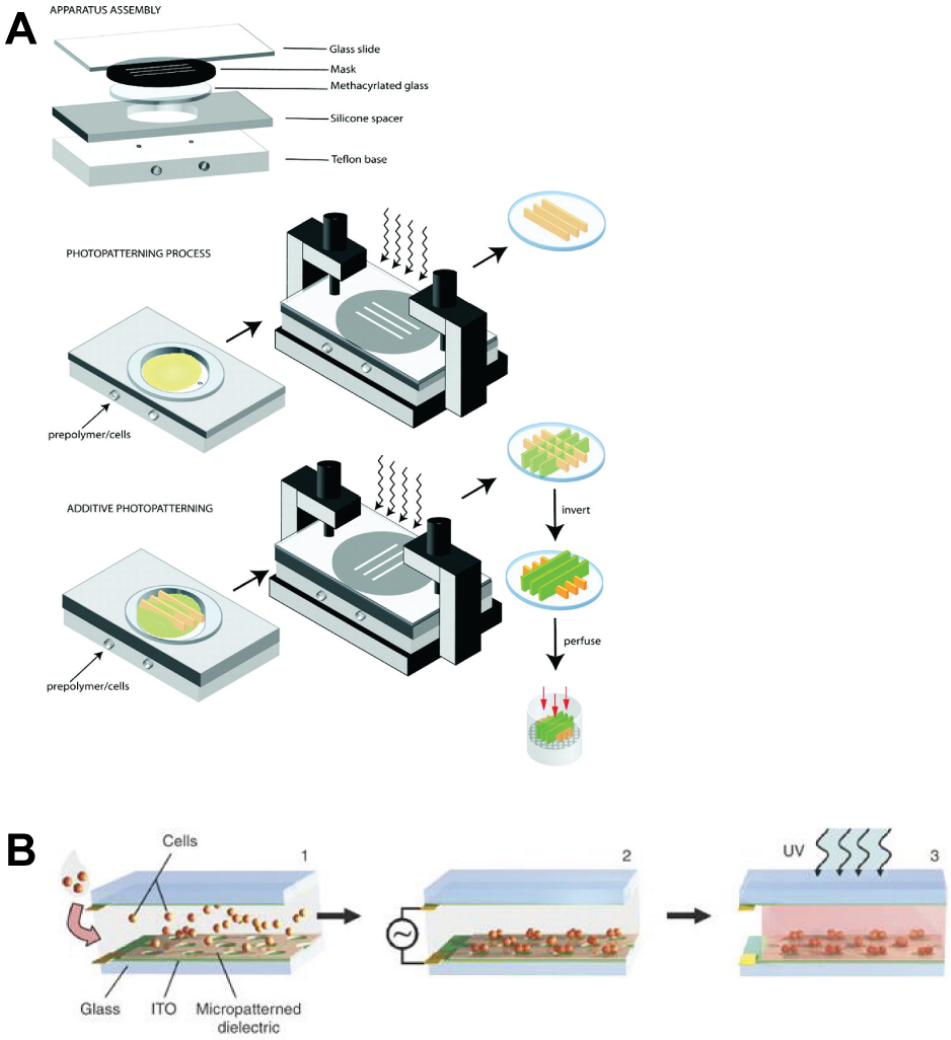

Figure 1.3: Micropatterning of cells utilizing photopolymerization of hydrogels. Masks can be used to expose certain regions of the hydrogel to light creating specific hydrogel patterns (adapted from [88]) (A). Dielectrophoretic forces can be used to push cells into certain locations, followed by photopolymerization of the hydrogel trapping the cells in place (adapted from [6]) (B).

Another technique for trapping cells in particular orientations involves the use of dielectrophoretic forces to move cells to specific locations within a hydrogel [6]. Cells were suspended in a photosensitive hydrogel solution sandwiched between two tin-oxide coated glass slides. One of the glass slides contained an insulating layer with only certain

predetermined shapes of no insulation. When an electrical current was applied from one glass slide to the other, the cells were pushed only to the areas of the hydrogel over the non-insulated areas. Then light was supplied to the hydrogel solution causing polymerization trapping the cells in place. This procedure was repeated resulting in multiple layers of patterned cells (Fig. 1.3B) [6].

Microfabrication and microelectromechanical systems (MEMS) techniques are being used to more precisely position cells and matrix in particular spatial orientations. For tissue engineering applications, a two-step process first designed by Anderson *et al.,* and Unger *et al.,* is typically employed for the generation of scaffolds, stamps, or devices [8, 183]. The first step is the creation of a silicon- based master mold, which can be accomplished either by traditional silicon etching techniques or by soft lithography (i.e. photolithothography) (Fig. 1.4A). The second step is a process known as replica molding whereby an elastomeric substance is poured over the master mold and then cured to form an elastomeric mold (Fig. 1.4B). The elastomeric mold can then be used in a number of different ways. Polydimethylsilxone (PDMS) is the most commonly used elastomeric substance due to its durability and adhesive characteristics [8].

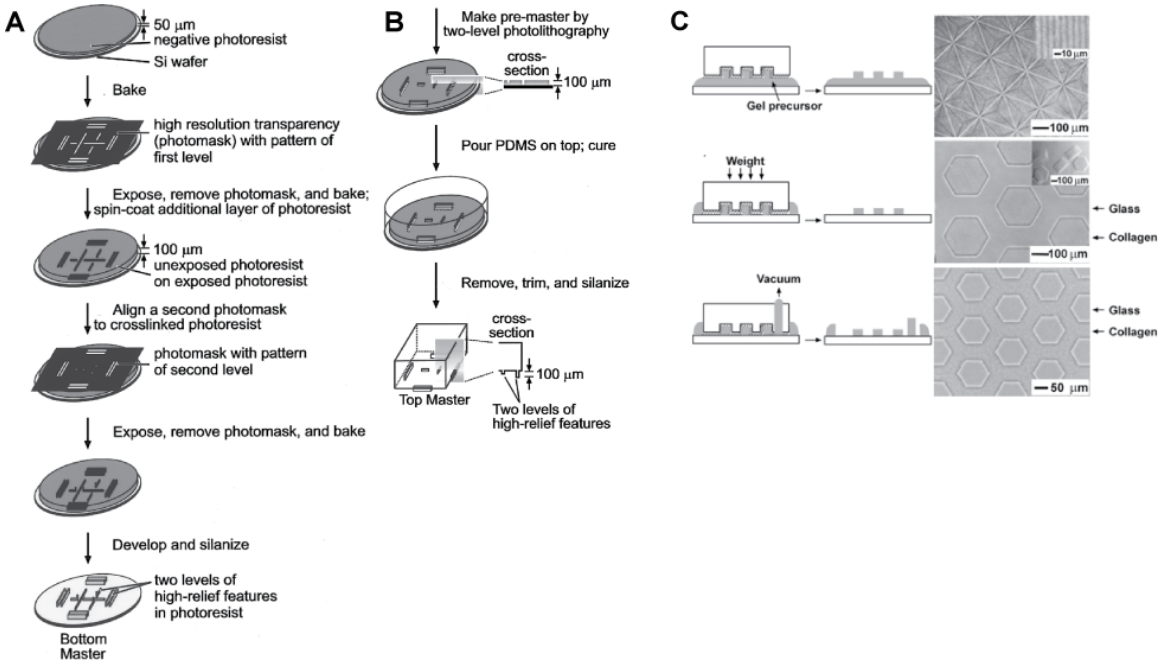

Figure 1.4: Microfabrication of molds for micropatterning of tissue engineered constructs. Soft photolithography was used to create a master mold (A). Then, PDMS was poured over the mold and cured resulting in a PDMS mold (A and B adapted from [8]) (B). The PDMS mold can then be used as a stamp to create hydrogels containing cells with specific 3D shapes and orientations (adapted from [174]) (C).

Tang *et al*., first suggested that PDMS molds created as described above could be used as stamps to create imprints in hydrogels that could then be solidified to achieve a particular shape (Fig. 1.4C) [174]. Yeh *et al.,* demonstrated how various shapes of hydrogels can be created by filling in the spaces of a PDMS mold with a photopolymerizable hydrogel containing cells. The hydrogel was then exposed to light causing polymerization and resulting in a hydrogel containing cells in a particular shape [195].

Nelson *et al.,* used this approach to create an imprint of a tubule in a type I collagen gel [119]. A cell solution was then placed in the imprint and covered by another

layer of solidified collagen trapping the cells in a tubule orientation. The cells adhered to the collagen and proliferated along the walls of the collagen resulting in an epithelial tubule with predetermined shape and dimensions.

Rather than creating a PDMS mold, Fidkowski *et al.,* created a mold using poly(glycerol sebacate), an elastomeric material known for being biodegradable and biocompatible [38]. A flat poly(glycerol sebacate) sheet was sandwiched together with a molded poly(glycerol sebacate) sheet resulting in a fluidic chamber. Endothelial cells were then injected into the chamber. The endothelial cells attached to the walls of the chamber resulting in a microvasculature structure.

1.2.3 Cell Printing and Cell Sheet Engineering

Inkjet printers have been modified to allow for the deposition of extracellular matrix molecules and cells in specific orientations, which has led to the idea of organ printing. Organ printing can work either by printing cell/matrix solutions that will polymerize once placed in a particular orientation (Fig. 1.5A), by printing cells in a particular orientation on a prefabricated scaffold (Fig. 1.5B), or by printing a scaffold that is later seeded with cells [140]. Xu et al., utilized cell printing technology to create complex patterns and structures of embryonic primary hippocampal and cortical neurons [190]. After being printed on to fibrin gels, the neurons exhibited normal, healthy neuronal phenotypes and electrophysiological characteristics suggesting that cell printing could be used to build functional neuronal structures. Lee *et al.,* utilized inkjet printing to create a scaffold in the shape of intestinal villi [81]. The printed scaffold was used as a mold for creating a poly(lactide co-glycolide) based scaffold that was then seeded with

intestinal epithelial cells. The epithelial cells attached to the scaffold and grew preferentially in the villi region of the scaffold.

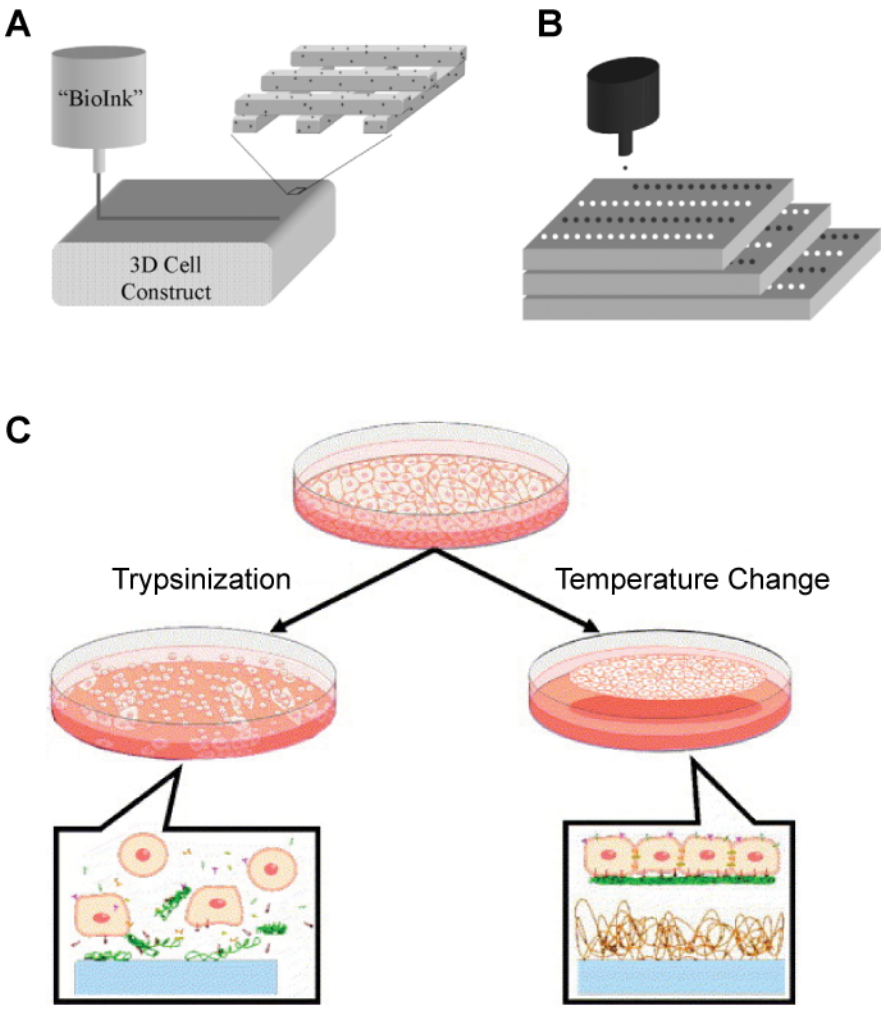

Figure 1.5: Inkjet printing and cell sheet engineering technologies. Cells and matrix can be printed together (A) or cells can be printed alone onto a prefabricated scaffold (B) (A and B adapted from [140]). Monolayers of cells can be safely isolated as sheets by culturing the cells on a substrate whose hydrophobicity changes in response to temperature (C) (adapted from [193]).

Cell sheet engineering has emerged as another method of creating layers of cells that can then be stacked to construct 3D tissues (Fig. 1.5C) [193]. Kushida et al., first

demonstrated how endothelial cells could be cultured on a plate coated with a temperature-responsive polymer, poly(N-isopropylacrylamide) [75]. Once the cells reached confluency, the temperature of the culture was decreased causing the polymer to become hydrophilic and resulting in a weak attachment of the cells to the plate. This allowed for the cells to be removed from the plate as an intact sheet. Masuda *et al.,* used this technique with myocardial cells to create multilayer myocardial tissues [104]. The constructed myocardial tissues were demonstrated to improve the heart function of damaged hearts in multiple animal models.

L'Heureux *et al*., utilized cell sheet engineering to create blood vessels containing three cell layers utilizing human cells [76]. First, a cell sheet of vascular smooth muscle cells was wrapped around a support tubule. Then a sheet of fibroblast cells was wrapped around the smooth muscle layer to create the adventitia. After the cell sheets matured, the support tubule was removed and the lumen of the tubule was seeded with endothelial cells. The resulting vessel expressed multiple markers of mature blood vessels and contained burst strengths comparable to that of human blood vessels.

1.3 Engineering New Treatments for ESRD

New potential ESRD treatments attempt to address the drawbacks of dialysis and renal transplantation described in Section 1.1.2. Research towards alternative treatments for ESRD or alternative sources of kidneys for transplantation has focused on five areas: improving the efficacy of hemodialysis, adding cellular components to hemodialysis, creating biological based kidney substitutes, complete organ reconstruction, and adapting animal sources of kidneys for human use.

1.3.1 Micro and Nano-scale Dialysis Devices

Microelectromechanical systems (MEMS) are being use to create smaller, microscale objects for use in biomedical applications. Kaazempur-Mofrad *et al.,* created a bilayered microscale device out of two microetched polydimethylsiloxane (a MEMS substrate) films sandwiched around a polyethersulfone membrane (Fig. 1.6A). The microscale size of the device resulted in a more optimal urea and creatinine clearance at physiologic blood-flow conditions [64]. Currently this device does not include the use of any renal cells; however, Fissell *et al.,* has demonstrated that renal cells can attach and differentiate when cultured on various silicon-based MEMS substrates [40]. Another group has created a computer model of a wearable device that contains two membranes in series with nano-sized pores and synthetic channels that can operate continuously without the need for a dialysate solution [121, 122]. While this device is promising, a working model has yet to be constructed. A device constructed of biocompatible silicone hollow fibers with nano-sized pores has achieved significant capillary bed formation around the device when implanted into a host rat, but total filtrate volume is currently very limited [177].

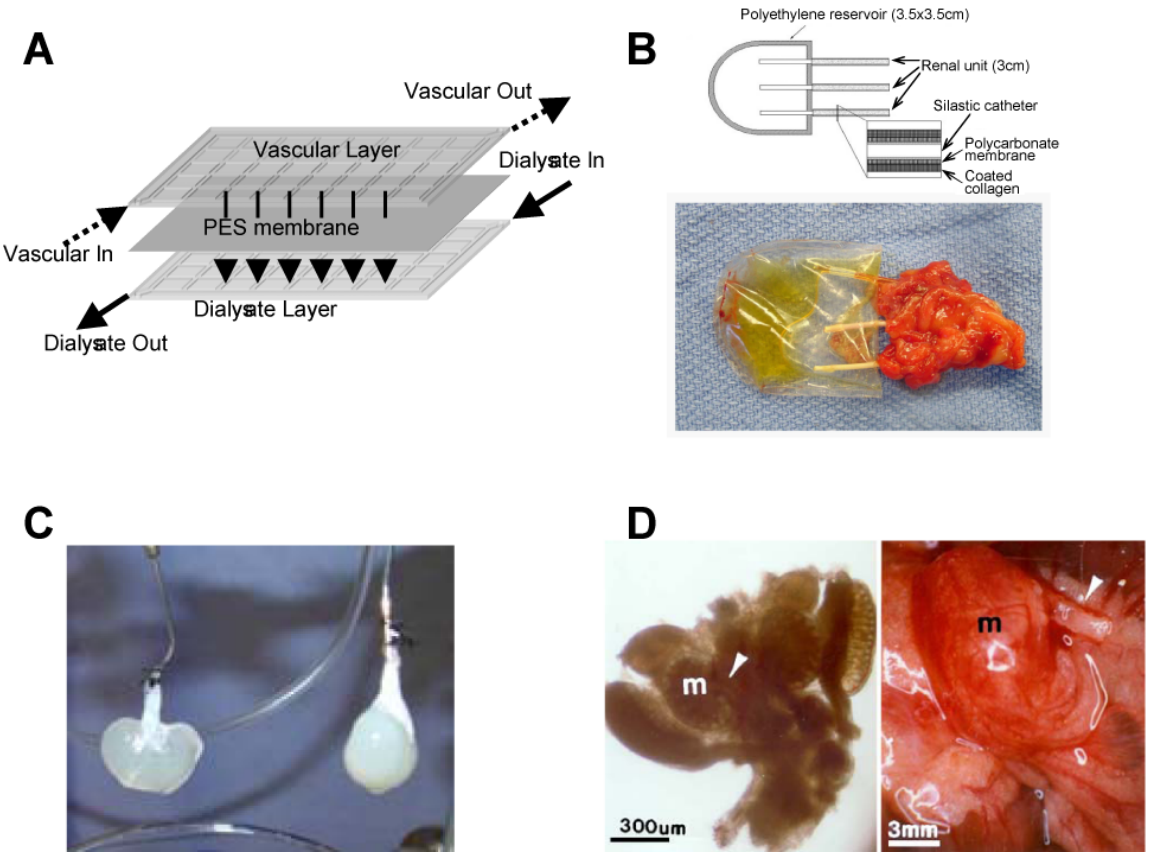

Figure 1.6: ESRD treatment strategies. A bilayered microscale dialysis device (adapted from [64]) (A), implantable cell-seeded tubules (adapted from [78]) (B) the decellularized kidney scaffold (from [146]) (C), and the implanted embryonic metanephroi (rat metanephroi indicated with the "m") (adapted from [52]) (D) all represent potential ESRD treatment strategies.

Although micro and nano-scale dialysis devices may provide improved waste filtering over traditional hemodialysis, they cannot provide the endocrine and metabolic functions of the kidney and, even with improved membranes, will unlikely be able to provide the same level of selectivity of molecules for secretion and reabsorption as the kidney. Consequently, these approaches may present the same quality of life issues and secondary complications as dialysis, such as osteomalacia or anemia. These limitations may render the technologies temporary, rather than permanent treatment options for

patients with ESRD, keeping allogenic renal transplantation as the best available treatment option.

1.3.2 The Bioartificial Kidney

Another strategy for improving the efficacy of hemodialysis is to incorporate live renal cells that can perform specific reabsorption of molecules filtered out by standard dialysis membranes and contribute endocrine functions similar to the kidney. The extracorporeal bioartificial kidney is a traditional hemodialysis machine with an additional cartridge containing human proximal tubule cells seeded on the luminal side of hollow pronectin-L coated polysulfone fibers [39, 57, 58]. The seeded human proximal tubule cells have been shown to activate vitamin D_3 and the cell-laden cartridge has demonstrated durability, viability, and functionality in the clinical setting [58]. An alternative implantable cell-based strategy involves seeding histocompatible renal cells created by nuclear transplantation on to collagen-coated cylindrical polycarbonate membranes connected to a collection device [78]. When implanted into a host animal this device produced a urine-like substance containing concentrated urea (Fig. 1.6B) [78].

Both of these strategies utilize live renal cells to provide renal functionality; however, limitations exist for these strategies as well. Both of these strategies rely on having large numbers of renal cells available for seeding, which could pose problems for larger scale production of the extracorporeal bioartificial kidney. Also, it is unknown how long these cells could survive in the artificial environment; therefore, it is unknown how often the cells in either of these devices would need to be replaced. These devices only replace the function of certain renal populations and not the many different cell types of

the nephron, limiting their ability to provide full renal function. Furthermore, the extracorporeal bioartificial kidney, currently in clinical trials, has yet to demonstrate significant improvements over traditional dialysis. The implantable bioartificial kidney would seem to be susceptible to the same issue of improved function as the extracorporeal bioartificial kidney, and may be at risk of short survival time due to the artificial materials used in the device construction (assuming that the cells themselves are not at risk of short survival times).

1.3.3 Cell-based Organ Reconstruction

Two other cell-based approaches aim to construct kidneys by either layering sheets of cells [74, 193] or seeding cells on to scaffolds created from decellularized rat kidneys [146]. While a 3D kidney tissue has not yet been created with cell sheet engineering technology, this technology has been used to engineer renal tubule cell sheets [74]. Additionally, cell sheet engineering technology has already been used to engineer 3D miniature liver systems displaying persistent survivability *in vivo* [126]. Ross *et al.,* created a kidney scaffold by decellularizing a rat kidney (Fig. 1.6C). This scaffold was then seeded with a mouse ES cell line through the renal artery. After 10 days, ES cells showed some scaffold-dependent migration, altered cell morphology, and differentiation [146].

One limitation of both of these strategies is based on the fact that the adult kidney contains many different cell types, including 26 cell types in the nephron alone. Adult kidney reconstruction techniques would require either having a source of all the different cell types, in addition to properly placing them in 3D orientation, or assuming that

progenitor cells placed in a certain orientation will differentiate into the appropriate cell type (including the many renal tubular cell types and the endothelial cells of the vasculature). Since the collecting duct system, nephrons, and vasculature originate from different progenitor tissues, this may represent a difficult challenge to overcome. Similar to the extracorporeal bioartificial kidney, these strategies would require a large number of cells to reconstruct an entire organ, ehich may present a problem for large scale production.

1.3.4 Organ-based Kidney Replacements

Another possibility for addressing the shortage of available kidneys is to use animal sources of organs. While adult animal organs elicit an overwhelming immune response, embryonic tissues have been demonstrated to be more immunocompatible than adult organs [30, 42, 167, 185]. Rogers *et al.,* demonstrated how an embryonic rat metanephroi (at embryonic day 15) when implanted in to a host adult rat could grow in size, differentiate, and have the ureter connected to the host animal, resulting in function of the implanted metanephroi (Fig. 1.6D) [142]. Marshal *et al.,* were able to connect multiple rat metanephroi when they were implanted in the peritoneum of a host rat, resulting in increased survival time of anephric rats over single metanephroi implantation [103]. The xenogenic barrier has also been proven to be crossable by experiments in which human (E56) and porcine (E28) embryonic kidney tissues were able to grow, differentiate and produce urine-like substances eight weeks post-transplantation into a host immunodefficient mouse [31]. Additionally, both Rogers *et al.,* and Dekel *et al.,* have demonstrated that porcine renal primordia (E28) can grow and differentiate when

implanted into immunocompetent host mice or rats, although immunosuppression was required [31, 141]. It may also be possible to propagate renal primordia to create many potential implantable tissues from one embryonic kidney derivative [168].

Ultimately, this technique relies on the ability of the embryonic kidney to further develop in to a fully functional kidney in a foreign environment, which has yet to be achieved. It is also unknown how many embryonic kidneys would be necessary to provide adequate function for use as a treatment for ESRD. It would also be unlikely that a xenogenic tissue, even with reduced antigenicity, would have a graft survival rate greater than the allogenic sources currently used for renal transplantation, and they would likely still require some level of immunosuppression.

1.3.5 Sources of Cells for Engineering Kidney Tissues

Some of the potential therapies described above rely on a source of cells. While some of the technologies are utilizing cells available right now, including the extracorporeal bioartificial kidney that utilizes human proximal tubule cells from kidneys not suitable for transplantation as the biological component, others are relying on new techniques to generate immunocompatible cells. The problem with adult renal cells is that they are not easily propagated *in vitro* resulting in limited availability. Additionally, they would likely elicit the same immune response as current renal transplants. Ideally, immunocompatibility would be derived from using autologous cells or cells that are somehow altered to be non-immunogenic, so that immunosupression (one of the drawbacks to current renal transplantation therapy) would not be necessary for treatment.

Embryonic stem cells are propagatable cells that can potentially be created from a patient's own cells via techniques such as nuclear transplantation to create embryos containing immunocompatible kidney cells [78]. While the creation and development of new embryos raises bioethical questions, the use of embryonic stem (ES) cells in the form of the embryoid body (a non-viable *in vitro* culture) may be less controversial. Mouse ES cells cultured in embryoid bodies have been demonstrated to differentiate into intermediate mesoderm-like cells [69] (the precursors to metanephric mesenchyme that epithelialize to form nephrons) or ureteric bud-like ducts [192] (the precursor to the collecting duct system). Amniotic stem cells are an alternative cell source to embryonic stem cells that also may retain the ability to differentiate in to any tissue cell type and be propagated *in vitro* [27].

Another potential source of renal cells that are both propagatable and immunocompatible may be adult stem cells from the patient's own body. Many groups have identified populations of renal cells within adult kidneys with many properties of stem or progenitor cells [19, 32, 50, 71, 100, 149]. One population of adult tubular cells has demonstrated an ability to form tubule-like structures and to migrate and integrate into epithelial components of both the nephrons and collecting ducts when injected into a metanephric kidney culture [98]. Additionally, both hematopoietic stem cells [87] and bone marrow stem cells [65] have been demonstrated to contribute to the repair of injured kidneys. All of these adult cells represent immunocompatible cells with the potential to be used in kidney engineering techniques.

1.4 Metanephric Kidney Development

This dissertation aims to convey the potential of a developmental approach to engineering kidney tissues to address many of the issues that other strategies do not. However, before the approach can be explained, first the origin of the metanephric kidney and its development in to a fully functional organ must be introduced. Metanephric kidney development begins with the outgrowth of the ureteric bud (UB) from the Wolffian duct (WD) at approximately week 5 in human development, day 12 of rat development, or day 10.5 in mouse development. The mesenchymal cells surrounding the bud, known as the metanephric mesenchyme (MM), coalesce around the tips of the branching UB and are induced to undergo a mesenchymal-to-epithelial transformation (MET). Meanwhile, the invading UB is induced to undergo repetitive rounds of branching morphogenesis. The MM provides factors that promote UB branching and maturation while the UB releases factors that promote MM differentiation. The UB branches for approximately twenty generations in humans to form the collecting duct system, while the MM epithelializes and differentiates to form the various components of the nephron (Fig. 1.7) [159].

The developmental events that comprise kidney development can be modeled as a series of distinct stages [153]. The initial stage of UB outgrowth (or WD budding) is followed by UB branching and finally by UB maturation. The MM proceeds through its own stages of condensation, epithlialization (forming comma and then s-shaped bodies), and maturation in to a full nephron.

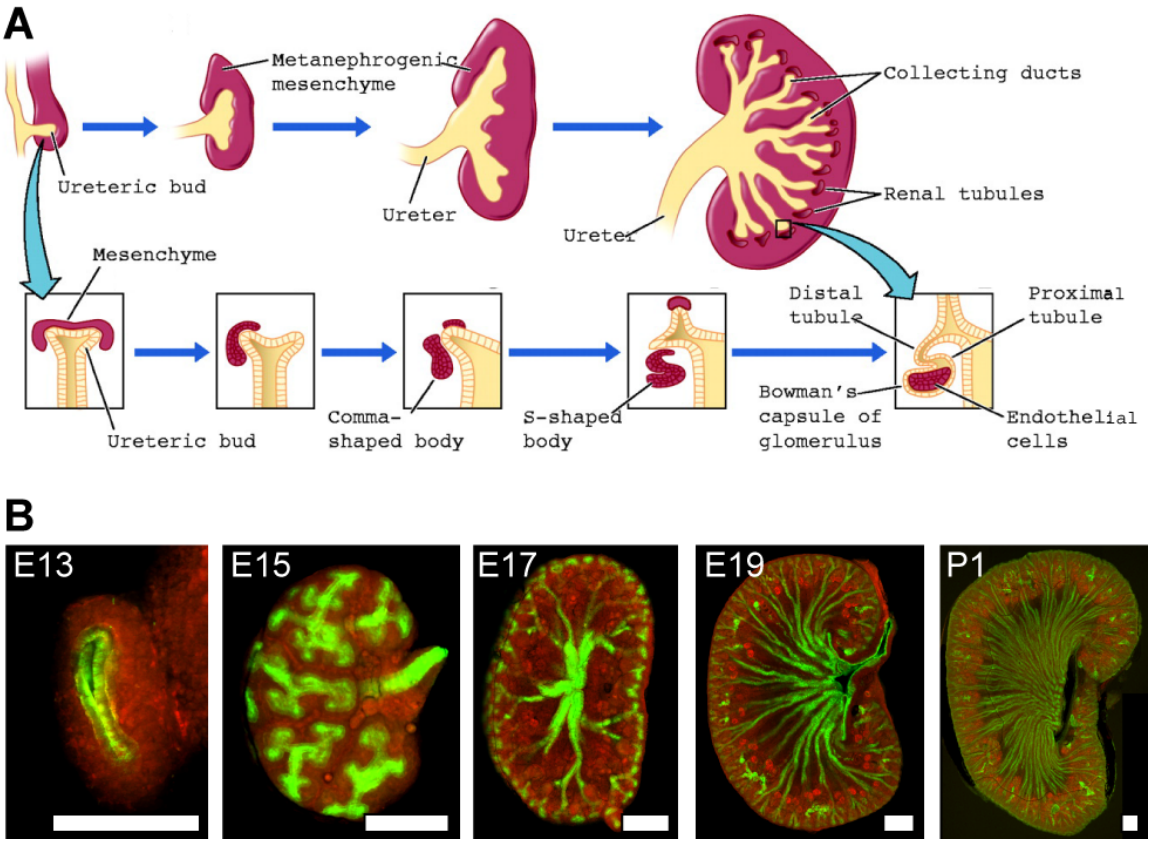

Figure 1.7: Kidney development. This kidney development scheme illustrates the stages of kidney development whereby the MM and UB undergo a mutual induction resulting in the nephrons and collecting ducts, respectively (adapted from [153]) (A). The UB undergoes extensive branching and patterning during the course of kidney development; scale bar corresponds to 300 μm (B).

1.4.1 The Natural Scaffold for 3D Kidney Development

The processes of branching morphogenesis and MET are both invasive and highly three dimensional. Accordingly, the cells of these tissues must constantly be removing, remodeling, and depositing extracellular matrix (ECM) molecules around themselves in a restricted spatiotemporal manner. These ECM molecules play a major role in kidney organogenesis by providing the physical substratum for spatial organization, binding various growth factors, and regulating development directly by ECM receptor signaling

[66]. The structural support for kidney development is provided by type I, type III and type IV collagens. Types I and III collagens are mostly present at the beginning of kidney development and are primarily expressed by the MM. As MET occurs, the newly differentiated MM begins to express more of the basement membrane specific proteins, including type IV collagen [34, 66]. Scaffolding is an important aspect of engineering 3D tissues and understanding the natural ECM scaffold of the developing kidney could provide valuable insight as to how best to design an artificial scaffold for *in vitro* engineering of kidney tissues.

1.4.2 *In Vitro* Kidney Culture Systems

Traditionally, kidney development has been studied *in vitro* by utilizing a whole metanephric kidney culture in which the kidney is cultured flat on a filter at the air/media interface [158]. This culture system replicates many of the developmental events that occur *in vivo*, but does not allow for the development of the renal vasculature and the 3D structure (the kidney grows flat along the filter). The individual stages of kidney development can be investigated separately through various *in vitro* models (Table 1.1). For example, Wolffian duct budding, isolated UB branching, and nephron formation (via a recombination of branched UB and MM or isolated MM induction) have all been reproduced in controlled *in vitro* environments [11, 49, 99, 136, 158, 168]. Vascularization of the embryonic kidney has been reproduced and studied by implantation of embryonic kidneys into host animal sites such as the chorioallantoic membrane (quail), the anterior eye (mature rat), and beneath the renal capsule (mature rat) [4, 155, 156]. UB, Madin-Darby canine kidney (MDCK), and inner medullary

collecdting duct (IMCD) cell lines have all been suspended in extracellular matrix gels and induced to undergo tubulogenesis under certain growth factor and matrix conditions [22, 113, 150]; however, the exact relevance of the cell tubulogenesis model to *in vivo* kidney development is not certain. These individual models allow for the investigation of signaling pathways, mechanisms, growth factor influences, or matrix requirements without interference from other processes that normally occur concurrently *in vivo*. Additionally, these culture systems allow for the potential of controlling the *in vitro* growth and development of kidney tissues, thus forming the basis behind the developmental approaches to engineering kidney tissues presented in this dissertation.

Table 1.1: *In vitro* models of kidney development

***In Vitro* Kidney Development Model**	**References**
Cell tubulogenesis (UB, MDCK, IMCD cell lines)	[22, 113, 150]
Wolffian duct budding	[99]
Isolated ureteric bud branching	[136]
Metanephric mesenchyme/spinal cord co-culture (for mesenchymal-to-epithelial transformation)	[49]
Isolated metanephric mesenchyme induction	[11]
Branched ureteric bud/metanephric mesenchyme recombination	[168]
Embryonic kidney implantation (for vascularization)	[4, 155, 156]
Whole embryonic kidney culture	[158]

1.5 Hyaluronic Acid

While *in vitro* metanephric embryonic kidney culture reproduces many features of *in vivo* kidney development, it is essentially a 2D culture growing along a filter and,

therefore, does not replicate the 3D structure of the kidney known to be vital for kidney function. The developmental approaches presented in this thesis propose a 3D *in vitro* culture system to engineer tissues that have the potential to recapitulate the proper 3D structure of the kidney. A successful 3D *in vitro* culture system would require a scaffold material that is biocompatible, capable of supporting the 3D structure of the tissue, capable of being remodeled by the developing tissue, and composed of nontoxic subunits. Often in tissue engineering, scaffold materials are selected because they have properties that allow them to be crosslinked or because they are readily available. However, there is rarely a strong reason supported by biological and optimization data behind the pairing of a particular polymer with a particular cell type. Since tissue engineering involves coaxing cells and tissues to act in a particular manner, the effect of the environment surrounding the cells and the breakdown products of the environment could play a vital role in engineering the best possible tissue product.

Hyaluronic acid is a natural polymer found in the tissues of nearly all vertebrates and many bacteria [43] and is particularly prevalent throughout the extracellular matrix during mammalian embryogenesis [107]. Based on the roles of endogenous hyaluronic acid and the characteristics of the polymer, both of which are explored below, this thesis will investigate the potential roles of endogenous hyaluronic acid in kidney development and the potential of HA to be a scaffolding material for future developmental approaches to *in vitro* engineering of kidney tissues.

1.5.1 Hyaluronic Acid Structure and Function

Hyaluronic acid (HA) is a simple polysaccharide, or glycosaminoglycan (GAG), consisting of repeating disaccharide units of D-glucuronic acid (1-β-3) N-acetyl-D-glucosamine (1-β-4) (Fig. 1.8), existing at sizes up to 10^7 Da [80]. Unlike other GAG molecules, HA does not require a protein linker molecule. In its larger forms, HA is a negatively charged chain that exists in a nearly random coiled configuration that, despite the negative charge, also contains hydrophobic regions [43].

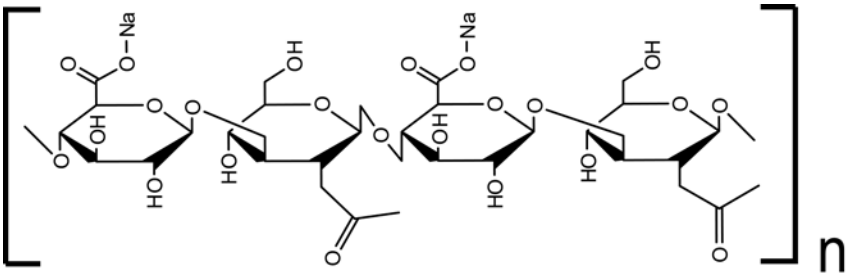

Figure 1.8: Single hyaluronic acid repeating unit**.** Hyaluronic acid consists of repeating units D-glucuronic acid (1-β-3) N-acetyl-D-glucosamine (1-β-4).

This structure gives HA unique characteristics, including water absorption, steric exclusion, and visco-elasticity, that are directly related to its functions. For instance, HA solutions present in joints have very high viscosities at low shear rates, which protects tissues from friction and abrasion, but very low viscosities at high shear rates allowing rapid movements with little resistance [43]. Steric exclusion keeps HA molecules as part of the synovial fluid during compression or joint articulation [25]. The steric exclusion property of HA is also known to provide an immunosuppressive function by preventing

ligand access to cell surface receptors. This is thought to be one of the mechanisms involved in immunosuppression in the developing fetus [105].

HA also functions as a signaling molecule. The two most studied hyaluronic acid receptors (or hyaladherins) are CD44 and Receptor for Hyaluronic Acid Mediated Motility (RHAMM). HA signaling through CD44 has been demonstrated to be involved in regulating the cell cycle [114], promoting angiogenesis [181], and modulating cell migration [110, 176]. In particular, HA-CD44 signalling has been found to be important for T-Cell extravasation [29]. RHAMM has been suggested as the primary HA receptor in certain primary human endothelial cell lines [90]. Similar to CD44, RHAMM has also been demonstrated to be involved in cell migration [51] and angiogenesis [157]. The shared function is not unexpected; compensation of one receptor for the other is believed to explain why gene deletions of either RHAMM or CD44 do not influence mouse viability [161, 178], while the deletion of a hyaluronic acid synthase gene results in embryonic lethality [107].

HA is also known to bind a variety of extracellular matrix molecules, including other GAG chains, proteoglycans, multiple collagens, fibronectin, and linker proteins, giving HA the potential to influence both the structure of the tissue and the sequestering of signaling molecules [68, 106, 118, 160, 182]. HA is known to be an important functional component of cartilage [53], skin [108], and brain extracellular matrices [191].

HA chains can exist in lengths varying from under 20 kDa to $2x10^4$ kDa. As the chain length changes, so does its physical properties and functions. The smaller chain lengths do not form the coiled structure that longer chains do and do not have the same high viscosity; therefore, the roles of HA as an immunosuppressant and joint lubricant

only apply to the longer chains of HA. The different sizes are also known to have opposing functions *in vivo*. Longer chains of HA have been demonstrated to act as an angiogenesis suppressant [36], while shorter oligosaccharides of HA have been shown to promote angiogenesis [28]. Additionally, although all sizes of HA interact with HA receptors, smaller sizes of HA are believed to be more involved in HA signaling while larger molecules can actually inhibit signaling [28].

1.5.2 Hyaluronic Acid Regulation in Mammalian Development

HA is synthesized by three hyaluronic acid synthase genes, *HAS-1*, *HAS-2* and *HAS-3* [107], and it is degraded by six different genes; however, only *HYAL-1* and *HYAL-2* are believed to be the primary functional hyaluronidases of mammalian somatic cells [26]. While HYAL-1 is a secreted protein and breaks down HA to a tetrasaccharide [83], HYAL-2 exists as a cell anchored protein and degrades HA to 20 kDa fragments [83, 137]. HAS-2 is believed to be the primary synthesizer of hyaluronic acid during embryonic development, synthesizing HA chains between $2x10^5$ – $2x10^6$ Da. Murine embryos lacking the *Has-2* gene possess only 3% of the normal embryo HA content, exhibit growth retardation evident by embryonic day 9, and die by day 9.5 [107]. Furthermore, exogenous HA has been shown to improve the development of *in vitro* produced bovine embryos and porcine parthenogenic embryos [44, 180]. This evidence suggests a vital role for HA during mammalian development.

Since the *Has-2* null mouse dies before the beginning of metanephric kidney development (which does not begin until day E10.5 in the mouse), it is unknown whether HA is also vital for kidney development and renal organogenesis. However, HA has been

implicated in the branching morphogenesis of a UB cell line and was found to be expressed along with its receptor, CD44, along the basal surface of the branching UB [134]. Additionally, HA was found to be ubiquitously present throughout the developing rat kidney until well after birth, at which point HA localizes to the renal interstitium of the inner medulla [166]. While HA and its receptors are known to be present in the developing kidney, the role of HA in kidney development is still unclear. Additionally, given that HA action depends heavily on HA size, it may be possible that HA plays multiple or even opposing roles in kidney development as it does in other tissues. If HA is to be used as a tool for engineering kidney tissues, then one must understand the effects of the larger sizes of HA as well as the potential degradation products (smaller sizes).

1.6 Hyaluronic Acid in Tissue Engineering

Many of the biological and physical properties of HA (described above) make the molecule an attractive candidate for use in tissue engineering. HA is a polysaccharide synthesized by a single protein without postsynthesis modifications. Additionally, the structure of HA is the same in bacteria as it is in humans. The lack of necessary modification and the ability of bacteria to produce HA make mass production of HA polymers a relatively simple and cheap process. Because HA is a molecule that is naturally present in the body, it is non-antigenic, non-immunogenic, biocompatible and naturally degraded in the body [138, 139]. HA contains many functional groups that allow the molecule to be manipulated and crosslinked to create hydrogels that can be used as scaffolds for cell and tissue growth. Additionally, the natural role of HA as an extracellular matrix component and as a space-filler means that HA should be compatible

with a large variety of different cell and tissue types. One common issue with engineering new tissues is achieving vascularization, but HA may be able to act as both a scaffold and as a source of small HA fragments that promote angiogenesis [28, 181].

Hyaluronic acid has already been demonstrated to be a safe and clinically applicable biomaterial when used as an injectible gel to replace endogenous HA lost over time or due to injury (both in joints and in skin). Injectible HA gels are currently being used clinically for viscosupplementation of osteoarthritic joints [9, 13]. HA is an essential component of the skin extracellular matrix responsible for volume and suppleness, but HA concentration in the skin decreases as humans age [46, 108]. Therefore, injectible HA gels are being used as dermatological fillers and as a treatment for wrinkles [91, 92, 111].

1.6.1 Hyaluronic Acid-based Hydrogels

For a biomaterial to be used as a scaffold for tissue engineering, it must be able to keep cells or tissues suspended in a 3D volume. Because of its hydroxyl and carboxylic acid groups, HA molecules can be modified to contain desired functional groups and can be easily crosslinked to form a scaffold that, due to its hydrophilic properties, retains water (hydrogel). HA has been crosslinked by a variety of methods including water-soluble carbodiimide crosslinking [179], polyvalent hydrazide crosslinking (via carbodiimide crosslinking) [186], divinyl sulfone crosslinking [10, 79], disulfide crosslinking [89], and photocrosslinking through glycidyl methacrylate–HA conjugates [17] (Fig. 1.9).

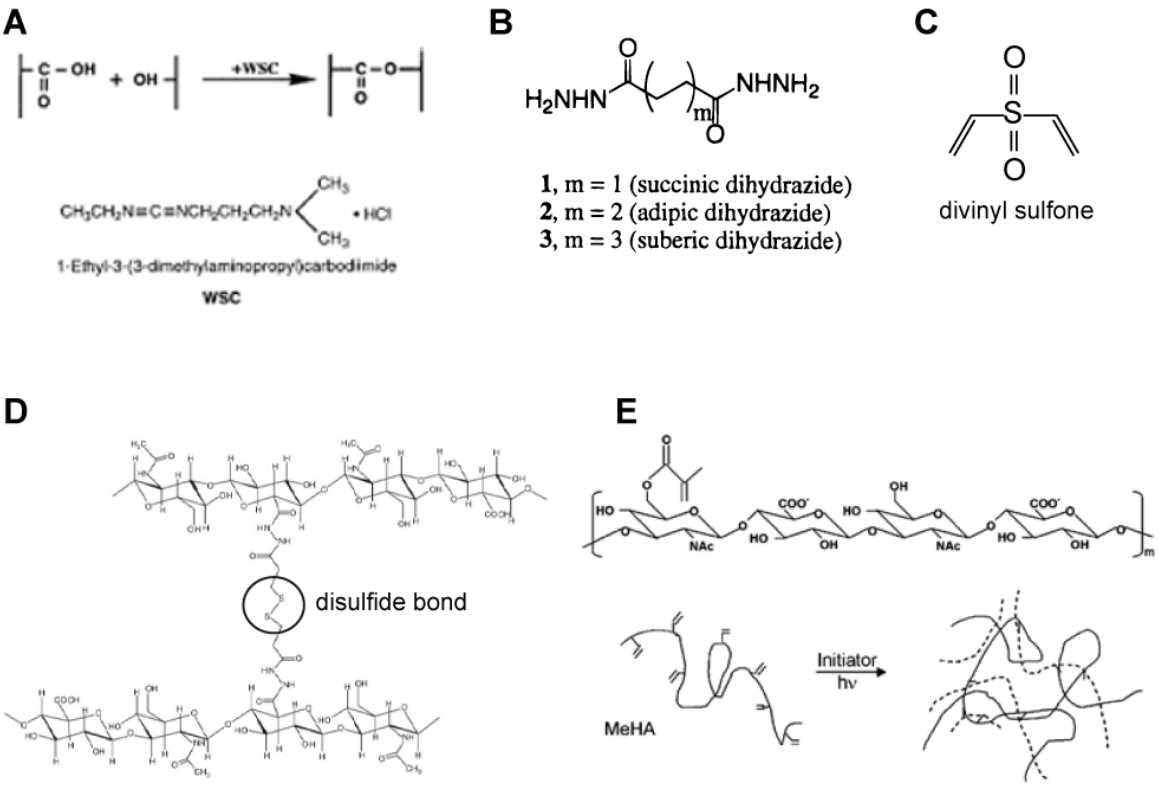

Fig. 1.9: Hyaluronic acid crosslinking methods. Water-soluble carbodiimide (WSC) can be used as a catalyst to directly crosslink HA molecules to each other (adapted from [179]) (A) or to crosslink amide groups of dihydrazide molecules (B) to carboxylic acid groups of HA (adapted from [186]). Vinyl groups of divinyl sulfone (C) can react with the hydroxyl groups of HA to form crosslinked gels. HA can be modified to have terminal thiol groups that will form disulfide bonds (adapted from [89]) (D). Exposure of an initiator to light leads to the formation of radicals that propagate through the vinyl groups of the methacrylated HA (MeHA) to form kinetic chains (shown as dashed lines) (adapted from [17]) (E).

Only some of these crosslinking methods have been demonstrated safe for suspending cells. Both divinyl sulfone crosslinking and methacrylate-based photolymerization have been used to retain chondrocytes in polyethylene glycol-based hydrogels without significant cell death [86, 129]. Park *et al.,* suspended primary bovine calf chondrocytes in a solution of branched polytheylene glycol (PEG) modified with vinyl sulfone terminal groups. A crosslinker containing two thiol end groups (that are

reactive with the vinyl sulfone end groups of the modified PEG) was added to the solution resulting in crosslinking of the PEG-based hydrogel. The encapsulated chondrocytes were still viable after 1 month of culture [129]. Lin Gibson *et al.,* modified PEG to contain methacrylate end groups similar to HA in Figure 1.6E. The methacrylated PEG solution was exposed to 365 nm wavelength light causing the methacrylate groups to crosslink, thus encapsulating the cells. After 2 weeks, nearly all suspended cells were determined to be viable [86].

One of the aims of this thesis is to grow kidney-like tissues in a 3D culture environment. While crosslinked hydrogels support the growth and differentiation of cells, larger tissues may have additional scaffold requirements for growth and differentiation. Cells can proliferate and migrate through the pores of a scaffold to occupy the entire volume of that scaffold, but larger tissues cannot be constrained to grow through these pores. Larger tissues must be able to remodel the scaffolds to make room for new growth. One potential solution to this problem is the concept of matrix-metalloprotease (MMP) sensitive crosslinked hydrogels. Lutolf *et al.,* have developed polyethyleneglycol-based scaffolds containing a protease-sensitive peptide sequence as a crosslinker molecule, which allows for the scaffold to be degraded and remodeled by the cells suspended within the scaffold [93, 129, 162]. This technique was utilized by Park *et al.,* as described above for culturing bovine primary calf chondrocytes. The limitation of the technique designed by Lutolf *et al.,* is that it is designed particularly for polyethylene glycol and cannot be used in conjunction with other polymers such as HA. Because of the evidence provided on the role of HA in kidney development, part of this thesis aims to investigate a method of synthesizing a MMP-sensitive crosslinker that could be used to crosslink many

polymers including HA; although, the quality control and application is beyond the scope.

1.7 Scope of the Dissertation

Current strategies for therapies to treat ESRD all have limitations of either lack of complete renal function, overwhelming technical hurdles, or the need for immunosupression. The objective of this dissertation is to investigate the hypothesis that an *in vitro* developmental approach to engineering kidney tissues is both feasible and has the potential to address the limitations of the alternative strategies offering the advantages of 1) potentially beginning with only two cell types, 2) requiring the construction of relatively small and simple embryonic tissues, thereby requiring a small number of cells, 3) offering multiple potential points of cell or tissue propagation, and 4) resulting in a kidney tissue with a 3D structure known to be important for renal function. Furthermore, this work aims to investigate the hypothesis that hyaluronic acid is involved in guiding renal organogenesis and that this role can be utilized in the process of engineering 3D kidney tissues. This dissertation is divided in to four experimental chapters with each chapter presented in a manuscript format.

Chapter 2 investigates whether *in vitro* culture systems could be used to sequentially recapitulate the stages of kidney development beginning with the renal progenitor tissues, Wolffian duct and metanephric mesenchyme. Culture conditions for each step of *in vitro* development are described using optimization studies. The resulting kidney-like tissue is analyzed for gene expression, functional transport, and the ability to attain a vasculature when implanted into a host animal.

In Chapter 3, the potential to create renal progenitor tissues from two homogenous cell sources are used to investigate the hypothesis that the metanephric embryonic kidney can be modeled as a tissue composed of only two homogenous cell types. Additionally, it is hypothesized that embryonic kidneys can be cultured in an *in vitro* 3D environment to achieve more "anatomically correct" 3D kidney growth and collecting duct formation. The ability of various extracellular matrix molecules to support *in vitro* 3D embryonic kidney growth is investigated.

In Chapter 4, the role of hyaluronic acid, a biocompatible and endogenous extracellular matrix molecule, modulating renal organogenesis is investigated using *in vitro* kidney culture techniques. Both hyaluronic acid size and concentration were varied to examine potential differences in effect on kidney growth and differentiation.

A method of crosslinking polymers with free hydroxyl groups, such as hyaluronic acid, is explored in Chapter 5. The synthesis of a MMP-sensitive peptide sequence with functional vinyl sulfone ends is described.

The final chapter of this dissertation summarizes all the work performed for this thesis and elaborates on how the knowledge and techniques developed in this thesis represent potential tools to be utilized in developing an ESRD kidney replacement therapy.

CHAPTER 2:

Staged *In Vitro* Reconstitution and Implantation of Engineered Rat Kidney Tissue

2.1 Abstract

A major hurdle for current xenogenic-based and other approaches aimed at engineering kidney tissues is reproducing the complex three dimensional structure of the kidney. Here a stepwise, *in vitro* method of engineering rat kidney-like tissue capable of being implanted is described. Based on the fact that the stages of kidney development are separable into *in vitro* modules, an approach was devised which sequentially induces an epithelial tubule (the Wolffian duct) to undergo *in vitro* budding, followed by branching of a single isolated bud, and its recombination with metanephric mesenchyme. Implantation of the recombined tissue results in apparent early vascularization. Thus, in principle, an unbranched epithelial tubular structure (potentially constructed from cultured cells) can be induced to form kidney tissue such that this *in vitro* engineered tissue is capable of being implanted in host rats, and developing glomeruli with evidence of early vascularization. Optimization studies (of growth factor and matrix) indicate multiple suitable combinations and suggest both a most robust and a minimal system. A whole genome microarray analysis suggested that recombined tissue recapitulated gene

expression changes that occur *in vivo* during later stages of kidney development, and a functional assay demonstrated that the recombined tissue was capable of transport characteristic of the differentiating nephron. The approach includes several points where tissue can be propagated. The data also shows how functional, three dimensional kidney tissue can assemble via interactions of independent modules separable *in vitro*, potentially facilitating systems level analyses of kidney development.

2.2 Introduction

Given the prevalence of chronic kidney disease and the shortage of donor organs [1], a variety of tissue engineering strategies are being pursued. For example, the extracorporeal renal tubule assist device utilizes a synthetic hemofilter connected in series with a bioreactor cartridge containing human proximal tubule cells [59]. In addition, renal primordia obtained at a sufficiently early developmental stage have been demonstrated to undergo differentiation and grow when transplanted into animal hosts [4, 31, 63, 142, 155, 156]. *In vitro* propagation of the branching ureteric bud or subdivided progenitor tissue has been proposed as a method for generating a number of kidneys from a single progenitor tissue [168]. Cellular components and scaffolding have been combined in order to create cell-based filtering devices and nephron components [78, 187]. Additional cell-based strategies have included the use of adult renal stem-like cells [19, 32, 50, 54, 65, 71, 98, 100, 127, 149]. Certain populations of these cells are capable of forming tubules in culture and migrating to developing tubules in organ culture [98]. Injection of stem-like cells into diseased kidneys may promote healing [54, 73, 87, 149]. However, engineering a kidney-like tissue from cells with appropriate three dimensional (3D) spatial relationships of nephrons has yet to be achieved [169].

Here we have devised a method that (based upon the stages of metanephric kidney development [112, 153]) utilizes elements of kidney primordia, the Wolffian duct (WD) and metanephric mesenchyme (MM), to engineer *in vitro* kidney-like tissue containing functional tubular transporters and glomeruli with apparent early vascularization. Moreover, this *in vitro* stepwise approach provides not only the potential

for propagation at several levels, but also the potential for introduction of immunomodulatory or other genes. Perhaps most importantly, if a tubular structure can be formed from adult, amniotic, embryonic stem cells, or other cell types, this approach provides a potential strategy for engineering a 3D vascularized kidney-like tissue from cells *in vitro*.

2.3 Results

2.3.1 WD Budding

The initiating event in metanephric kidney development is the outgrowth of the ureteric bud (UB) from the WD [159]. Using three separate culture systems, this developmental event was replicated *in vitro* (Fig. 2.1, Table 2.1). First, the whole mesonephros was isolated and cultured in the presence of 10 ng/mL glial-cell derived neurotrophic factor (GDNF) as described previously [99]. After threee days in culture, numerous budding events occurred at multiple foci along the WD (Fig. 2.1A and B). In the second method, the mesonephric tubules, along with most of the non-epithelial mesoderm, were removed from the WD prior to *in vitro* culture. Although the GDNF concentration had to be increased from ~10 ng/mL to ~125 ng/mL and an additional soluble growth factor was required (either fibroblast growth factor-1 (FGF1), ~250 ng/mL, or fibroblast growth factor-7 (FGF7), ~50 ng/mL), similar impressive budding of multiple UB-like structures was observed (Fig. 2.1C and D). In the third method, the WD was cleared of all surrounding mesoderm prior to *in vitro* culture, leaving essentially a "naked" epithelial tube. In this "minimal" system, the WD was able to bud in the

presence of soluble growth factors only when suspended in a 3D extracellular matrix gel (Fig. 2.1E and F). Under all three culture conditions, while the overall surface area of the WD increases due to budding at multiple foci, the WD did not appear to lengthen significantly.

2.3.2 Isolated *In Vitro*-formed UB Branching

Following its emergence from the WD, the UB penetrates the MM where it is induced to undergo extensive branching morphogenesis leading to the formation of the renal collecting system. Previously we have shown that embryonic rat isolated UBs suspended in an extracellular matrix gel undergo robust branching in the presence of GDNF and a conditioned medium (CM) secreted by a MM-derived cell line (BSN-cells) [136]. Here, we demonstrated that a single isolated bud induced from a WD as described above (an *in vitro*-formed UB) retains the ability to branch in 3D culture (Fig. 2.2) using conditions similar to those described for the "T-shaped" UB dissected from E13 rat kidneys [136]. Thus, *in vitro*-formed UBs, while not achieving a characteristic T-shaped structure assumed to be necessary for normal development of the kidney based on knockout studies [16, 112, 120], can grow and branch *in vitro* in a fashion similar to the excised T-shaped bud. This suggests that the T-shaped bud stage can be bypassed in our developmental strategy for tissue engineering.

2.3.3 Extracellular Matrix Requirements for Isolated 3-D UB Culture

Given that the extracellular matrix plays a significant role as a scaffold for isolated UB growth and branching as well as modulation of growth factor effects, we

attempted to optimize the growth conditions for 3D UB branching. While previous studies of isolated UB branching utilized a matrix of "growth factor-reduced" Matrigel and type I collagen (50:50 v/v) [136], we found that type I collagen alone did not support branching morphogenesis and was, in fact, inhibitory, while Matrigel supported branching, although diminished branching was observed at extreme concentrations (Table 1). In addition to these two original components, a 1% alginate solution, crosslinked with 100 mM $CaCl_2$, and Puramatrix, an inert self assembling peptide matrix, were also tested in the isolated UB system; neither supported UB branching (Table 2.2). Pure type IV collagen (the network forming component of Matrigel is type IV collagen [72]) also supported UB branching while additional basement membrane components such as laminin I had little apparent effect on branching (Table 2.3). However, UBs cultured in type IV collagen did not grow as well as those in Matrigel (data not shown), possibly because Matrigel contains a concentration of type IV collagen (~3.3 mg/mL) [72], more than triple that of the pure type IV collagen commercially available (~1 mg/mL).

Taken together with our previous studies [18, 109, 136, 151, 152], a minimal set of conditions can be defined for UB growth/branching as pleiotrophin (PTN) plus GDNF [151] in a type IV collagen matrix. The most robust system for both tip and stalk formation, as well as growth, of the *in vivo* isolated bud, however, appears to be BSN-CM supplemented with GDNF and FGF1 [18, 135] in a 50% Matrigel solution, which were the culture conditions employed for the *in vitro*-formed UB described below.

2.3.4 *In Vitro*-formed UB and MM Recombination

Once the WD has formed buds *in vitro* and the dissected *in vitro*-formed UB had branched, we sought to determine whether 3D nephron formation would occur; our approach was to recombine the branched structure with fresh MM. These experiments differ from previous studies [136] in that the branched UB was derived from an *in vitro* budded WD (that does not form a T-shaped structure, considered a key developmental stage [16, 112, 120]). The recombined tissue was cultured on a Transwell filter without additional growth factors (Fig. 2.3B). Several days after recombination, branched structures had grown and elongated (Fig. 2.3E), and induction was evident by both phase contrast and fluorescent lectin staining (Fig. 2.3C-F). Connections between the collecting system and the more proximal portions of the tubule derived from the MM were evident (Fig. 2.3F).

Recombinations between MM and the branched *in vitro*-formed UB, the branched isolated T-shaped UB, or the induced WD (containing multiple non-branched *in vitro*-formed UBs) were highly similar; conceivably, any of these recombination systems could be used to engineer kidney-like tissue. For convenience, many subsequent experiments were carried out in the latter two systems.

While the recombined tissues were comprised of nephron structures resembling late stages of renal development, it was important to verify that the induced MM was not only undergoing mesenchymal to epithelial transformation (MET), but also that the MM-derived tubules were expressing functional transporters. 6-Carboxyfluorescein (6-CF) is a fluorescent organic anion taken up by specific tubular transporters[‖]. When the recombined tissue (branched T-shaped UB and MM) was incubated with 6-CF, cellular

uptake was observed in the cells of mesenchymally-derived tubules, suggesting both differentiation and function of the MM-derived nascent proximal tubules (Fig. 2.4A and B). This uptake was blocked by 2mM probenecid, an organic anion transport competitive inhibitor [173] (Fig. 2.4C).

In addition to demonstrating the functional capacity of the recombined tissues, the global gene expression of recombined tissue (non-branched *in vitro*-formed UBs and MM) was analyzed and compared to the gene expression of early, late, and post developmental kidneys in order to determine whether normal developmental pathways were being followed. Briefly, genes with at least a 3-fold difference in expression between any of the 4 conditions (E13, E18, Wk4, recombined tissue) were analyzed and grouped into one of ten expression patterns (Fig. 2.5). The expression of each group of genes was analyzed in the recombined tissue to compare the recombined tissue gene expression levels to the three *in vivo* time points (Table 2.4). The comparison suggested that developmental pathways are similarly modulated/regulated in tissue engineered from *in vitro* induced WD recombined for four days with fresh MM. Almost 50% of the genes that were up-regulated at E18 *in vivo* were up-regulated in the recombined tissue. In addition, 72% of the down-regulated genes also down-regulated in the recombined tissue to at least E18 levels. Nevertheless, there were a few genes expressed at much higher or lower levels in the recombined tissue that did not change in the stages compared; these genes represented less than 5% of the total number of genes in the analysis.

2.3.5 Implantation and Apparent Vascularization of the Recombined Kidney-like Tissue

In order for a kidney tissue to be functional *in vivo* it must contain a vasculature and glomeruli. While the microarray analysis demonstrated that the recombined tissue recapitulates many of the gene expression patterns of renal development, few vascular genes were up-regulated. However, this does not predict whether the recombined tissue will be able to successfully integrate into a host animal. Previous studies have demonstrated that early avascular embryonic kidneys can be implanted into a host animal to recruit a vasculature with functional glomeruli [4, 31, 63, 142, 155, 156]. Therefore, we implanted the recombined kidney-like tissue (from a recombination of branched T-shaped UB and MM) under the renal capsule of a host rat. After 14 days, the host animal was sacrificed and the implanted tissue was analyzed (Fig. 2.6). The implanted recombined tissue had multiple glomeruli and expressed the endothelial marker PECAM-1 in the cells of the glomerulus (Fig. 2.6D). Erythrocytes could be seen in the glomeruli of the recombined tissue, suggesting blood flow to the implanted tissue (Fig. 2.6C, arrows). The long term viability and *in vivo* functionality, as well as the optimal location and procedure for implantation, remains to be determined.

2.4 Discussion

We present a strategy for tissue engineering a propagatable kidney-like tissue by following key kidney developmental events *in vitro* in a stepwise fashion beginning with a WD. We describe the optimization and elaborate on a variety of conditions that can be used at several *in vitro* steps, potentially offering multiple approaches and points of

propagation within this strategy. The strategy results in tissues with nephrons, glomeruli and an apparent early vasculature in three dimensions. Figure 2.7 illustrates how these systems can be assembled in order to create *in vitro* engineered renal structures from the initial components.

Our optimization studies revealed that the WD requires only the presence of GDNF for budding if the whole mesonephros is cultured *in vitro*, but requires additional growth factors like FGF-1 or FGF-7 if the mesonephric tubules and surrounding mesoderm are removed (Fig. 2.1). The recent detection of a GDNF bypass pathway, however, raises the possibility that even GDNF may not be essential for this step [97]. Furthermore, a suspended culture system using a diluted Matrigel solution, in addition to the soluble growth factors, is required for the WD devoid of surrounding mesoderm to undergo *in vitro* budding. These experiments suggest that the surrounding mesoderm plays a key role in budding by providing growth factors and/or necessary matrix components, which for tissue engineering purposes, we supply exogenously. Moreover, each of the many buds can be excised, suspended in a 3D matrix, and induced to undergo extensive branching morphogenesis. The branched *in vitro*-formed UB appears highly similar to the *ex vivo* isolated T-shaped UB grown in culture [136]. Since a single focus of budding yields a kidney *in vivo*, if each of the multiple buds were cultured individually, then many kidney-like tissues could potentially arise from a single WD cultured *in vitro*.

Branching growth was optimized for the T-shaped UB; optimal branching and growth occurred when we combined FGF-1, a growth factor that supports branching and growth of the isolated UB culture system, with non-FGF branch-promoting growth factor

combinations (i.e. GDNF plus either PTN or BSN-CM). *In vitro*, these growth factor conditions provided the most robust branch-stimulating conditions (i.e. growth plus most *in vivo*-like patterning) among the many soluble factor combinations that we have tested [18, 109, 135, 151, 152]. The fact that a combination of BSN-CM, FGF-1, and GDNF gave more consistent branching growth than PTN, FGF-1 and GDNF, suggests one or more factors within BSN-CM will need to be isolated to achieve ideal "minimal" conditions. Conceivably these could include factors such as TGFβ-superfamily members, including bone morphogenetic proteins 2 and 4 and activin, which can modulate branching and are involved in sculpting of the isolated UB culture system [18]. Thus, it is possible that a combination of PTN plus one additional "UB-sculpting factor" could replace BSN-CM to attain an ideal minimal set of conditions for a tissue engineering approach. Until such conditions are discovered, data indicate that the combination of BSN-CM, FGF-1, and GDNF supports the most robust growth and branching of the UB *in vitro*.

Given the recent work on matrices and scaffolds for tissue engineering of bone, cartilage and other organs (reviewed in [67, 94]), both artificial and natural matrix conditions were analyzed for isolated 3D UB branching. Our data suggest that *in vitro* isolated UB branching morphogenesis is largely dependent upon type IV collagen and does not require additional matrix components (the UB only branched in type IV collagen or type IV collagen-based Matrigel), although one can not rule out the possibility that the growth of the UB is affected by other Matrigel components. Surprisingly, adding laminin I, which enhances branching of cultured cells [154], to a type IV collagen matrix did not appreciably increase branching morphogenesis (Table 2.3). This suggests that the initial

extracellular matrix scaffold does not require all components of the final basement membrane and that the UB itself might synthesize any necessary supplementary proteins in an isolated system. In addition, two inert ECM molecules, alginate, which has been used extensively in cartilage tissue engineering [23, 56, 102], and Puramatrix, which was successfully used to support neuronal migration [163] as well as to promote osteoblast differentiation [45], did not support UB branching. This may be due to the inability of the UB to remodel the artificial matrix to allow room for new branches. Nevertheless, an "ideal minimal system" for tissue engineering of the kidney according to our scheme ought to continue consideration of other artificial matrices as they become available.

The branched *in vitro*-formed UB (derived from the WD) when placed adjacent to freshly isolated MM, caused a mesenchymal-to-epithelial transformation and tubule formation (as well as connections to nascent collecting ducts) resulting in nephron-containing tissues. This indicates that the *in vitro*-formed UB, after being induced to branch *in vitro*, retains the capability to form kidney-like tissues.

The recombined tissue was found to form nephron structures that not only phenotypically appeared normal, but also resembled the transcriptome of the developing E18 rat kidney. Recombined tissue was also demonstrated to be functionally capable of organic anion transport (Fig. 2.4). The probenecid-inhibitable transport of the fluorescent organic anion, 6-CF, was only observed in cells of MM-derived structures that appear to be nascent proximal tubules.

For the recombination step we utilized fresh MM tissue reported to contain pluripotent renal progenitor cells [127]. It may be most ideal, however, to begin with cells alone. We have demonstrated here the ability of secreted products from the BSN

cell line (derived from MM) to induce optimal branching of the *in vitro*-formed UB, but thus far have been unable to show that the cells themselves will recombine to form nephron-containing structures (data not shown). This may require a matrix-based strategy to make cells cohere or, alternatively, it is possible that BSN cells are too differentiated (perhaps more like mesenchymal "cap" cells) to be used for this application. Recently, it has been reported that mouse ES cells can be induced to form MM-like cells, suggesting an alternative approach [69].

Similar considerations apply to the creation of an epithelial tubule like the WD from cells. Of note, it has been shown that the UB cell line can form tubules under conditions somewhat similar to those we have shown as optimal for branching of the isolated UB [150]. It has also been shown that adult "progenitor-like" cells from the injured mouse kidney can form tubular epithelial structures *in vitro* and migrate to multiple compartments of the developing kidney in organ culture [98]. These types of cells, or possibly others which have recently been described [20, 27, 78], may be more suitable.

In addition to using WD-like or MM-like tissues potentially constructed from cells, the methods we describe may be suitable for xeno-based approaches. Given the fact that they are tissue/organ culture-based, and that there are at least two points for propagation (at the level of the *in vitro* cultured WD and at the level of the *in vitro*-formed UB), it may be possible to "humanize" the tissue through transfection or similar strategies, or to induce expression of immunomodulatory or other genes to diminish the possibility of rejection and, potentially, improve functionality. These techniques, not currently feasible in mammalian adult organs, could provide considerable flexibility for

the goal of creating immunocompatible tissues suitable for a particular genetic profile. Beginning with a single or limited *in vitro* propagatable tissue may also help address the concern about animal viruses with xeno-based approaches by creating a single or limited set of key points in a tissue engineering strategy where intense quality control or surveillance can be applied. Embryonic-derived tissues seem to elicit a reduced immune response in rodents [31, 142]; therefore, *in vitro* manipulation of xeno-tissues or primitive cells to engineer kidney-like tissue may result in a less antigenic transplant than alternative options.

The recombined tissue seems to recruit an early vasculature, forming glomeruli that appropriately express a key endothelial marker when implanted underneath the renal capsule of a host animal, although, *in vivo* functionality remains to be determined. Whether this technique will be successful as a therapy for chronic kidney disease is unknown, but it provides "proof of concept" that an *in vitro* engineered kidney-like tissue, designed in the manner we describe, can survive over the short term and begin to recruit a vasculature when placed in a host animal. Sites other than the renal capsule may prove as, or even more, hospitable for recombined tissue [142].

Each step of this tissue engineering procedure reflects one or more independent stages of kidney development. Therefore, in addition to being an important tool for engineering implantable kidney-like tissues, this method further demonstrates that developing kidneys consist of a number of separable but reconstitutable modules [18, 112, 153, 172]. This approach may be useful for future systems biology work on nephrogenesis [112, 153]. Early vascularization of the recombined tissue appears to occur distinct from the morphogenetic processes of budding, branching and MET.

While many approaches are being taken towards engineering kidney substitutes, we suggest that a kidney-like tissue formed by following the normal developmental progression will likely recapitulate the three dimensional relationships necessary to maintain vital renal functions. Here, we have provided the guidelines for such a strategy, in rodents, to stimulate renal progenitor tissues to follow the natural developmental program resulting in an *in vitro* engineered kidney-like tissue containing a branched collecting duct system, nephrons with functional transporters, glomeruli and an apparent vasculature. That the strategy has strong potential for propagation of the engineered kidney-like tissue, as well as modulation of functionality and immunogenicity by transfection-type methods, adds to its possible utility.

2.5 Methods

2.5.1 Materials

All growth factors are from R&D Systems (Minneapolis, MN) and all other reagents are from Sigma (St. Louis, MO) unless otherwise noted.

2.5.2 Budding of WD

The urogenital tract was isolated from timed pregnant Holtzman rats (Harlan, Indianapolis, Indiana) at embryonic day 13 (E13) and WDs were dissected free of surrounding tissue [99]. The mesonephric tubules and most of the surrounding intermediate mesoderm were mechanically separated from the WD or, in some cases, the remaining intermediate mesoderm was carefully stripped away leaving only the WD. Tissues were placed on 0.4 μm Transwell filters (Costar, Cambridge, MA) and cultured

at the air-media interface (except the WD devoid of intermediate mesoderm, which was suspended in a 3D extracellular matrix of growth factor-reduced Matrigel (Becton Dickenson, Franklin Lakes, NJ) and DMEM/F12 (50:50 v/v) (GIBCO-BRL, Grand Island, NY) on a Transwell filter. DMEM/F12 media supplemented with 10% FCS (Biowhittaker, East Rutherford, NJ), 1% antibiotics and growth factors at the noted concentrations were placed in the well beneath the filter. All cultures were carried out at 37º C in a humidified 5% CO2 atmosphere unless otherwise noted and all cultures were performed at least three independent times.

2.5.3 Isolation and 3D Branching of *In Vitro*-formed UBs

Budded WDs were removed from the filter, lightly digested with trypsin (2 mg/mL trypsin in L-15 for 5 min. at 37°), and the buds were separated from the WD and surrounding attached cells using microsurgery forceps. Microdissected *in vitro*-formed buds were suspended in a matrix of growth factor-reduced Matrigel and DMEM/F12 (50:50 v/v) on a Transwell filter and cultured in the presence of BSN-conditioned media (prepared as described previously [136]), supplemented with 10% FCS, 1% antibiotics, GDNF (125 ng/ml), and FGF1 (250 ng/ml).

2.5.4 Optimization of Extracellular Matrix (Natural and Artificial) Conditions for Isolated UB Branching

E13 UBs and MM were isolated from rat kidney rudiments as previously described [18, 136, 151, 152]. UBs were cultured in the presence of BSN-CM supplemented with 10% FCS, GDNF (125 ng/ml), FGF1 (250 ng/ml), and 1% antibiotics.

UBs were suspended in matrices (natural and artificial) consisting of growth factor-reduced Matrigel diluted with DMEM/F12, type I collagen, Puramatrix, 1% alginate solution (crosslinked with 100 mM $CaCl_2$), and type IV collagen at noted concentrations and combinations. All matrix solutions were supplemented with DMEM and buffered by HEPES and $NaHCO_3$ to a pH of approximately 7.2.

2.5.5 Recombination of *In Vitro*-formed UBs and T-shaped UBs with MM

After 4-6 days the branched *in vitro*-formed UBs or branched T-shaped UBs were separated from the surrounding matrix by blunt dissection. Branched buds with minimal matrix were placed on a new Transwell filter and cultured with DMEM/F12 (50:50) supplemented with 10% FCS. MM from E13 kidneys was placed next to and on the branched UB (Alternatively, the non-branched, non-isolated *in vitro*-formed UBs were directly recombined with MM). After 4-7 days of culture, the recombined kidney-like tissues were fixed in 4% parafomaldehyde, extensively washed in PBS and processed for fluorescent lectin staining.

2.5.6 Fluorescent Lectin Staining

Samples were fixed with 2% paraformaldehyde for 30 min at 4°C, blocked with 50 mM NH_4Cl overnight at 4°C, and incubated with 1% gelatin in 0.075% Saponin for 30 min at 37°C. After two washes with Neuraminidase buffer (150 mM NaCl, 50 mM sodium acetate, pH 5.5), tissues were incubated with Neuraminidase (1 unit/ml) for 4 hr at 37°C and then with rhodamine-conjugated PNA (50 μg/ml) and FITC-conjugated DB

(50 µg/ml) for 60 min at 37°C. Samples were postfixed with 2% paraformaldehyde and viewed with a laser-scanning confocal microscope.

2.5.7 Microarray Analysis

The E13 kidney, E18 kidney, adult kidney, and recombined kidney-like tissues (from a recombination of non-branched *in vitro*-formed UB and MM) were dissolved in lysis buffer and the RNA was isolated using the RNAqueous Micro kit from Ambion (Austin, TX). RNA was submitted to the UCSD Genechip core facility for processing with the Affymetrix (Santa Clara, CA) rat 230 2.0 whole genome chip. *In vivo* time points were analyzed in biological triplicates, while the recombined tissues were analyzed in biological duplicates. All gene expression analysis was performed using Agilent (Santa Clara, CA) Genespring GX 7.3 software.

2.5.8 Functional Organic Anion Transport Assay

Recombined tissues (branched T-shaped UB - MM) on culture day 7 were assayed as described previously [173], with 1 µM 6-carboxyfluorescein (6-CF) (Sigma, St. Louis, MO) in place of fluorescein. Briefly, recombined tissues were left on the transwell filter and washed twice with PBS followed by incubation in a minimal saline solution (PBS, 0.1 mM $CaCl_2$, 1 mM $MgCl_2$) with 1µM 6-carboxyfluorescein (6-CF) (Sigma, St. Louis, MO), 20 µg/mL TRITC-conjugated DB, and in the presence or absence of the organic anion transport (OAT) inhibitor, 2 mM probenecid, for 1 hour at 25°C. Following the incubation, the tissues were washed 3 times with 4°C PBS, mounted

on a glass slide with Fluoromount G (Electron Microscopy Sciences, Hatfield, PA) and immediately imaged on the Nikon EZC1 confocal microscope system.

2.5.9 Implantation of Recombined Kidney-like Tissue

Recombined tissues (branched T-shaped UB - MM) on culture day 6 were detached from the Transwell filter, and suspended in cold L-15 medium. The abdominal cavity of an adult male rat was opened under inhalant anesthesia with isoflurane. A subcapsular tunnel was prepared on the right kidney using the tip of microsurgery forceps. 2-6 recombined tissues were inserted into the subcapsular region together with a small volume of L-15 medium (~40 μl) by micropipette. The abdominal cavity was closed by suturing muscle and skin layers. After 14 days, the kidneys with implants were excised and provided for histological analyses (described in detail in the online supplementary information).

2.5.10 Histological Analyses

Host kidneys bearing implants were excised, fixed in 4% paraformaldehyde/0.1M PBS, pH 7.4 for 24 hr at 4ºC, and incubated in graded concentrations of sucrose solutions (10%, 15%, and 20%). Samples were embedded in Tissue Tek O.C.T. compound (Sakura Finetek, Torrance, CA), and frozen rapidly in liquid nitrogen. 4 μm sections were cut and stained with anti-rat PECAM-1 (CD31) antibody (1:100; clone TLD-3A12, mouse IgG1k, Pharmingen) and anti-collagen type IV antibody (1:100; rabbit polyclonal, Chemicon) at 4ºC overnight. After washing in PBS, samples were then reacted with donkey anti-mouse IgG-Alexa Fluor 488, goat anti-rabbit IgG-Alexa Fluor 568, and 4’,6-

diamidino-2-phenylindole dihydrochloride (DAPI) (all from Molecular Probes (Eugene, OR)) at room temperature for 1 hr. Specimens were observed with a Nikon D-Eclipse C1 confocal microscope. Some cryosections were processed for routine histology using hematoxylin and eosin staining, and observed with a Nikon Eclipse TE300 light microscope.

2.6 Footnotes

‖This work performed by David Truong is currently unpublished

2.7 Acknowledgments

This work was supported by NIH grants DK057286, DK065831and HL035018 (to S.K.N.) and AHA grant 0330182 (to H.S.). E.R. was supported by the NSF graduate research fellowship. We also acknowledge Kevin Bush, David Truong, Thomas Gallegos, Derina Sweeney, and Ankur Dnyanmote for their critical reading of this manuscript.

This chapter, in full, is a reprint of the material as it appears in "Staged *in vitro* reconstitution and implantation of engineered rat kidney tissue" by Rosines E., Sampogna R.V., Johkura K., Vaughn D.A., Choi Y., Sakurai H., Shah M.M., Nigam S.K. in Proceedings of the National Academy of Sciences, 2007. 104(52): p. 20938-43. Reprinted with permission from the Proceedings of the National Academy of Sciences USA. Table 2.1, Table 2.4, and Figure 2.5 appeared in the online supplementary information. The dissertation author was the primary investigator and author of this paper.

Table 2.1: Wolffian duct budding conditions

WD condition	Factors Promoting Budding
Whole Mesonephros	▪ 2D filter culture, 10 ng/ml GDNF
WD + intermediate mesoderm	• 2D filter culture, 125 ng/ml GDNF + 50 ng/ml FGF7 • 2D filter culture, 125 ng/ml GDNF + 250 ng/ml FGF1
WD (devoid of intermediate mesoderm)	• 3D-matrix (Matrigel), 125ng/ml GDNF + 50 ng/ml FGF7 • 3D-matrix (Matrigel), 125 ng/ml GDNF + 250 ng/ml FGF1

Table 2.2: Extracellular matrix effects on ureteric bud branching, network-forming matrices

Matrices	**Branching Effect**
Matrigel (15 - 100%)	Supports
Type IV Coll. (0.75 mg/mL)	Supports
Type I Coll. (0.4 - 4.0 mg/mL)	Does not support
Alginate (0.3 - 1.5%)	Does not support
Puramatrix (50 - 100%)	Does not support

Table 2.3: Extracellular matrix effects on ureteric bud branching, Matrigel/Coll IV additions

Addition	**Branching Effect**
Laminin (0.2 – 0.75 mg/mL)	No effect
Alginate (0.1 - 0.9%)	Diminished
Type I Coll. (0.4 - 3.0 mg/mL)	Diminished
Type IV Coll. (0.25 - 0.75 mg/mL)	No effect

Table 2.4: Global microarray analysis of recombined tissue

Up-regulated Genes	**Up-regulated Genes in Recombined Tissue**
Group I (743 genes)	13.19 % (98)
Group II (164 genes)	50.00 % (82)
Group III (1246 genes)	49.76 % (620)
Down-regulated Genes	**Down-regulated Genes in Recombined Tissue**
Group IV (1304 genes)	15.03 % (196)
Group V (104 genes)	49.04 % (51)
Group VI (1025 genes)	74.34 % (762)
Developmentally Up-regulated Genes	**Up-regulated Genes in Recombined Tissue**
Group VII (315 genes)	53.65 % (169)
Developmentally Down-regulated Genes	**Down-regulated Genes in Recombined Tissue**
Group VIII (451 genes)	27.94 % (126)
Recombined Tissue Abnormally High	**Number of Genes**
Group IX	241
Recombined Tissue Abnormally Low	**Number of Genes**
Group X	90

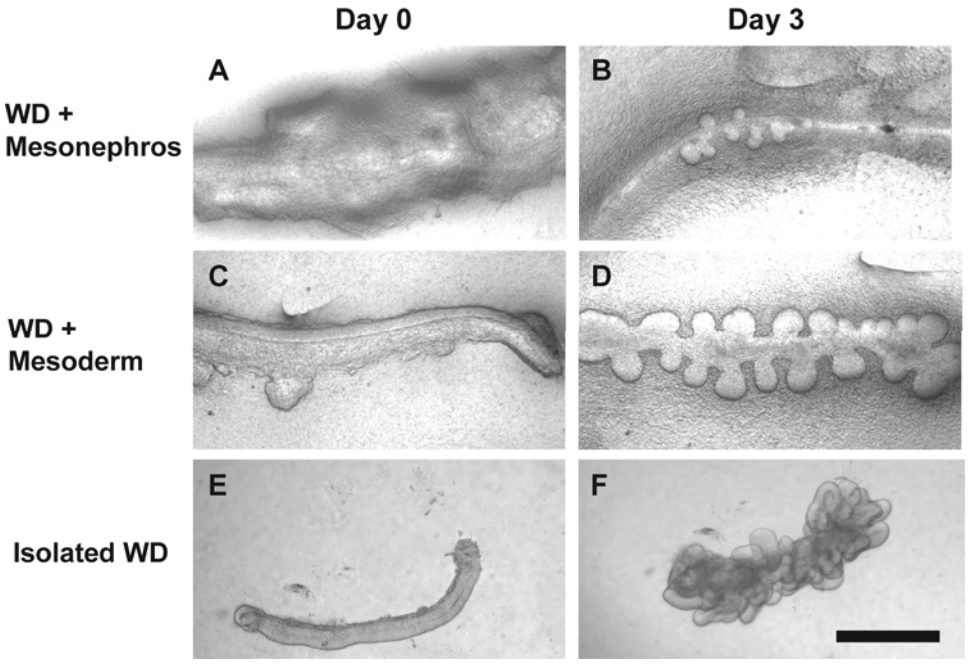

Figure 2.1: WD budding systems. The whole mesonephros (A and B), the WD with a thin layer of intermediate mesoderm (C and D), and the WD devoid of other cell layers (E and F) can be induced to bud according to the conditions outlined in the text and Table 2.1. (Scale bar, 500 μm.)

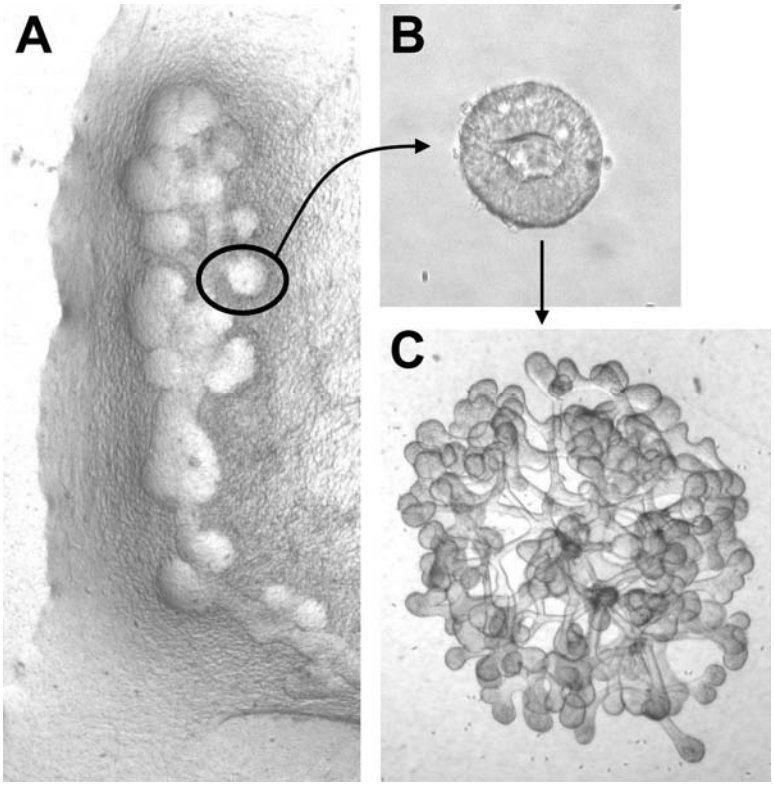

Figure 2.2: WD budding to isolated *in vitro*-formed UB branching. One bud from a budded WD after 4 days in culture (A) can be excised, suspended in a 3D extracellular matrix gel (B), and induced to branch (C). Please also see Table 2.2.

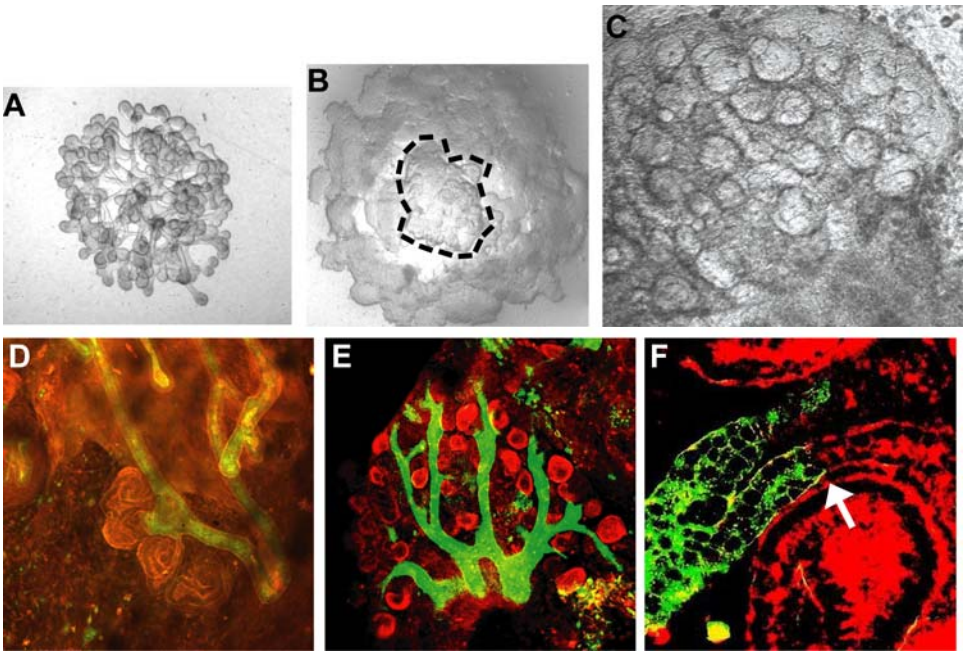

Figure 2.3: Recombination of branched *in vitro*-formed UB with MM. (A and B) The branched *in vitro*-formed UB from Fig. 2C (A) was mechanically separated from the matrix (delineated by the dotted line) and recombined with freshly dissected undifferentiated MM(B). (C–F) Recombined tissues were grown for approximately 4–6 days (C). A x10 dual fluorescent micrograph of the recombined tissue stained with FITC-labeled *D. biflorus* (green) and rhodamine conjugated peanut agglutinin (PNA) lectin (red) shows the mesenchymal-to-epithelial transition occurring around the UB branches (green) (D and E x4). A higher-magnification (x40) at the fusion (arrow) of the WD-derived (green) and MM-derived (red) epithelial cells demonstrates a contiguous tubule lumen (F).

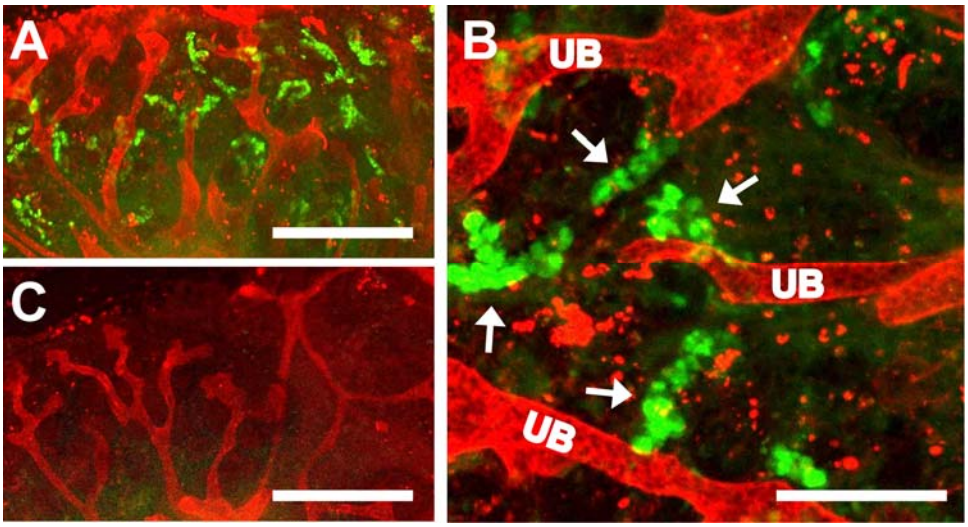

Figure 2.4: Differentiated tubules of the recombined tissue are functionally capable of organic anion transport. (A) Accumulation of 6-CF (green), a fluorescent organic anion, in the MM-derived tubules (UB-derived tubules stained with TRITC-conjugated *D. biflorus*, red) of the recombined tissue (branched T-shaped UB, MM) suggests both differentiation and function of mesenchymal tubules. (B) The accumulation is seen only in the cells of non-UB-derived tubules (arrows). (C) The accumulation is probenecid- (a competitive inhibitor of organic anion transport) sensitive, confirming that the accumulation was transporter mediated. (Scale bars, 500 μm for A and C and 200 μm for B.)

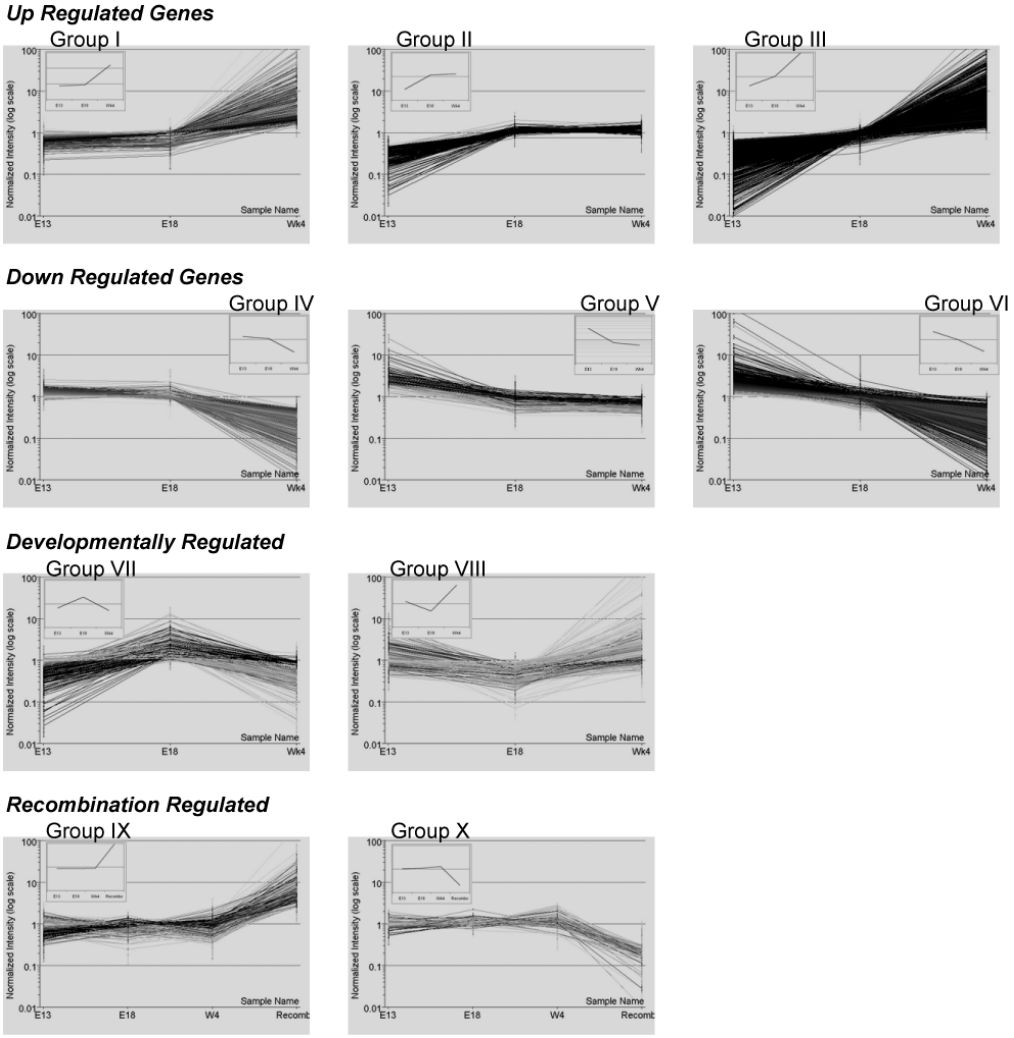

Figure 2.5: Grouping of the genes based on developmental expression patterns. Before the gene expression of the recombined tissue (from a recombination of nonbranched *in vitro*-formed UB and MM) was analyzed, the genes on the chip were grouped according to their kidney developmental expression pattern. Up-regulated genes (Groups I, II, III) were defined as genes with 3-fold expression increases from E13 to Wk4. The genes were further grouped based on E18 expression level; if E18 was within 1.5-fold of E13 or Wk 4, then the gene was defined as Group I (late rise) or Group II (early rise), respectively. If E18 was in between those criteria, then the gene was defined as Group III. An analogous grouping was performed for down-regulated genes (Groups IV, V, VI - late drop, early drop, and neither, respectively). Developmentally regulated genes were defined as genes whose E18 expression was at least 3-fold higher (Group VII) or lower (Group VII) than E13 or Wk4 (and 1.5-fold higher or lower than the other); thus, these genes had a maximum (Group VII) or minimum (Group VIII) gene expression at E18. Recombination regulated genes represent genes that were 3-fold higher (Group IX) or lower (Group X) in the recombined tissue than all three developmental time points. Raw data are available at the NCBI GEO website with accession number GSE9570.

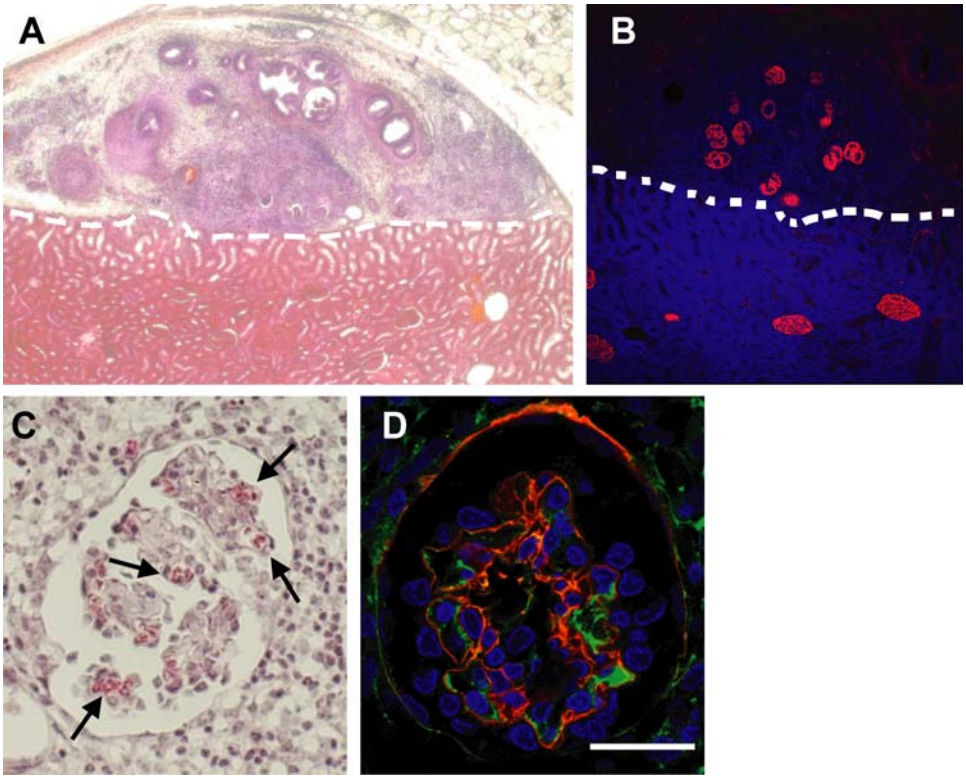

Figure 2.6: Recombined tissue 14 days after implantation into a host rat. (A and B) The dashed line separates recombined tissue (above) from host tissue (below) (A, 4); glomeruli are stained with PNA (red) (B, x10). (C and D) The presence of erythrocytes (arrows) in the glomeruli suggests blood flow in the recombined tissue (C, x40). The cells of the glomerulus express the endothelial marker PECAM-1 (green) and type IV collagen (red) along its basement membrane (D, x60). DAPI nuclear stain is blue. (Scale bar, 50 μm.)

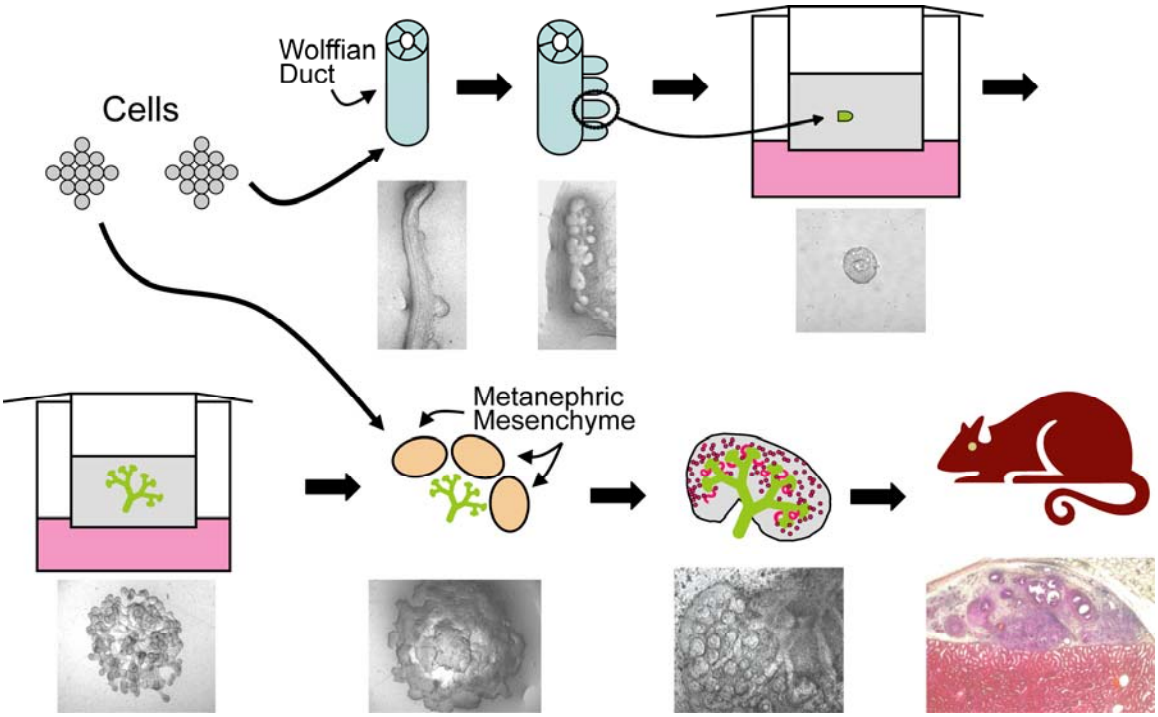

Figure 2.7: Proposed *in vitro* kidney engineering strategy. First, the WD is isolated and induced to bud. Then, each bud can be isolated and induced to undergo branching. The branched *in vitro*-formed UB is then recombined with MM; after 4–6 days of mutual induction, the recombined tissue resembles a late-stage embryonic kidney. The recombined tissue is then implanted into a host animal where it is vascularized and forms glomeruli. The possibility of using cells to engineer WD and/or MM-like tissue is also indicated.

CHAPTER 3:

Constructing Embryonic Kidney Progenitor Tissues from Cells and Three-dimensional *In Vitro* Kidney Culture: Towards a Broader Method of *In Vitro* Engineering of Kidney Tissues

3.1 Abstract

It has previously been determined that kidney-like tissues engineered *in vitro* from renal progenitor tissues contain functional organic anion transporters and can be implanted into host animals to achieve an early vasculature. Here we address the possibility of constructing the renal progenitor tissues from cells. We also propose an alternate approach to engineering 3D kidney tissues by assembling renal progenitor tissues into an anatomically appropriate embryonic kidney-like structure containing an epithelial tube with the potential to form the collecting duct system and mesenchyme competent of differentiation. Wolffian duct tissues were demonstrated to be capable of replacing the ureteric bud (UB) in embryonic kidney culture, suggesting that the UB can be replaced by an epithelial tube with a more homogenous cell composition. Cell aggregates of an immortalized UB cell line were able to induce metanephric mesenchyme to epithelialize and to connect with the UB cell aggregate, although they were not able to branch under these conditions. Finally, we demonstrated that 3D embryonic kidney

development can occur in a 3D *in vitro* culture system. 3D reconstructions of HoxB7-GFP mouse embryonic kidneys (E12) cultured on a filter, or suspended in type I collagen or type IV collagen, revealed that type IV collagen supports the thickest tissue growth (600 ± 8 μm) and the largest kidney volume (0.22 ± 0.02 mm^3), followed by type I collagen culture (371 ± 7 μm, 0.184 ± 0.008 mm^3) and the filter culture system (79 ± 2 μm, 0.12 ± 0.02 mm^3). Furthermore, only kidneys in type IV collagen exhibited a 3D umbrella-like branching pattern characteristic *in vivo* kidney development. Thus, we address two issues: 1) the potential of progenitor cells to form epithelial tubes that can induce MM and integrate and, 2) the potential for culturing a more anatomically correct kidney-like tissue in 3D. Much more needs to be done, but this work supports the feasibility of both developmental approaches.

3.2 Introduction

With over 76,000 people in the U.S. alone awaiting a kidney transplant, the necessity for additional kidneys or alternatives to allogenic renal transplantation is well established [2]. Currently, the best alternative to transplantation is dialysis. While improvements in dialysis are forthcoming, including the use of renal cells in conjunction with dialysis [59], even these improved dialysis techniques are both unable to recapitulate all functions of the kidney and, thus far, unable to demonstrate a significantly increased efficacy that could eliminate the need for transplantation. One potential solution to the shortage of kidneys available for transplantation is to engineer new kidneys or kidney-like tissues for therapeutic purposes. The human kidney employs a complex three dimensional structure, including structures such as the loop of Henle, the juxtaglomerular apparatus and complex microvasculature, to achieve its many functions. Rather than attempt to engineer an adult kidney or kidney-like tissue with this level of complexity, we have demonstrated a strategy for the engineering of kidney tissues by *in vitro* reconstitution of the renal developmental stages [144].

Metanephric kidney development begins with the outgrowth of the ureteric bud (UB) from the Wolffian duct (WD). The ureteric bud invades the surrounding metanephric mesenchyme (MM) and begins to undergo branching morphogenesis [159]. The branched UB structure will differentiate into the collecting duct system of the kidney. The cells of the MM, which induce branching morphogenesis of the UB, undergo a mesenchymal-to-epithelial transformation, connect to the tips of the UB, and ultimately form the various components of the nephron [159]. In the stepwise approach to

developmental engineering of kidney tissues, these same *in vivo* developmental events were reproduced *in vitro* beginning with rat WD and MM tissues to achieve an implantable kidney tissue with functional transport capabilities [144]. If one could construct the WD and MM tissues from cells, then it may then be possible to create implantable renal tissues in the stepwise fashion described above without requiring animal or human tissue sources.

In a potential alternative developmental approach to engineering kidney tissues, kidney progenitor tissues reconstructed from cells could be directly assembled into an embryonic kidney-like structure comprised of an epithelial tube surrounded by mesenchyme. The assembled embryonic kidney-like tissue could then be cultured *in vitro*, in a manner similar to metanephric kidney culture of the E13 rat embryonic kidney (which contains only a T-shaped UB and MM), resulting in a kidney-like tissue. This approach, however, would seem to require a three dimensional (3D) culture system for the assembled embryonic kidney in order to recapitulate the 3D structure of the adult kidney. It is currently unclear to what extent embryonic kidney development with whole kidney culture can occur in an *in vitro* 3D culture environment.

The goal of constructing MM and either the WD or UB tissues from cell lines (for use in either kidney engineering approach) requires the assumption that homogenous cell populations can be used to assemble tissues known to be heterogeneous. Here we provide support with rodent cell lines for the concept that it may be possible to model the renal embryonic tissues as homogenous cell types and that it may be possible to construct these tissues from homogenous cells. Furthermore, we introduce a culture system that demonstrates the embryonic kidney is capable of *in vitro* 3D growth and development

when suspended in a 3D extracellular matrix gel, and the effects of different matrix molecules on 3D growth are investigated. These results represent important advances in the developmental approaches to *in vitro* engineering of kidney tissues.

3.3 Methods

3.3.1 Materials and Reagents

Fibroblast growth factor-1 (FGF1) and glial cell-derived neurotrophic factor (GDNF) were obtained from R&D Systems (Minneapolis, MN). Mouse anti-E-cadherin antibodies were from BD Biosciences Pharmingen (San Diego, CA) and goat anti-mouse AlexaFluor 594 was from Molecular Probes (Eugene, OR). FITC-conjugated *D. biflorus* and (DB) lectin and rhodamine-conjugated PNA were from Vector Laboratories (Burlingame, CA). Type I and type IV collagens, and growth factor-reduced Matrigel were from BD Biosciences (San Jose, CA). Antibiotics, DMEM:F12 1:1 (v:v) and PBS were from GIBCO-BRL (Grand Island, NY). Unless otherwise noted, all other reagents are from Sigma (St. Louis, MO).

3.3.2 Embryonic Tissue Isolation

Embryos from timed pregnant Holtzman rats (Harlan, Indianapolis, IN) at day 13 (E13) of gestation (day 0 being the day of appearance of the vaginal plug) or timed pregnant HoxB7-GFP mice embryos at E12 were dissected free of surrounding tissues. The urogenital tract was isolated and WDs were dissected free of surrounding tissue. The mesonephric tubules and intermediate mesoderm was carefully stripped away leaving only the epithelial tube of the WD. Metanphric kidneys were isolated and directly used in

the kidney culture as described below or further separated in to the UB and MM tissues as described previously [136].

3.3.3 WD/MM Co-culture

An approximately 100 μm segment of WD was excised and suspended with the MM from one kidney in a 1 mg/mL type I collagen solution (supplemented with DMEM and buffered by HEPES and $NaHCO_3$ to a pH of approximately 7.2). Before the gel was completely solidified, the WD segment was placed in the crevice of the MM left behind from the removal of the UB. The WD/MM tissue was cultured in the presence of a DMEM:F12 medium supplemented with 10% FBS (Hyclone, Logan, UT) and 1% antibiotics for 7 or 12 days. All cultures were incubated at 37ºC in a humidified 5% CO_2 and 100% humidity atmosphere.

3.3.4 UB Cell Aggregate/MM Co-culture

Mouse SV40 large-T antigen transfected UB cells were cultured to confluence. The cells were then trypsonized and suspended in a DMEM:F12 media with 10% FBS and 1% antibiotics at a concentration of $1x10^5$ cells/mL. 20 μL of the cell solution was placed on the bottom of a Petri dish lid with 10 mL of PBS in the Petri dish. The cells were incubated for 2 days at 37°C in a humidified 5% CO_2 atmosphere. The UB cell aggregates were removed from the hanging drops and placed on a 0.4 μm Transwell filter surrounded by freshly isolated MM with 400 μL DMEM:F12 media supplemented with 10% FBS and 1% antibiotics placed below the filter and incubated for 7 days.

3.3.5 MM Cell Culture and Conditioned Medium

The MM primary cell line was created by placing freshly isolated MM cells directly on a cell-culture treated plate. The MM cells were cultured on the plate for 5 days after which time the MM cells were trypsinized and placed on new plates. To create conditioned medium BSN, RIMM-18, MM primary, or 3T3 cells were cultured on plates and allowed to reach confluence. After confluence was reached, the medium was replaced with DMEM:F12 (no antibiotics or FBS) and the cells were incubated for 3 days. After 3 days the conditioned medium was removed and concentrated 5 times with a 5000 MW cutoff Millipore (Billerica, MA) filter.

3.3.6 Isolated Ureteric Bud Culture

Isolated ureteric buds were suspended in a growth factor-reduced Matrigel solution (1:1 Matrigel:DMEM/F12), and cultured with conditioned medium from the BSN, RIMM-18, MM primary, or 3T3 cell lines supplemented with 10% FBS, 1% antbiotics, 125 ng/mL FGF1, and 125 ng/mL GDNF as described previously [18, 133, 136, 152, 170, 197]. The suspended UBs were then cultured for 7 days at which time tips were counted.

3.3.7 3D Kidney Culture

Embryonic metanephric kidneys were isolated and suspended in extracellular matrix solutions of type I collagen, type IV collagen, or growth factor-reduced Matrigel at the noted concentrations. All matrix solutions were supplemented with DMEM and buffered by HEPES and $NaHCO_3$ to a pH of approximately 7.2. Kidneys were cultured in

the presence of 600 μL DMEM:F12 supplemented with 10% FCS and 1% antibiotics for 7 days.

3.3.8 Immunofluorescence and Lectin Staining

After the indicated number of days, kidney cultures were fixed for 30 min with 4% paraformaldehyde in PBS. Fixed kidney cultures were rinsed with TBS and extracted in absolute methanol at -20°C for 20 min. Samples were then blocked for 1hr in 3% BSA in TBS-T at 4°C followed by incubation in anti-E-cadherin antibody (1:500 in blocking solution) for 24 hr at 4°C. Samples were then washed 3x8 hr in TBS-T, followed by incubation in AlexaFluor594 antibody (1:2000) and FITC-DB (1:500) for 24 hr at 4°C, and a final 3x8hr washes in TBS-T at 4°C. Samples were then mounted on slides with ProLong Gold antifade reagent (Invitrogen, Carlsbad, CA). For PNA staining, following the blocking step the tissues were washed twice with Neuraminidase buffer (150 mM NaCl, 50 mM sodium acetate, pH 5.5), incubated with Neuraminidase (1 unit/ml) for 4 hr at 37°C and then with rhodamine-conjugated PNA (50 μg/ml) and FITC-DB (1:500) for 24 hr at 4°C. Fluorescently stained samples were imaged using either the Nikon EZ-C1 confocal system.

3.3.9 3D Imaging and Morphometric Analysis

Kidney cultures from HoxB7-GFP mice were fixed for 30 min with 4% paraformaldehyde in PBS and rinsed 3x5 min in PBS. Kidneys were then cleared with Focus Clear (Cedarlane Laboratories, Burlington, NC) for 20 min and mounted on depression slides with Mount Clear (Cedarlane Laboratories, Burlington, NC). Samples

were imaged on the FV300 Olympus 2-photon microscopy system. 3D Reconstructions, isosurfacing, and 3D measurements of fluorescent stacks were performed using Image Pro Plus 3D Constructor 5.1 (Media Cybernetics, Bethesda, MD). Tissue thickness was determined as being the minimum distance between two planes (or Feret minimum). Length to thickness ratio was calculated as the Feret maximum to Feret minimum ratio. Kidney volumes were estimated as the volume of an ellipsoid with the dimensions of half the length, depth and width of a bounding box around the branching structure. All samples were analyzed with $n \geq 3$ and with errors reported as the standard error of the mean.

3.4 Results

3.4.3 Modeling the UB as an Epithelial Tube of Homogenous Cells

While the WD represents a starting tissue for the *in vitro* reconstitution of kidney development in stages, direct assembly of an embryonic kidney aims to reconstruct the equivalent of an E13 rat/E11.5 mouse embryonic kidney comprised of an unbranched (T-shaped) UB and MM. However, unlike the WD, the UB is known to be comprised of a heterogeneous cell population containing cells at the tip region distinct from cells of the stalk region (differentially expressed genes include C-RET, FGFR1, FGFR2, MT1-MMP [109]); the non-budded WD from which the UB protrudes does not appear to have these different regions. Therefore, a small segment of WD tissue would presumably represent a homogenous epithelial tube with the inherent potential to form the collecting duct of a developing kidney.

To investigate whether an epithelial tube with a homogenous cell population could function as a UB and retain the capacities to undergo branching morphogenesis and induce MET, the UB was removed from an E13 rat kidney and a segment of the WD from an E13 rat kidney was put in its place (Fig. 3.1a). The E13 kidney with the UB replaced by a segment of WD developed a branched collecting duct system and induced MM to epithelialize in a manner similar to that of traditional *in vitro* metanephric kidney culture (Fig. 3.1b-d). After 7 days of *in vitro* culture, convoluted MM-derived epithelial structures expressing E-Cadherin were visible, suggesting the formation of nascent nephrons (Fig. 3.1c). After 12 days of *in vitro* culture, in addition to increased growth of the collecting duct system, a large number of developing glomeruli were evident by PNA lectin staining (Fig. 3.1d). This demonstrates that the homogenous epithelial tube of the WD can branch and form a collecting duct structure that induces MM epithelialization and glomerulus formation.

3.4.1 Constructing an Epithelial Tube from Cells

For both developmental approaches to engineering kidney tissues (*in vitro* reconstitution in stages and *in vitro* culture via direct assembly), it would be ideal to be able to construct from cells the renal progenitor tissues needed to form kidney tissues, thus, bypassing the need to harvest tissues from animal or human donors. While it is currently unknown what source of cells (potential cells including mature cells or stem cells - embryonic, amniotic, or adult) may work best for this purpose or whether progenitor cells could be differentiated into the renal lineages, it is necessary to develop strategies to construct tissues from cells should they become available. Since both

developmental approaches to tissue engineering can potentially begin with a homogenous epithelial tube, the next step was to attempt to construct an epithelial tube from a homogenous cell line possessing the potential to act as a UB or WD.

The process of constructing an epithelial tissue from cells was simulated using the SV40 large-T antigen transfected mouse UB cell line. This UB cell line is capable of undergoing tubulogenesis in response to a conditioned medium (CM) from a metanephric mesenchyme cell line (BSN cell line) (Fig. 3.2a) similar to what has been described previously [150]. To test whether these UB cells could transform in to a UB tissue, UB cells were suspended in hanging drops to create UB cell aggregates. The inductive and branching capacity of these UB cell aggregates was tested by establishing a co-culture with primary isolated E13 rat MM (Fig. 3.2b). The UB cell aggregate was capable of inducing mesenchymal-to-epithelial transition of the isolated E13 rat MM (Fig. 3.2c-e). Furthermore, it was capable of connecting to form contiguous tissue segments. The E-cadherin positive MM-derived tubule continued its curvature and connected with the *D. biflorus* (DB) staining from the UB derived cells (Fig. 3.2e, white arrow). While the UB cell aggregate did not display a branching phenotype, it did demonstrate an ability to generate multicellular structures (Fig. 3.2e, yellow arrows) with maintained epithelial polarity.

3.4.2 Constructing a MM Tissue from MM Cells

In addition to an epithelial tubule, a MM tissue constructed from cells is also necessary for the developmental approaches to engineering kidney tissues. Therefore, it was investigated what potential MM cells are available to simulate this procedure and

whether the MM can be modeled as a homogenous cell line. Three different MM-derived cell types (BSN cell line, RIMM-18 cell line, and primary rat E13 MM cell cultures) and a 3T3 fibroblast cell line (as a control) were tested for the ability to secrete factors that induce UB differentiation following cell propagation. A rat primary MM cell culture created from primary MM tissue was demonstrated to be vimentin positive and cytokeratin negative, similar to the BSN, RIMM-18, and 3T3 cell lines (Fig. 3.3a-d). Next, the conditioned medium from each of the 4 cell types was substituted as the medium in the isolated UB culture system. Only conditioned media from the BSN and primary MM cell types were capable of inducing UB branching morphogenesis (Fig. 3.3e,g); however, the BSN-CM was substantially more potent than the primary MM-CM (Fig. 3.3i). The RIMM-18 and 3T3 conditioned media did not induce UB branching, but the 3T3-CM did seem to induce slight globular growth (Fig. 3.3h) while the RIMM-18-CM did not induce appreciable growth (Fig. 3.3f).

Cell aggregates from each of the three MM cell types, created by hanging drops and/or centrifugation, were unable to reproduce the differentiation of MM tissue (mesenchymal-to-epithelial transition) or induce UB branching when cultured together with an isolated E13 rat UB (data not shown).

3.4.4 3D Whole Embryonic Kidney Culture

Metanephric kidney culture has traditionally been performed by culturing the embryonic kidney explant on a filter, resulting in relatively 2D growth and development morphology. This culture system does not appear to reproduce the 3D structure known to be important for kidney function. If renal progenitor tissues were to

be constructed from cells and those tissues were assembled to reproduce an embryonic kidney-like structure (an epithelial tube and mesenchyme), then the next step would be to culture the early embryonic kidney-like tissues in a system that allows for recapitulation of 3D kidney structures. Therefore, we investigated whether an E13 rat embryonic kidney could reproduce 3D growth and branching morphogenesis when suspended in an extracellular matrix gel. Type I collagen, type IV collagen, and Matrigel all supported kidney growth and development (Fig. 3.4). A concentration dependence was evident, with lower concentrations resulting in larger growth. The highest concentration of Matrigel (100%) seemed to result in very little explant growth after 7 days compared to the day 0 kidney (Fig. 3.4k). Although an increasing opacity of the kidneys imaged with brightfield microscopy (type IV collagen = Matrigel > type I collagen > filter) suggested a thicker more 3D tissue, the degree of branching morphogenesis taking place in those tissues could not be determined. The artificial matrices of alginate and puramatrix were also tested; however, neither supported appreciable growth (data not shown).

To quantify the 3D growth and to visualize the extent of 3D branching in the gel suspension culture, E12 embryonic kidneys from the HoxB7-GFP mouse were cultured in three culture conditions that exhibited different brightfield microscopy opacity levels; traditional filter culture, 1 mg/mL type I collagen, and 0.65mg/mL type IV collagen. After 7 days of culture, the kidneys were imaged on a 2-photon microscope, 3D reconstructions of the branching structures were performed (Fig. 3.5), and morphometric measurements were taken (Table 3.1). Filter kidney cultures grew along the filter with little appreciable growth or branching in the z-direction, while both type I

collagen and type IV collagen embryonic kidney cultures exhibited extensive 3D branching growth in the z-direction. Type I collagen cultures (371 ± 7 μm) were 4.7 times thicker than the filter cultures (79 ± 2 μm) and type IV collagen cultures (600 ± 8 μm) were 7.6 times thicker than filter cultures. Total culture volume was larger in the thicker tissues (Table 3.1), although this difference is not as significant as the thickness because the branches of the kidneys cultured in the collagen gels did not extend as far from the origin as kidneys grown on a filter.

Type IV collagen and type I collagen promoted different 3D growth patterns. Kidneys in type I collagen only branched upwards in the z-direction away from the filter (Fig. 3.6a), while the branching of kidneys growing in type IV collagen exhibited an umbrella-shape branching pattern (Fig. 3.6b) more similar to what is seen during *in vivo* kidney development (Fig. 3.6c). Although the kidneys in the type IV collagen branched farther in the z-direction and exhibited a more umbrella-like pattern, their branches did not extend as far in the horizontal (x-y) plane of the kidney than the branches of kidneys cultured in type I collagen. Kidneys grown in type I collagen always grew upwards from the filter, but more so along the filter as if the kidneys could sense the direction of gravity, exhibiting a length to thickness ratio of 2.79 ± 0.08. Kidneys grown in type IV collagen, however, had no consistent orientation relative to the filter and exhibited a smaller length to thickness ratio, 1.51 ± 0.07, suggesting a fundamental difference in how the structural properties of type I collagen and type IV collagen gels affect the direction the tissue will branch.

3.5 Discussion

We have previously demonstrated how one could recreate the key stages of metanephric kidney development, *in vitro*, for the purpose of creating a functional, implantable kidney tissue starting from renal progenitor tissues, WD and MM [144]. Here we built upon that stepwise approach for *in vitro* engineering of kidney tissues by addressing the issue of creating the renal progenitor tissues from cells and demonstrating important proofs of principles necessary for the construction of renal progenitor tissues from cells (Fig. 3.7a). In addition, we have proposed an alternative approach to engineering 3D kidney tissues that would utilize renal progenitor tissues (potentially constructed from cells) to assemble an early embryonic kidney-like tissue that can potentially be cultured similar to the whole embryonic kidney (Fig. 3.7b). We demonstrated that 3D *in vitro* whole embryonic kidney development is possible, and we investigated the conditions under which a whole embryonic kidney can achieve *in vitro* 3D growth and development.

The ideal kidney engineering solution would be to create a kidney tissue that would have little to no immune response when implanted. One way to address that issue would be to construct transplantable tissues from a source of either autologous cells or other cells that could be transformed in to immunocompetent cells. The ability to expand a cell line *in vitro* and construct an organ from these cells would also alleviate the problem of finding sources of tissues or organs. There are many potential sources for cells from which to engineer kidney tissues, including mature renal cells, cells created by

nuclear transplantation [78], embryonic stem cells [69], amniotic stem cells [27], or adult renal stem-like cells [19, 32, 50, 54, 65, 71, 98, 100, 127, 149].

Once a cell source is identified, the next step would be to organize those cells in to the renal progenitor tissues of an epithelial tube and metanephric mesenchyme. Since all of the aforementioned cell sources would likely exist as homogenous cell lines, this goal can only be accomplished if the tissue being constructed is capable of existing as a tissue of homogenous cells or a tissue of non-homogenous cells with high plasticity. In the case of the embryonic kidney, the two tissues that need to be reproduced are the UB and the MM. Since the goal is to create a UB from a homogenous cell line, first it had to be demonstrated that a homogenous epithelial tissue was capable of replacing a non-homogenous UB and retain the ability to recapitulate *in vitro* kidney development. Here we demonstrated that the UB can be replaced with a more homogenous epithelial tube of earlier cell lineage, the Wolffian duct, and the resulting structure can develop similar to traditional *in vitro* kidney cultures, both by undergoing branching morphogenesis and inducing mesenchymal differentiation. This provides evidence that the UB can be modeled as or a replaced by a homogenous epithelial tissue, but also represents an important finding in that WD cells can directly be used in the construction of an epithelial tube for use in assembling an embryonic kidney. As a result, the WD can now be considered a starting tissue for both of the developmental strategies presented here. This is a potential advantage in that the WD is thought to be an earlier cell lineage than the UB; it may prove to be easier to promote the differentiation of stem cells towards the earlier WD cell lineage.

Next we attempted to organize a homogenous epithelial cell line into an epithelial tissue. With a mouse UB cell line, we demonstrated that cells can be organized in to a cell aggregate that retains the ability to induce MET. When UB cells were aggregated by the hanging drop method and then placed on a filter with isolated rat E13 MM, the UB cell aggregate not only induced MM epithelialization, but also appeared to join and form a contiguous tissue segment. Furthermore, the UB cell aggregate formed multicellular extensions. While this is a very promising finding, the UB cell aggregates were unable to organize into a luminal structure and unable to reproduce branching morphogenesis. However, E-cadherin expression suggested that epithelial polarity was maintained. Additional attempts to create luminal UB cell aggregates included suspending the aggregates in various extracellular matrix gels in conjunction with stimulation by a MM-cell (BSN) conditioned medium supplemented with growth factors (data not shown) similar to what has been shown to stimulate UB branching in an isolated UB culture system [136]. Another study has shown that primary salivary gland cells can self organize in to epithelial structures when aggregated and suspended in a extracellular matrix gel [188]; however, this did not occur with the UB cell line. Newer technologies such as cell micropatterning may be necessary to achieve the creation of a luminal epithelial structure from cells retaining the MM-inductive capacity and UB branching capability [119].

While it may have seemed that the MM tissue would be easier to construct from cells than an epithelial tissue because there appears to be no specific cell orientation or structure, this was not the case. We demonstrated that the conditioned media from three different MM-derived cell types possessed different efficacies in inducing isolated UB branching morphogenesis indicating that MM-derived cells can be expanded *in vitro* and

retain the ability to induce UB branching morphogenesis. Primary MM cells had a branching induction level in between two other MM cell lines (BSN and RIMM-18) (Fig. 3.3i) suggesting that perhaps MM tissue is composed of both BSN-like (demonstrated to induce UB branching [136]) and RIMM-18-like (demonstrated to epithelialize in response to UB-derived growth factors [84]) cell types. Aggregates of each of the three MM-derived cell types were unable to differentiate similar to E13 rat MM in response to a UB co-culture. Suspending the cells (non-aggregated) within an extracellular matrix gel together with a UB also did not result in MM aggregation or differentiation (data not shown). These data may suggest that E13 rat MM tissue cannot be modeled as a tissue of homogenous cells; however, since primary cell aggregates could not act as primary MM tissue, perhaps the methods of aggregation or cell suspension were not allowing for the cells to act as MM tissue. It also may be possible that only certain sub-selected MM cells were proliferating when cultured on a plate, thus the primary MM cell line lacked all the necessary MM cells in the cell aggregates. Perhaps an earlier mesenchymal tissue potentially containing a less differentiated population of cells, such as the mesenchyme adjacent to the WD immediately prior to budding or intermediate mesodermal cell lines/cultures, would represent a better potential tissue to reconstruct from cells.

WD and MM tissues constructed from cells could potentially be assembled in to an embryonic kidney-like structure that could be cultured similar to traditional *in vitro* metanephric kidney culture (Fig. 3.7b). However, traditional embryonic kidney culture occurs as a flat 2D culture (Fig. 3.5a-c) and does not recapitulate the 3D growth and structure of *in vivo* development. Here we demonstrated that embryonic kidneys can recapitulate 3D growth and branching morphogenesis in an *in vitro* culture system.

Kidney growth increased with decreasing concentrations of extracellular matrix with both type I collagen and Matrigel kidney culture environments. The less dense matrices may have allowed for more growth because there was less material to remodel and breakdown. This may also be supported by the observation that neither alginate nor puramatrix substrates (both of which are non-remodelable artificial matrices) supported significant growth.

In order to visualize and quantify the extent of 3D branching morphogenesis taking place in the suspended cultures, embryonic kidneys from mice with GFP expression placed under the HoxB7 promoter were cultured for 7 days and then imaged with a 2-photon microscope. Type IV collagen appeared to support the thickest tissue growth and the largest kidney volume. In addition, only kidneys cultured in type IV collagen possessed a 3D curvilinear branching outline, or umbrella shape, similar to the *in vivo* developing kidney [21]. However, while the total volume of the kidneys cultured in type IV collagen were larger than kidneys cultured in type I collagen or those cultured on a filter, the 0.22 ± 0.02 mm^3 kidney culture volume only approached the volume of a E14.5 mouse kidney reported to be 0.25 ± 0.02 mm^3 [21]. While the branching pattern of the kidneys in type IV collagen were was highly three dimensional and exhibited a more *in vivo*-like shape than the other tested conditions, the branches lengthened half as long as the filter kidney cultures. This maybe a result of the lack of nutrients penetrating through the tissue and reaching the inner branches of the kidney that normally elongate during the development process. This may be supported by the fact that kidneys cultured on a filter, which grew much further from the origin of branching, were only 79 ± 2 μm thick,.

However, it may be possible for additional growth factors and known branching promoters to be added to the culture to alleviate this problem.

The adult kidney contains three distinct axes of growth, the medio-lateral axis (also known as the cortico-medullary axis); dorso-ventral axis (the shortest dimension), and the rostro-caudal axis (longest dimension). However, it is currently unknown whether the function of the kidney is dependent on the different lengths of those axes or what causes the different axes of growth [5]. The kidneys cultured in type IV or type I collagen did not appear to distinguish dorso-ventral and rostro-caudal axes of growth; rather the kidneys appear round when looking down upon the kidney culture. It may be that external factors during *in vivo* development, such as space constraints or soluble factors from nearby developing tissues, not present in the *in vitro* systems are responsible for those different axes of growth.

While a Matrigel or other animal derived matrices may not be suitable for use in a human renal therapy because of a potential immune response, these studies reveal that 3D kidney culture is possible when suspended in a compatible matrix. With the advent of MMP sensitive artificial matrices, it may be possible to culture embryonic kidneys in an artificial scaffold that allows for 3D growth and is biocompatible. Additionally, hyaluronic acid, which is often used in tissue engineering for creating artificial scaffolds, has been demonstrated to enhance *in vitro* kidney growth and development [145]. Thus, a hyaluronic acid based MMP-sensitive scaffold may represent a potential artificial scaffold that could simultaneously support and enhance 3D kidney growth and development.

The ultimate goal of this kidney engineering research is to be able to construct from cells a kidney or kidney-like tissue that can be implanted as a therapy for those without full renal function. We have previously demonstrated how one can create implantable tissues *in vitro* from renal progenitor tissues, and now we have advanced the method by addressing the feasibility of using cells to construct those renal progenitor tissues. Furthermore, we have demonstrated the ability to grow embryonic kidneys in 3D culture supporting an additional strategy for engineering kidney tissues. The results of this paper represent advances in the techniques that may ultimately be necessary to achieve *in vitro* engineered kidney tissues following the developmental approaches presented here.

3.6 Acknowledgments

This work was supported by NIH grants DK057286, DK065831and HL035018 (to S.K.N.). E.R. was supported by the NSF graduate research fellowship. We would like to thank the UCSD Neuroscience microscopy shared facility and NINDS grant NS047101 for providing us access to their 2-photon imaging facilities.

Table 3.1: Measurements of kidneys grown in different *in vitro* culture conditions

	Volume, mm^3	Thickness, μm	Max Radius, μm	Length/Thickness
Filter	0.12 ± 0.02	79 ± 2	1120 ± 150	27 ± 4
Coll I	0.184 ± 0.008	371 ± 7	560 ± 14	2.79 ± 0.08
Coll IV	0.22 ± 0.02	600 ± 8	490 ± 21	1.51 ± 0.07

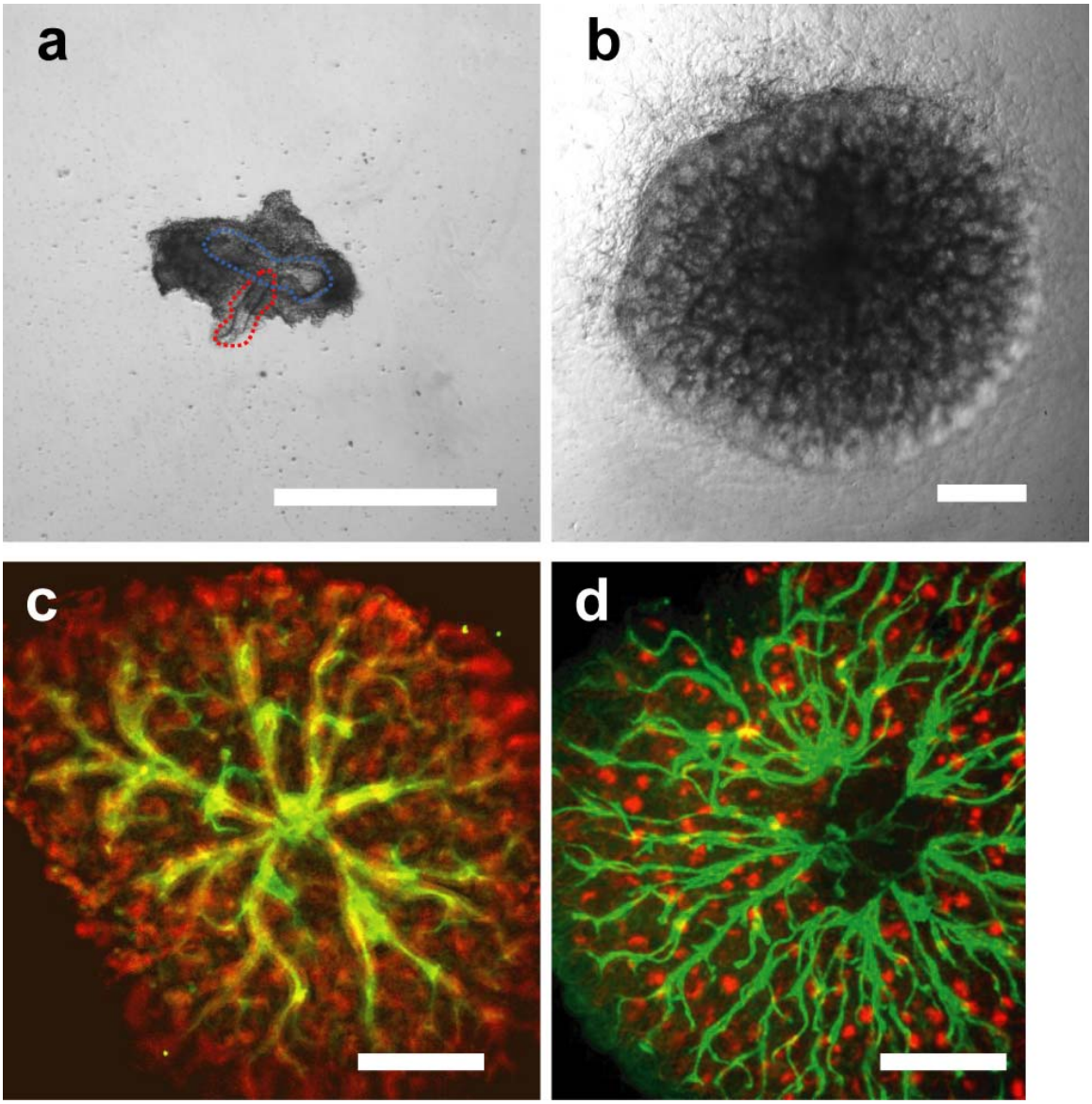

Figure 3.1: WD/MM co-culture. The UB was removed from an embryonic kidney (empty space circled in blue) and a WD (circled in red) was put in its place. After 7 days, the WD/MM co-culture grew similar to traditional *in vitro* kidney culture (b,c; green = DB lectin, UB derived tissues; red = E-Cadherin, UB and MM derived epithelial tissues) and after 12 days, PNA lectin staining (red) revealed differentiation of glomerular podocytes (d). Scale bars correspond to 300 µm.

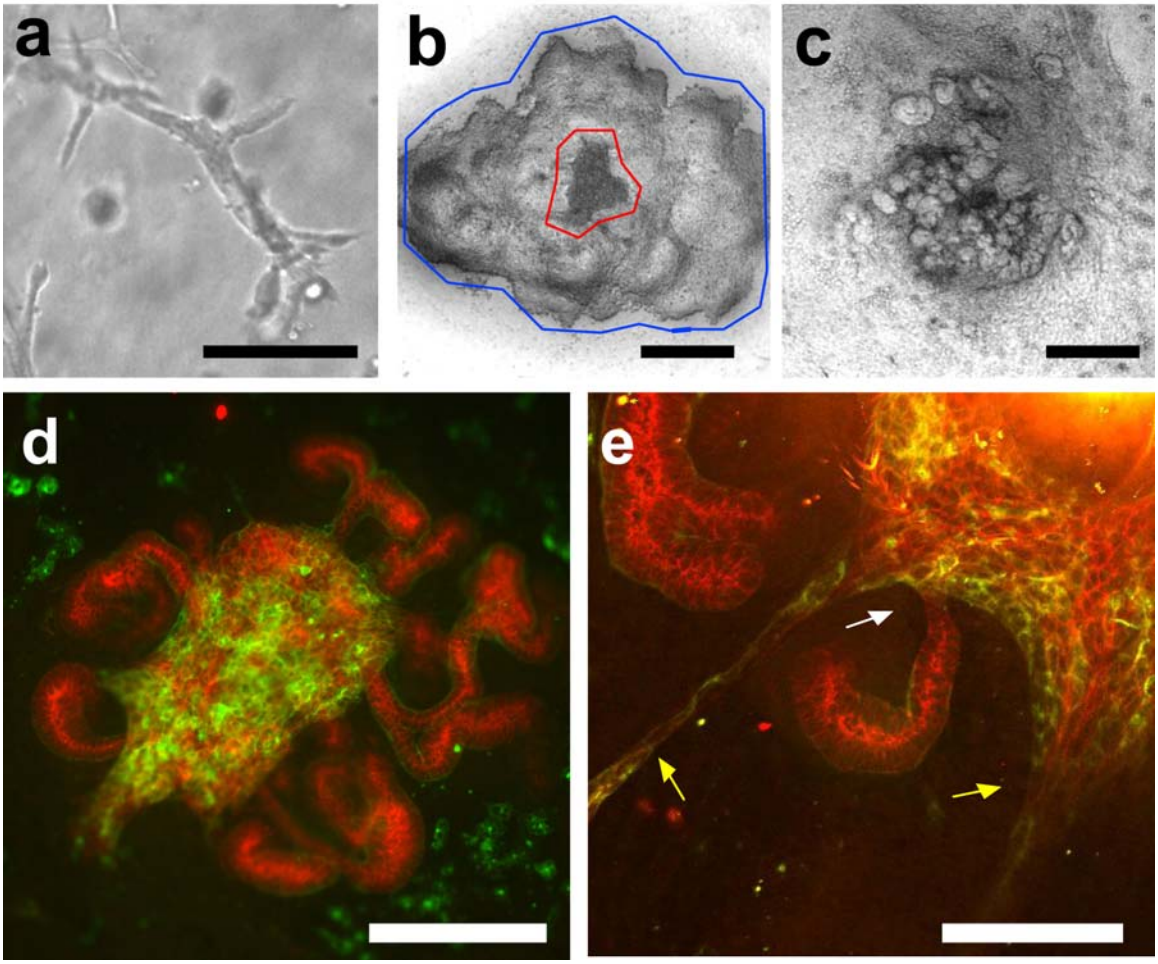

Figure 3.2: UB cell aggregate co-culture with MM. The UB cell is capable of undergoing tubulogenesis when suspended in an extracellular matrix gel - 50 μm scale bar (a). The UB cell aggregate (outlined in red) was recombined with E13 rat MM (outlined in blue) (b) and after 7 days comma and s-shaped bodies of the MM were evident (c). UB cells were stained green (*D. biflorus*) and both UB and MM derived cells were stained red (E-Cadeherin) (c) - 400 μm scale bar (b,c,d). The MM derived tubule was continuous with the green UB cells, white arrow - 100 μm scale bar (d). The yellow arrows indicate the multicellular structures of the UB cell aggregate.

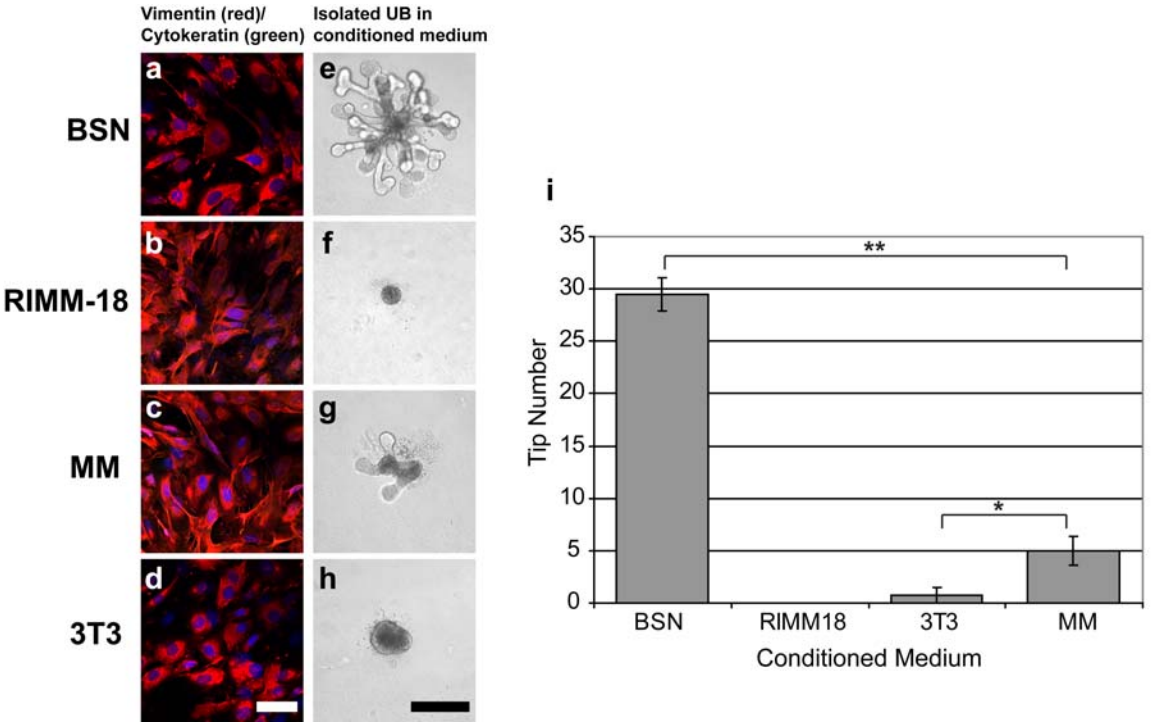

Figure 3.3: Three MM derived cell lines were tested for the ability to induce isolated UB branching. The BSN (a), RIMM-18 (b), and MM primary (c) cell lines are all MM derived cell lines that are vimentin positive, cytokeratin negative. 3T3 fibroblasts (d) are also vimentin positive, cytokeratin negative cells, but are not MM derived. The conditioned medium from BSN cells strongly induced isolated UB branching (e) whereas the conditioned medium from primary MM cells only slightly induced branching (g). The conditioned medium from RIMM-18 and 3T3 cells did not induce branching morphogenesis (f, h, respectively). Plot of tip number vs. cell-conditioned medium used (i) (ANOVA, $P \leq 0.00001$); * = $P \leq 0.05$, ** = $P \leq 0.00005$. Scale bars correspond to 50 μm (a,b,c,d) or 250 μm (e,f,g,h).

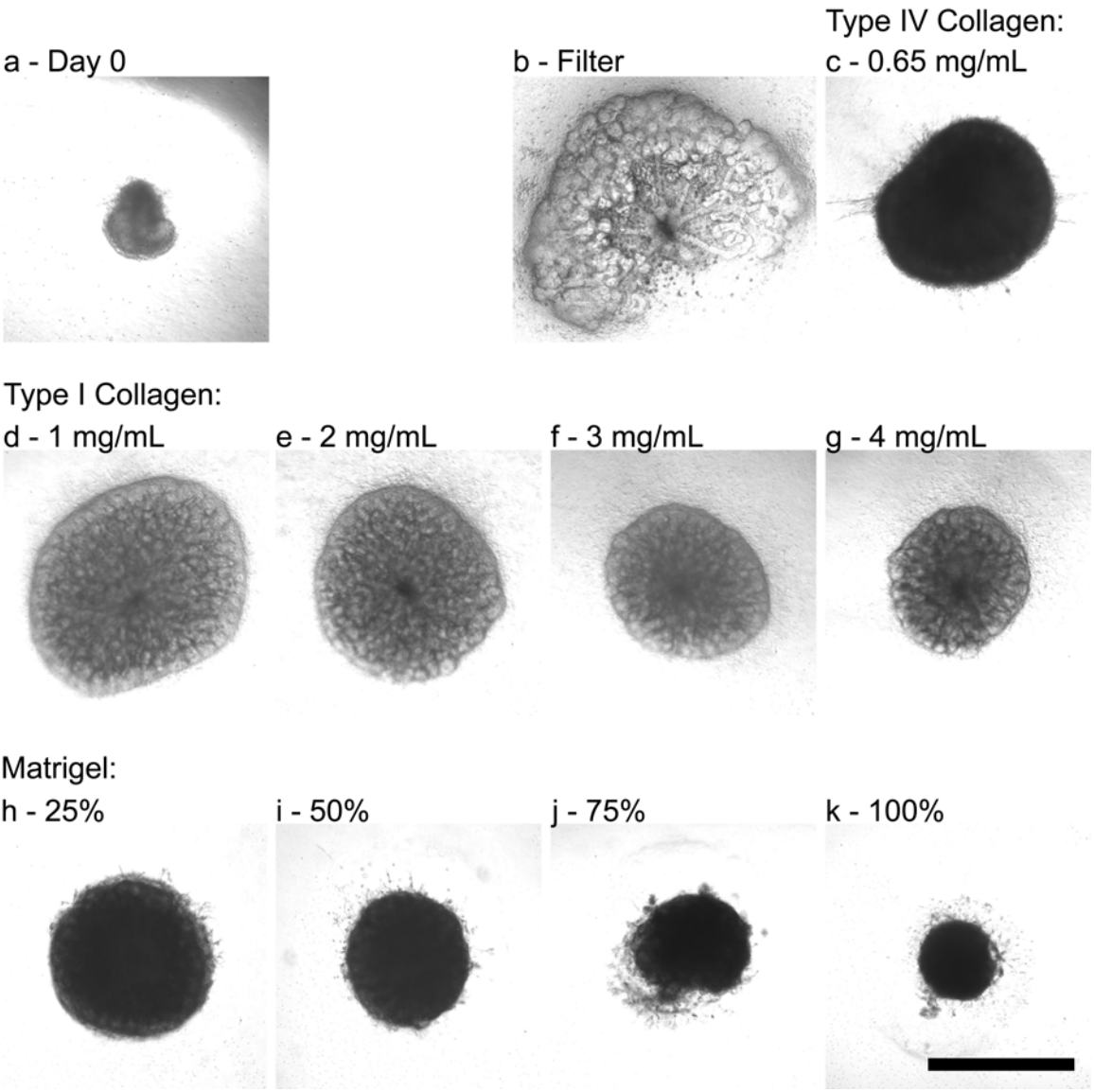

Figure 3.4: 3D metanephric kidney culture. Scale bar corresponds to 1000 μm.

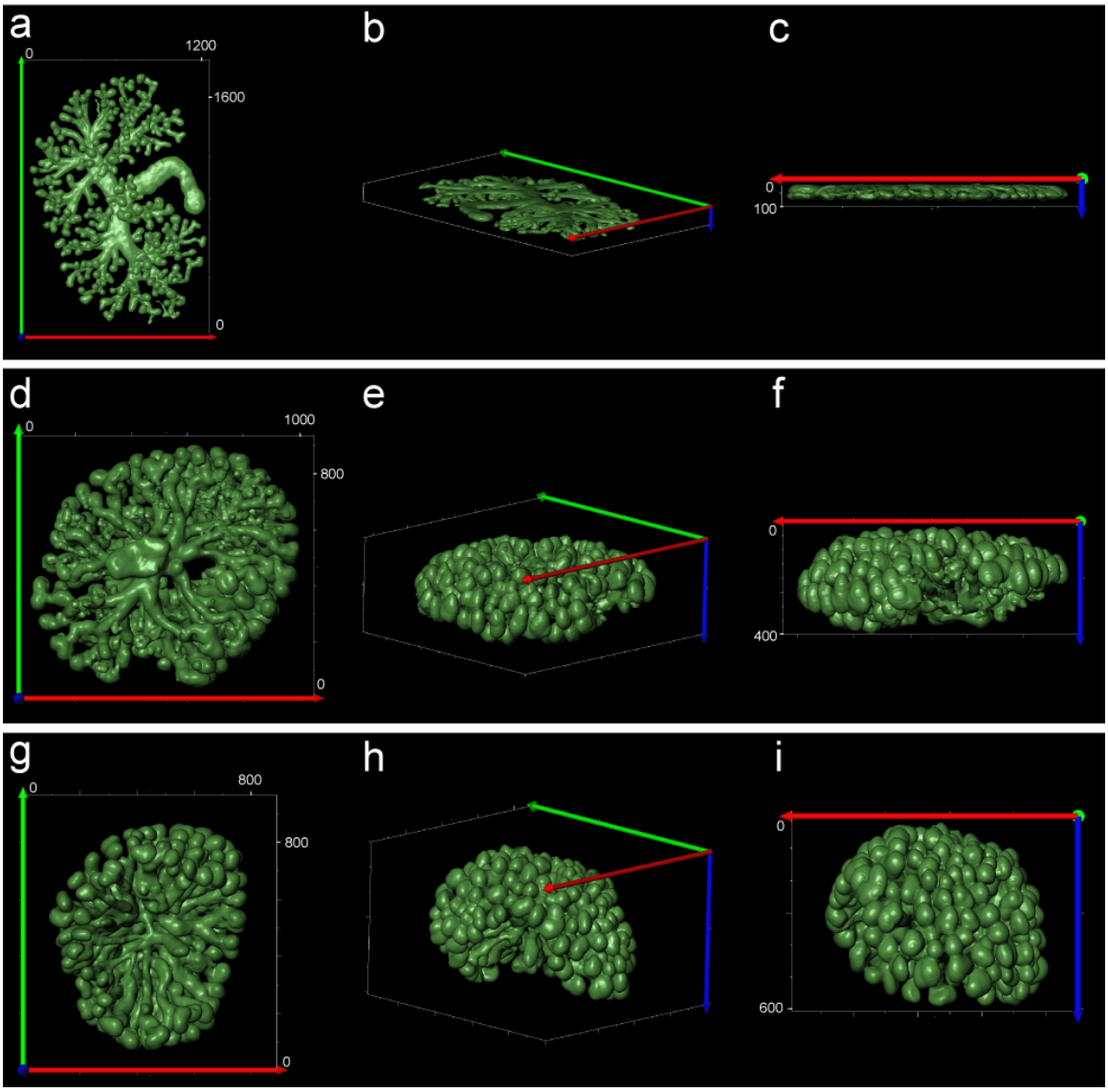

Figure 3.5: 3D projection of the branching ureteric bud of E12 HoxB7-GFP mouse kidneys cultured for 7 days. Kidneys in the traditional filter culture grew flat and along the filter (a-c), while kidneys cultured in type I collagen (d-f) or type IV collagen (g-i) grew much thicker and in a more 3D manner (units, μm).

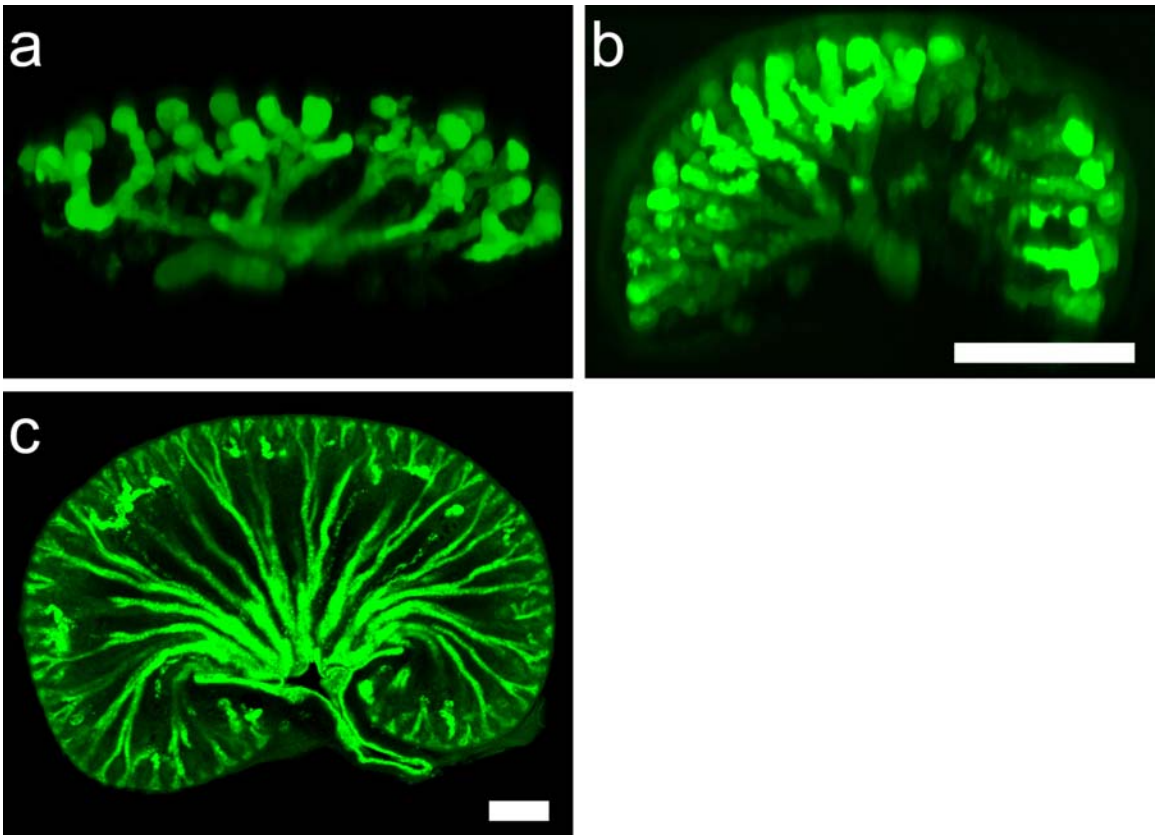

Figure 3.6: Cross sections of E12 HoxB7-GFP mouse kidneys cultured for 7 days in collagen gels. Kidneys cultured in type I collagen (a) exhibit less of the umbrella shape seen in kidneys cultured in type IV collagen (b). A cross section of an E19 rat kidney demonstrates the curving of the branches and umbrella shape typical of *in vivo* kidney development (c). Scale bars correspond to 300 μm.

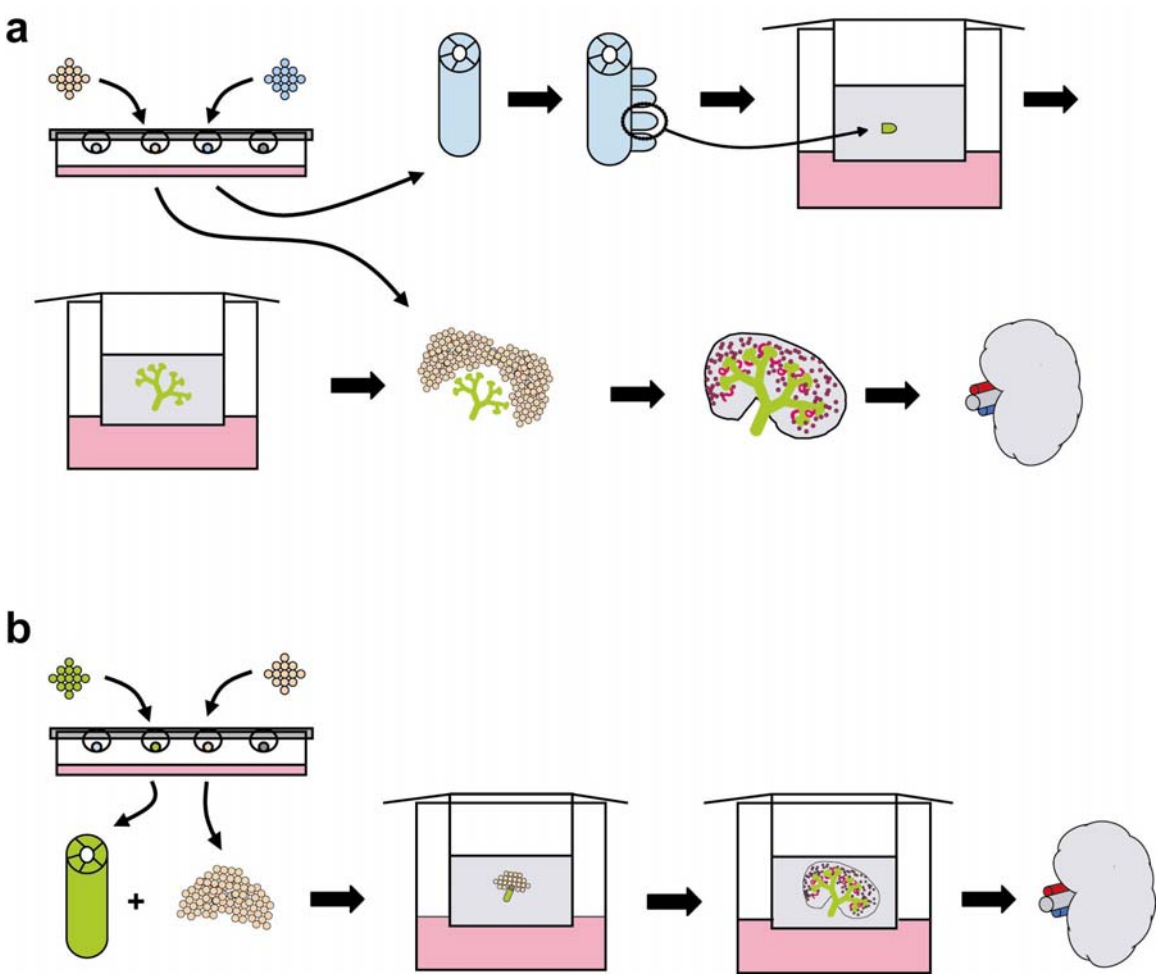

Figure 3.7: Developmental approaches to *in vitro* engineering of kidney tissues. In the first method, the Wolffian duct and metanephric mesenchyme progenitor tissues are constructed from cells and then induced to recapitulate kidney development in a stepwise fashion (a). In the second method, a Wolffian duct is constructed from cells and placed adjacent to mesenchyme in a 3D culture system recreating the embryonic kidney (b).

CHAPTER 4:

The Effect of Hyaluronic Acid Size and Concentration on Branching Morphogenesis and Tubule Differentiation in Developing Kidney Culture Systems: Potential Applications to Engineering of Renal Tissues

4.1 Abstract

Hyaluronic acid (HA) is a glycosaminoglycan of tissue engineering importance that plays a vital role in mammalian development. *In vitro* kidney culture methods were utilized to investigate the importance of HA during renal organogenesis. We found that HA has the ability to simultaneously modulate ureteric bud (UB) branching, promote mesenchymal-to-epithelial transformation, and promote differentiation of both metanephric mesenchyme (MM) and the UB depending on the concentration and molecular weight (MW) of HA. Hyaluronidase inhibited branching morphogenesis in both isolated UB and whole kidney cultures, suggesting endogenous HA is required for branching morphogenesis. HA exhibited morphogen-like properties, stimulating branching morphogenesis at low concentrations (0.1%) and low MW (6.55 kDa) but inhibiting at high concentrations (3.75%) and high MW (234.4 kDa). Furthermore, HA of every MW tested promoted collecting duct differentiation as measured by AQP-2 expression. E-cadherin immunostaining and qPCR of nephron differentiation markers

(OAT-1, NaP_i-2, AQP-1, and THP), demonstrated that HA of a variety of MWs strongly promotes mesenchymal epithelialization and nephron differentiation in a concentration-dependent manner. Since the HA synthesis and degradation genes, *has-2* and *hyal-2*, are highly expressed during kidney development, this data suggests that specific sizes and concentrations of HA may act to independently regulate UB branching and promote tubular maturation, representing a potential switch for ending branching morphogenesis, as well as initiating nephron differentiation. In addition, the ability of HA to promote *in vitro* embryonic kidney growth and maturation, together with the biocompatibility and crosslinking capability of HA, suggests a potential use of HA for both creating an instructive, 3D scaffold for *in vitro* kidney engineering from developmental tissues, as well as promoting tubule regeneration in injured or cryopreserved kidneys.

4.2 Introduction

Metanephric kidney development begins with the outgrowth of the ureteric bud (UB) from the Wolffian duct at week 5 in human development and approximately day 12 of rat development. The UB invades the surrounding metanephric mesenchyme (MM) and begins the process of branching morphogenesis. MM cells coalesce around the tips of the branching UB, thereby providing factors that promote UB branching morphogenesis and maturation, while the UB releases factors that promote epithelialization and differentiation of MM cells [159]. While many branching morphogenesis and mesenechymal-to-epithelial transformation (MET) regulatory factors have been identified [11, 18, 132, 136, 151, 152], the mechanism(s) for stopping branching morphogenesis and beginning collecting duct and nephron differentiation is poorly understood. Here we demonstrate that hyaluronic acid (HA) is a molecule that depending on size and concentration can modulate branching morphogenesis and promote differentiation of both the collecting duct and nephrons. Since the majority of nephron formation occurs in the phases of renal development following branching morphogenesis, HA represents a possible switch molecule that stops branching morphogenesis and promotes nephron differentiation.

HA is a simple polysaccharide consisting of repeating disaccharide units of D-glucuronic acid (1-β-3) N-acetyl-D-glucosamine (1-β-4) [80] synthesized by three hyaluronic acid synthase genes, *has-1*, *has-2* and *has-3* [107]. *Has-2* has been demonstrated to be the most important of these genes responsible for at least 97% of HA synthesized during murine embryonic development and murine embryos lacking the *has-*

2 gene exhibit growth retardation evident by embryonic day 9 and lethality by day 9.5 (before ureteric bud outgrowth) [107]. Moreover, exogenous HA has been shown to improve the development of *in vitro* produced bovine embryos and porcine parthenogenic embryos [44, 180]. Together, this data indicates a vital role for HA during mammalian organogenesis and development. In renal organogenesis, HA has been implicated in the branching morphogenesis of ureteric bud (UB) cell lines and has been found to be expressed along with its receptor, CD44, along the basal surface of the branching UB [134]. Furthermore, HA has been demonstrated to be ubiquitously present throughout the interstitial space of the developing kidney [166]. However, much remains to be elucidated about the role of HA in kidney development.

Has-2 synthesizes HA chains between $2x10^5$ – $2x10^6$ Da, yet HA is known to exist *in vivo* at much smaller molecular weights and have different *in vivo* roles based on its molecular weight [62]. The molecular weight of HA is controlled *in vivo* by the degradative hyaluronidases (hyal). Although six different hyaluronidases are potentially involved in HA degradation, *hyal-1* and *hyal-2* are believed to be the primary functional hyaluronidases of mammalian somatic cells [26]. The different hyaluronidases play different roles in regulating HA; for example, *hyal-1* is a secreted protein and breaks down HA to a tetrasaccharide [83], while *hyal-2* exists as a cell anchored protein and degrades HA to 20 kDa fragments [83, 137]. If smaller molecular weights of HA (less than ~20kD) are regulatory molecules for kidney development, then *hyal-2* would be expected to be expressed during kidney development.

HA has been researched extensively for a wide variety of tissue engineering purposes (reviewed in [7]). HA is a non-antigenic, immunocompatible extracellular

macromolecule [138, 139] which has already demonstrated prevalent medical use as an injectible gel for viscosupplementation of osteoarthritic joints [9, 13] and as a dermatological treatment for wrinkles [91, 92, 111]. Because of its hydroxyl and carboxylic acid groups, HA is easily modified to achieve particular characteristics and easily crosslinked to form hydrogels [10, 17, 79, 89, 179, 186]. The ability of HA to promote *in vitro* embryonic kidney growth and maturation demonstrated here, together with the proven biocompatibility and crosslinking of HA, provide evidence for the potential use of HA towards creating an instructive, 3D scaffold for *in vitro* kidney engineering from developmental tissues.

In this study, we used *in vitro* models of kidney development to examine the role of HA in kidney development and its potential role as a scaffold material for *in vitro* kidney tissue engineering. The temporal expression of *has-2* and *hyal-2* during *in vivo* kidney development was characterized by qPCR. Next, hyaluronidase and hyaluronic acid of various molecular weights and concentrations were added to both *in vitro* metanephric kidney and isolated ureteric bud culture systems. Morphometric analysis was used to quantify the effects on branching morphogenesis. UB/MM differentiation was measured by quantitative PCR of functional renal differentiation markers. We found that HA simultaneously modulates UB branching morphogenesis, induces MET, and promotes differentiation in both MM and UB depending on the MW and concentration of HA.

4.3 Methods

4.3.1 Materials and Reagents

Primers were synthesized by Allele Biotechnology (San Diego, CA). Hyaluronidase from *Streptomyces hyalurolyticus* was obtained from Sigma (St. Louis, MO). HA of the following molecular weights were obtained from Lifecore Biomedical (Chaska, MN): 234.4, 132.3, 64.0, 17.0 and 6.55 kDa. BSN cell conditioned media (BSN-CM) was harvested as described previously [136]. Recombinant growth factors, fibroblast growth factor-1 (FGF1) and glial cell-derived neurotrophic factor (GDNF) were obtained from R&D Systems (Minneapolis, MN). Mouse anti-E-cadherin antibodies were from BD Biosciences Pharmingen (San Diego, CA) and goat anti-mouse AlexaFluor 594 was from Molecular Probes (Eugene, OR). FITC-conjugated dolichos biflorus (DB) lectin was from Vector Laboratories (Burlingame, CA). Unless otherwise noted, all other reagents are from Sigma (St. Louis, MO).

4.3.2 Organ Culture

Embryos from timed pregnant Holtzman rats (Harlan, Indianapolis, IN) at day 13 (E13) of gestation (day 0 being the day of appearance of the vaginal plug) were dissected free of surrounding tissues. The metanephric kidneys were isolated and placed on Transwell filters (0.4 μm pore size) (Costar, Cambridge, MA) in 12-well plates. The isolated kidneys were cultured at the media-air interface with 600 μL DMEM/F12 (GIBCO-BRL, Grand Island, NY) supplemented with 10% fetal bovine serum (FBS) (Hyclone, Logan, Utah) and 1% antibiotics (GIBCO-BRL, Grand Island, NY) below the

filter at 37°C and 5% CO_2/100% humidity. When samples were treated with hyaluronidase, the enzyme was added to the media for a final concentration of 50 U/mL. HA was dissolved in sterile 0.2 μm filtered and autoclaved water (Hyclone, Logan, Utah) and then diluted to a 1X DMEM solution, buffered with HEPES (pH 7.2). 270 μL of the HA solution were placed on top of the tissue sample for HA treatment. All treatments were present throughout the indicated culture period.

4.3.3 Isolated Ureteric Bud Culture

Ureteric buds were dissected from E13 kidneys, suspended in a growth factor-reduced Matrigel (BD Biosciences, San Jose, CA) solution (1:1 Matrigel:DMEM/F12), and cultured with BSN-CM supplemented with 10% FBS, 1% antbiotics, 250 ng/mL FGF1, and 125 ng/mL GDNF as described previously [18, 133, 136, 152, 170, 197]. The low growth factor condition utilized a 1:2 BSN-CM:DMEM/F12 media with 30 ng/mL FGF1 (all else remained constant). When samples were treated with hyaluronidase, the enzyme was added to the media for a final concentration of 50 U/mL. For the HA conditions, a HA solution (prepared as described above) was used to dilute the Matrigel to 50% instead of DMEM/F12 to create a gel with the final HA concentration indicated.

4.3.4 Immunofluorescence and Lectin Staining

After the indicated number of days, kidney cultures were fixed for 30 min with 4% paraformaldehyde in PBS. Fixed kidney cultures were rinsed with TBS and extracted in absolute methanol at -20°C for 20 min. Samples were then blocked for 1hr in 3% BSA in TBS-T at 4°C followed by incubation in anti-E-cadherin antibody (1:500 in blocking

solution) for 24 hr at 4°C. Samples were then washed 3x8hr in TBS-T, followed by incubation in AlexaFluor594 antibody (1:2000) and FITC-DB (1:500) for 24 hr at 4°C, and a final 3x8hr washes in TBS-T at 4°C. Samples were then mounted on slides with ProLong Gold antifade reagent (Invitrogen, Carlsbad, CA).

4.3.5 qRT-PCR Analysis

Embryonic kidneys were isolated from time-pregnanat Holtzman rats (Harlan, Indianapolis, IN) at embryonic days 13 - 20 and 8 weeks. The RNA from tissues (either freshly isolated or from tissue culture) was isolated using the RNAqueous Micro kit from Ambion (Austin, TX). Invitrogen's (Carlsbad, CA) SuperScript III Platinum Two-Step qRT-PCR Kit with SYBR Green and the ABI 7500 Fast Real-time PCR System (Applied Biosystems, Foster City, CA) were used to perform qPCR analysis. All primers were designed using the Primer3 website. The following primer sets were used for qPCR: rat AQP-2 (sense and anti-sense: 5'-agagctcttcctgaccatgc-3' and 5'-ccggtgaaatagatcccaag-3', respectively), rat OAT-1 (sense and anti-sense: 5'-gaagagcaggagcagaggaa-3' and 5'-accccactccctttagtgct-3', respectively), rat NaPi-2 (sense and anti-sense: 5'-gccaatgtcatccagaaggt-3' and 5'-tgctctggacaacaaacgtc-3', respectively), rat AQP-1 (sense and anti-sense: 5'-cctggtctcagagcttcctg-3' and 5'-actttggagtgaggggact-3', respectively), rat THP (sense and anti-sense: 5'-atcacacgacaaggtgtcca-3' and 5'-gccacaccaggttttctgtt-3', respectively), and rat GAPDH (sense and anti-sense: 5'-aaggtcatcccagagctgaa-3' and 5'-cctgcttcaccaccttcttg-3', respectively). Samples were incubated at 50°C for 2 min followed by 95°C for 2 min followed by 45 cycles of 15 s at 95°C, 30 s at 56°C, 30 s at 72°C. Dissociation steps were run on all samples.

4.3.6 Imaging and Morphometric Analysis

Fluorescently stained samples were imaged using either the Nikon EZ-C1 confocal system or the FV300 Olympus 2-photon microscopy system. Image and tip number analysis were performed with ImageJ (NIH, Bethesda, Maryland). Isolated UB cultures were imaged by light brightfield microscopy and tips were counted using the Spot RT Slider digital camera attached to a Nikon microscope and Spot Advanced software v4.5 (Diagnostic Instruments, Sterling Heights, MI). The translucent isolated UB sample was divided into three distinct and non-overlapping planes of focus along the z axis. While focused on one plane, the tips of the other two planes were visible but blurred, supporting the view that tips were accounted for in only one plane. Tips were counted by focusing on each plane in sequence, finally summing the total number of tips from each plane to represent the whole 3-D structure.

4.3.7 Statistical Analysis

Statistical significance among conditions was determined by analysis of variance (ANOVA). Additionally, the differences between means of counted tips and gene expression values were compared by Student's *t* test, with *P*-values <0.05 considered significant. All *P*-values compare the experimental value to the untreated control unless otherwise noted with a connecting line. All tip counting experiments, isolated UB and organ culture, represent biological replicates of $n \geq 4$ and gene expression data represents biological replicates of $n \geq 3$. Error bars represent the standard error of the mean.

4.4 Results

4.4.1 *In Vivo* Regulation of HA during Kidney Development

The expression pattern of *has-2* was determined in the whole metanephric kidney throughout development. We performed a qPCR of *has-2* for each day of kidney development from E13 to E20 and at adulthood (Fig. 4.1a). *Has-2* is highly expressed in the kidneys during development, but nearly absent in adult kidneys. Next, we performed the same qPCR for *hyal-2*. *Hyal-2* is a particularly interesting hyaluronidase because it reduces the molecular weight of HA rather than completely degrading HA [83]. In addition, *hyal-2* exists as a glycosylphosphatidyl-inositol linked [137], cell anchored protein and therefore may allow the cell to tightly control the MW of the HA with which it interacts. *Hyal-2* expression remained relatively constant throughout development, but dropped to one-third of the developmental level post-development (Fig. 4.1b). Thus, both the predominant HA synthesis gene (*has-2*) and its degradative enzyme (*hyal-2*) are developmentally regulated in the kidney.

4.4.2 HA-induced Stimulation or Inhibition of UB Branching Depending on Molecular Weight and Concentration

The *has-2* gene knockout mouse is lethal prior to kidney development [107]; therefore, it is difficult to study the effect of HA deficiency on kidney development. One

way to address this issue is to apply *Streptomyces hyalurolyticus* derived hyaluronidase (HA-ase), which is specific for HA and does not cleave chondroitin sulfates, to *in vitro* metanephric kidney cultures. Applying HA-ase to the whole embryonic kidney culture resulted in a 72% decrease in branching morphogenesis and kidney size as measured by tip number (Fig. 4.2). This decrease can be reversed by the addition of HA to the HA-ase.

Since hyaluronidase decreases branching morphogenesis, it would appear to follow that the addition of exogenous HA would promote branching morphogenesis. However, when exogenous HA was added to *in vitro* cultured kidneys, it was found that HA could either promote or inhibit branching morphogenesis depending on the concentration and MW of the applied HA. Decreasing concentrations of exogenous HA, down to 0.1%, led to increases in branching morphogenesis (Fig. 4.3). Concentrations below 1.5% significantly increased the number of tips compared to untreated controls (nearly 2.5x more tips in kidneys treated with 0.1% HA), while concentrations above 1.5% dramatically reduced the number of tips in the organ culture compared to controls (>75% reduction with 3.75% HA) (Fig. 4.3). Similarly, decreasing molecular weights of exogenous HA led to increases in branching morphogenesis (Fig. 4.4). Molecular weights of 17.0 kDa and 6.55 kDa resulted in more than 200% and 300% increases in tip numbers, respectively, compared to controls (Fig. 4.4). Both the inhibitory and stimulatory effects of exogenous HA are reversible by the addition of hyaluronidase (Fig. 4.2c).

To examine the effects of HA directly upon the UB and not in the presence of secondary effects via HA-based alterations to the MM, the effects of HA and HA-ase treatment were analyzed in the isolated UB culture system. Figure 4.5 shows that

treatment of the isolated UB with HA-ase diminishes branching, although to a lesser extent than that seen in whole kidney culture (Fig. 4.2). When high MW exogenous HA (MW = 234.4 KD) was added to the isolated UB, branching morphogenesis was strongly inhibited in a concentration dependent manner (Fig. 4.5a,c,e); hyaluronidase could reverse this inhibition. When a more dilute BSN-CM and lower FGF concentration was used for isolated UB branching stimulation (1:3 diluted BSN-CM and 30 ng/mL FGF1), the effect of hyaluronidase was much more evident (Fig. 4.5g,h). This suggests that higher growth factor concentrations compensate for the removal of HA by HA-ase, raising the possibility that HA may act as a growth factor sink to promote UB branching. If HA is acting as a growth factor sink for branching tissues, then the effect of HA absence (i.e. HA-ase treatment) would be more evident in a growth factor depleted culture condition. Since, low MW and low concentration HA did not affect branching in the isolated UB system as was the case in whole kidney culture (data not shown), it is likely that the mechanism of high MW HA-mediated inhibition of branching is different from the low MW/low concentration HA-mediated stimulation of branching. Moreover, these results suggest that HA-mediated regulation of UB branching is independent of other effects on the kidney.

4.4.3 UB Differentiation into Collecting Duct

While HA was demonstrated to promote UB branching in certain conditions, we also investigated whether HA could promote collecting duct differentiation in addition to its effects on UB growth and branching. Aquaporin-2 (AQP-2), a transporter expressed only in mature collecting ducts [70], was used as a marker of UB maturation; initial

expression of AQP-2 is seen at approximately embryonic day 17 of rat metanephric kidney development [171]. Quantitative PCR revealed that AQP-2 expression was 5.75 fold higher in HA treated kidneys than in untreated controls (Fig. 4.6). Hyaluronidase eliminated this increase, although it had no affect on untreated control kidneys. Every MW HA tested caused increases in AQP-2 expression; although, the lowest molecular weights tested (17.0 kDa and 6.55 kDa) resulted in additional increases in expression (more than 2 fold) over the 234.4, 132.3, and 64.0 kDa molecular weights. However, the data does suggest that HA is dispensable for collecting duct differentiation as exogenous HA-ase does not appear to reduce the level AQP-2 expression in control kidneys (Fig. 4.6). Interestingly, ureteric bud differentiation was stimulated by all tested MWs of HA, including those which inhibited branching morphogenesis, suggesting that UB branching and collecting duct differentiation are independent processes.

4.4.4 Promotion of Mesenchymal-to-Epithelial Transition and Nephron Differentiation by HA

Metanephric mesenchyme differentiates into the tubular epithelium which ultimately forms the various segments of the nephron [159]. E-cadherin is a junction protein that is expressed by the collecting duct and by all segments of the epithelialized mesenchyme [24]. In kidney organ culture, HA appeared to affect the MM by promoting MET evident by E-cadherin immunofluorescence (Fig. 4.7). After 7 days in culture, the mesenchyme of control kidneys formed comma and s-shaped bodies with a few extended tubules, but the mesenchyme-derived tubules of HA treated kidneys were much longer

and more convoluted (Fig. 4.7). This effect can be seen with HA of all molecular weights tested.

To test whether HA was only promoting MET or also promoting differentiation of the tubules into more mature nephrons, kidneys grown in various concentrations/MWs of HA were analyzed by qPCR for four proteins expressed by mature differentiated nephric tubules; organic anion transporter-1 (OAT-1), an early development proximal tubule marker; NaP_i-2, a mid-development proximal tubule marker [173]; Aquaporin 1 (AQP-1), a late development proximal tubule marker [189]; and Tamm-Horsfall protein (THP), an ascending loop of Henle specific maker [164]. E13 rat kidneys cultured with or without a 3.75% HA (MW = 234.4 kDa) solution were analyzed by qPCR after 3, 5, 7, and 9 days of *in vitro* culture for expression of each of the four differentiation markers. Figure 4.8 shows that HA cultured kidneys develop at least 2 days faster than the control kidney cultures evident by the OAT-1 and NaP_i-2 expression patterns. The ascending loop of Henle specific marker, THP, does not increase expression at all after 9 days of *in vitro* culture for the control kidneys, while HA treated kidneys display a 4.5 fold increase after 7 days and 86 fold after 9 days. Next, kidneys cultured for 7 days with different molecular weights of HA were tested for differentiation marker expression levels and compared to the untreated controls. With the exception of AQP1, HA appeared to strongly promote MM differentiation at all tested molecular weights after 7 days (Fig. 4.9); however, HA treated kidneys display a 2 fold greater AQP-1 expression than controls after 9 days in culture (Fig. 4.8c).

When the HA concentration was varied (MW was kept constant at 234.4 kDa), it was seen that the ability of HA to induce MM differentiation was concentration

dependent and absent at concentrations at or below 0.5% HA (Fig. 4.10). Hyaluronidase treatment eliminated the expression increases caused by HA. However, it did not inhibit differentiation marker expression in untreated control kidneys suggesting that HA is not necessary for MM differentiation despite its strong enhancement of this process.

4.5 Discussion

Here we have demonstrated that *has-2* and *hyal-2* are genes highly expressed during kidney development. Along with the observations that HA is ubiquitously present throughout the interstitial space of the developing kidney [166] and that *has-2* is known to be the predominant active enzyme in HA synthesis during embryogenesis [107], a key role for the involvement of *has-2* and HA in kidney morphogenesis seemed plausible. To investigate the role of HA in kidney development, multiple *in vitro* models of kidney development, which mimic various aspects of renal morphogenesis (together and in isolation), were studied in detail.

The removal of HA from the *in vitro* models of kidney development by HA-ase treatment significantly inhibited branching morphogenesis in both whole metanephric kidney and isolated UB *in vitro* cultures (Fig. 4.2). However, HA-ase treated metanephric kidney cultures do not display decreases in the expression of MM maturation markers (i.e. OAT-1, NaP_i-2, AQP-1, and THP) (Fig. 4.10) suggesting that the absence of HA inhibits UB branching morphogenesis, and thus kidney growth, independent of its effects on the MM in the *in vitro* developing kidney. This also suggests that HA may be vital for UB branching morphogenesis, but dispensable for MM maturation. Surprisingly, while

HA may not be necessary for MM maturation, HA addition did stimulate MET and the expression of multiple differentiation markers.

Even though HA-ase inhibited branching morphogenesis, the effect of exogenous HA was bimodal, either promoting or inhibiting branching morphogenesis depending on the concentration of exogenous HA added. Low concentrations of HA (0.1%) tripled the number of tips seen in the metanephric kidney culture compared to controls, while high concentrations of HA (3.75 %) reduced the number of tips by 75%. The inhibition of branching morphogenesis by the high concentrations of HA was found to occur independent of effects upon the MM utilizing the isolated UB system. While the inhibitory effects of high concentration HA could be demonstrated with the isolated UB system, the stimulatory effects of low concentration and low MW HA could not. This can perhaps be explained by the composition of the extracellular matrix in which the isolated UB is grown. This matrix contains Matrigel, which may have interfered with the actions of HA. HA is known to bind various extracellular matrix proteins (including various collagens, fibronectin and chondroitin sulfates, all of which are present in Matrigel [68, 72, 106, 118, 160, 182]) and may not have been able to freely diffuse through the matrix to come in to contact with the suspended UB and stimulate branching via signaling through CD44 or RHAMM (receptor for hyaluronic acid mediated motility) HA receptors. It is also possible that HA acts as a growth factor sink for the ureteric bud. If the exogenously added HA is not in the vicinity of the branching UB (because it is bound throughout the matrix), then it would not be attracting growth factors towards the UB. The latter may be supported by the amplified effect of HA-ase on the isolated UB system when lower growth factors concentrations are used. Higher growth factor concentrations

in the media may be counteracting the effect of HA absence in the isolated UB system by negating the need for a growth factor sink.

Additionally, the discrepancy between the isolated UB system and metanephric kidney culture suggests that the mechanism for inhibition of UB branching by high concentration and high MW HA differs from the mechanism of stimulation by low concentration and low MW HA. While the stimulation of branching by HA may be the result of the growth factor binding capabilities of HA or by direct signaling via the CD44 or RHAMM receptors, the inhibition of branching morphogenesis by HA may be related to the physical characteristics of the HA and the highly viscous nature of the solution. High concentration and high molecular weight HA is very viscous and may be acting as a physical barrier to the growth required for UB branching morphogenesis; this observation could have tissue engineering and developmental relevance.

HA concentration profiles were also found to affect the UB and MM differently. The UB responds to very small or large doses of HA to promote or inhibit branching morphogenesis, respectively, while the enhanced MM differentiation occurs only in response to larger concentrations of HA (1.5% and above). This difference in concentration dependence between the UB and MM in response to HA may represent a mechanism through which HA could act as a developmental switch molecule. During kidney development, branching morphogenesis occurs first, followed by large scale MM differentiation [21]. It is possible that HA is present in relatively low concentrations early in development, but accumulates in the embryonic kidney as development continues. This is supported by the high developmental expression of *has-2*. In this manner, HA would be promoting branching morphogenesis early in development, but as HA

accumulates (either by *has-2* synthesis of HA or perhaps by inhibition of hyaluronidases) branching is inhibited and MM differentiation is stimulated. It may also be possible that the UB and MM are independently controlling the local concentration of HA that is seen to achieve a desired effect. For instance, the UB may be keeping a higher local concentration of HA around stalks that have already branched to promote tubule differentiation, while keeping the concentration lower around the tips to promote branching morphogenesis.

If different MWs of HA play different roles in regulating kidney development, one would expect the *hyal-2* gene to be expressed by the developing kidney. Here we have shown that *hyal-2* is highly expressed during development (3-fold more than the adult kidney) suggesting the potential for HA molecular weight to be a factor in kidney development. Furthermore, we demonstrated that the different MWs of HA (at high concentrations) can have different effects on branching morphogenesis and maturation of the ureteric bud. While high MWs could inhibit branching morphogenesis, low MWs promoted branching morphogenesis. In addition, all MWs of HA tested induced increases in AQP-2 expression, although the lower MWs of HA (6.55 and 17.0 kDa) increased AQP-2 expression by an additional 2-fold compared to higher MWs.

While the multiple molecular weights of HA affected the UB in drastically different manners, the differentiation of MM was independent of the exogenous HA molecular weight. Since UB branching is dependent on HA molecular weight, but the stimulation of MM differentiation is not, it can be inferred that the HA stimulation of MM is independent of the HA effects on UB branching morphogenesis. This independence is important because it provides a second potential mechanism through

which HA can direct the morphogenetic processes of the two renal progenitor tissues and suggests how the kidney could regulate HA molecular weight to act as a developmental switch. It may be possible that the one of the kidney progenitor tissues increases or decreases hyaluronidase action to achieve a response without inhibiting the effect of HA on the other tissue. *Hyal-1* and *hyal-2* are believed to be the two primary hyalurondiases that act in concert to regulate HA size and accumulation [26]. Glycosylphosphatidyl-inositol-anchored *hyal-2* breaks down high molecular weight HA to 20 KD fragments at the cell surface, while *hyal-1* further degrades HA to extinction [83, 137]. It may be possible that the UB and MM are controlling the size and concentration of HA that it sees at the cell surface. Early in development the UB may be using *hyal-2* to keep HA molecular weight below 20 kDa, the size demonstrated to promote UB branching and differentiation, but as development continues, either hyaluronidase action decreases or HA accumulates faster than *hyal-2* can cleave it, leading to a local HA molecular weight increase and therefore cessation of branching morphogenesis. Since MM is not affected by HA molecular weight, MM-related processes would not be affected by the increase in MW, and would continue to mature.

Regulation of HA molecular weight and modulation of HA concentration represent two possibilities of how HA may be acting as a switch or controlling the development of the UB and MM simultaneously, but independently. It is more likely that a combination of these two modes of action is occurring rather than just one or the other. Only a few developmentally relevant molecules are known to affect both branching morphogenesis and mesenchymal differentiation. For example, leukemia inhibitory factor (LIF) and transforming growth factor-β (TGF- β) have both been demonstrated to inhibit

UB branching and promote MM differentiation [11, 18, 132]. However, unlike these growth factors, HA is also capable of stimulating branching morphogenesis and can be regulated by both concentration and molecular weight. A conditional knockout of *has-2* and/or *hyal-2* would assist in testing these ideas *in vivo*; however, the expression data and *in vitro* metanephric kidney culture presented here strongly support a role for HA in renal development, possibly as a switch molecule.

The potential of HA to be a guiding molecule in kidney development has many implications for organ development in general. In addition to gaining a further understanding of kidney development, these results may be useful for *in vitro* kidney engineering. The tissue engineering field has long been interested in HA as a biomaterial, and the results of this paper suggest additional reasons to pursue the application of HA towards *in vitro* organ engineering. In particular, some developmental approaches to kidney engineering involve the use of embryonic tissues as a therapy or as a source of tissues for *in vitro* kidney engineering [31, 142, 168, 169]. Here we have demonstrated that HA is an extracellular molecule that guides and promotes *in vitro* kidney maturation and development. A HA-based scaffold could be designed specifically to promote the *in vitro* development of these kidney tissues. For example, since lower MWs, at high concentrations, promote branching morphogenesis and MM differentiation, a crosslinked HA scaffold could be designed with a high concentration of low MW HA molecules that are released as the matrix is degraded. Alternatively, one could create a bilayered scaffold containing an inner layer of UB promoting low concentrations or low MWs of HA and an outer layer consisting of higher MW molecules that will limit kidney growth to a specified size, yet continue to promote maturation.

Since HA promotes renal tubule development and differentiation, it may also prove useful during renal repair. HA may be able to promote formation of new nephrons in adult kidneys with renal disease. HA receptors or HA analogs may represent a new set of drug targets or therapies to promote in renal tubule regeneration. Furthermore, the potential tubular regenerative capacity of HA may make it a useful additive to cryopreservation solutions. Kidneys used for transplantation are typically perfused with a solution containing an anionic, water absorbing substance to prevent cell swelling during transport [96]. HA could act both as the water absorbing, anionic substance to protect from cell swelling in addition to promoting tubule regeneration in damaged tubules caused by ischemia/reperfusion injury.

4.6 Conclusion

The mechanisms regulating the timing of events in kidney development are not well understood. However, the data we present here illustrates two possibilities of how the synthesis and size regulation of HA could act as a developmental mechanism that ends branching morphogenesis and promotes of nephron differentiation. Furthermore, the ability of HA to promote maturation in the *in vitro* models of kidney development, together with the prevalent use of HA as a biomaterial, suggests the potential of HA as an ideal scaffold for kidney tissue engineering.

4.7 Acknowledgements

This work was supported by NIH grants DK057286, DK065831and HL035018 (to S.K.N.). E.R. was supported by the NSF graduate research fellowship. We also

acknowledge Dr. Kevin Bush and Dr. Hiro Sakurai for their critical reading of this manuscript. We would like to thank the UCSD Neuroscience microscopy shared facility and NINDS grant NS047101 for providing us access to their 2-photon imaging facilities.

Chapter 4, in full, is a reprint of the material as it appears in "The effect of hyaluronic acid size and concentration on branching morphogenesis and tubule differentiation in developing kidney culture systems: Potential applications to engineering of renal tissues" by Rosines E., Schmidt H.J., and S.K. Nigam in Biomaterials, 2007. 28(32): p. 4806-17. Reprinted with permission from the Elsevier publishing company. The dissertation author was the primary investigator and author of this paper.

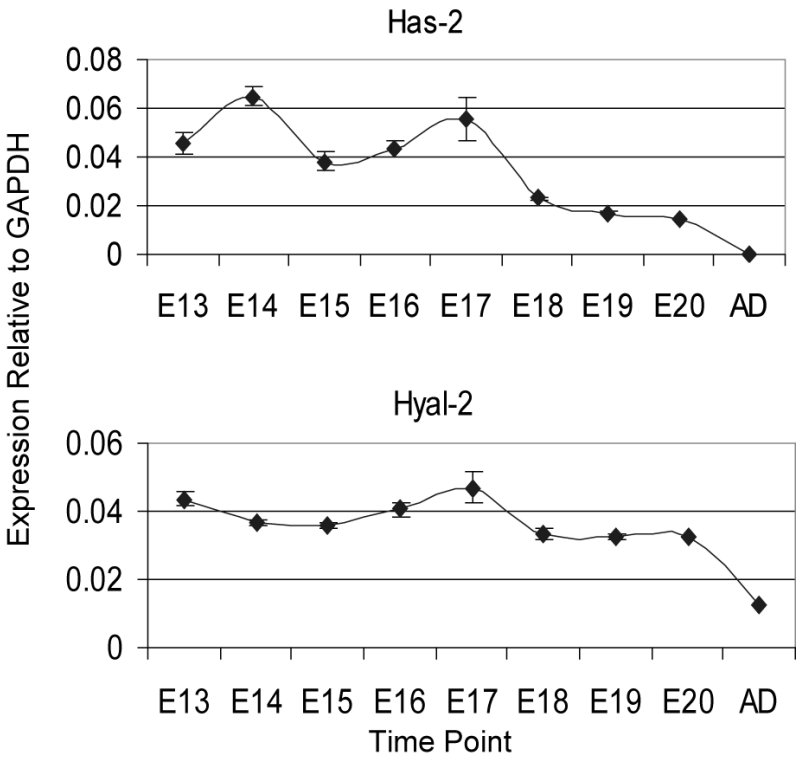

Figure 4.1: Expression of has-2 and hyal-2 in the developing rat metanephric kidney. Q-PCR analysis indicates that both *has-2* and *hyal-2* are highly expressed during kidney development.

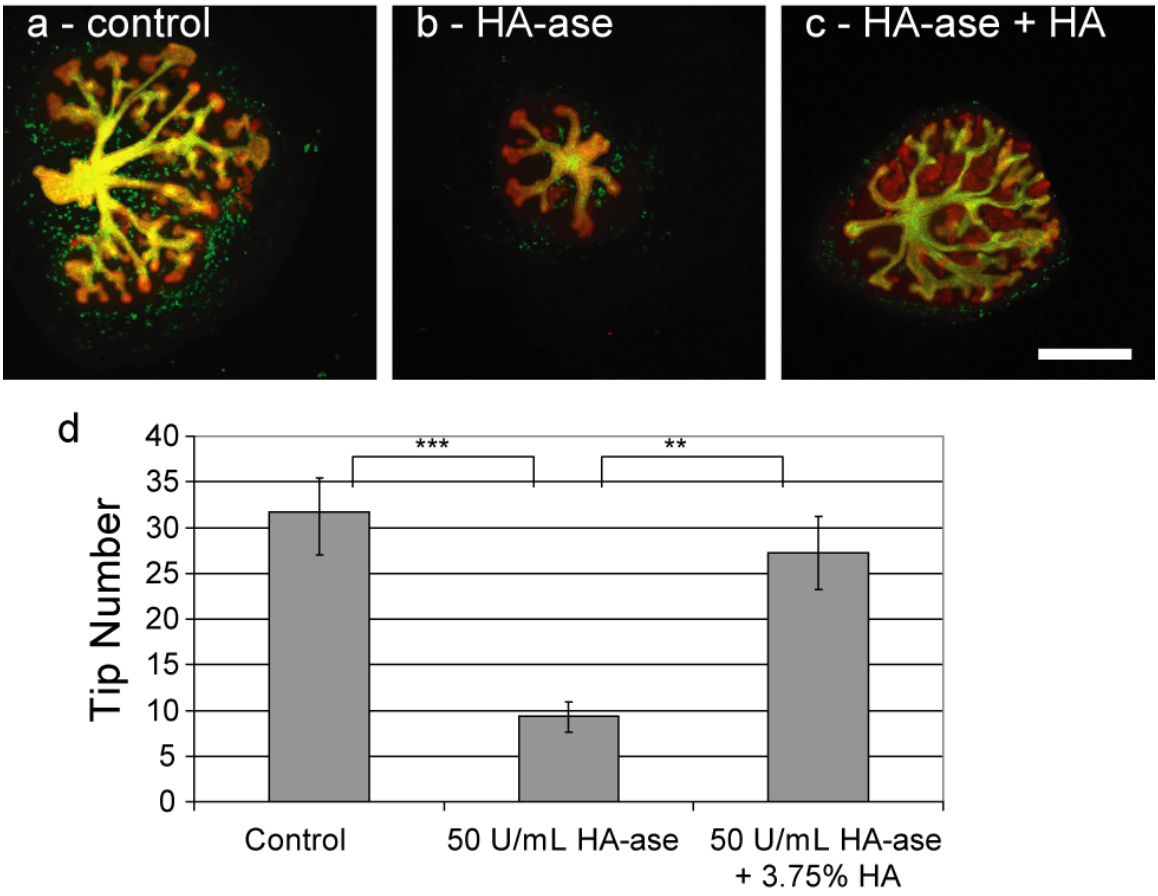

Figure 4.2: Whole embryonic kidney with or without hyaluronidase. (green = DB lectin, UB derived tissues; red = E-Cadherin, UB and MM derived epithelial tissues) (A) Control, (B) 50 U/mL hyaluronidase, (C) 50 U/mL hyaluronidase + 3.75% HA (MW = 234.4 kDa). (D) Plot of tip number vs. condition (ANOVA, $P \leq 0.05$). Tip number measurements of each condition after 7 days of *in vitro* culture. ** = $P \leq 0.005$, *** = $P \leq 0.0005$. Scale bar corresponds to 500 μm.

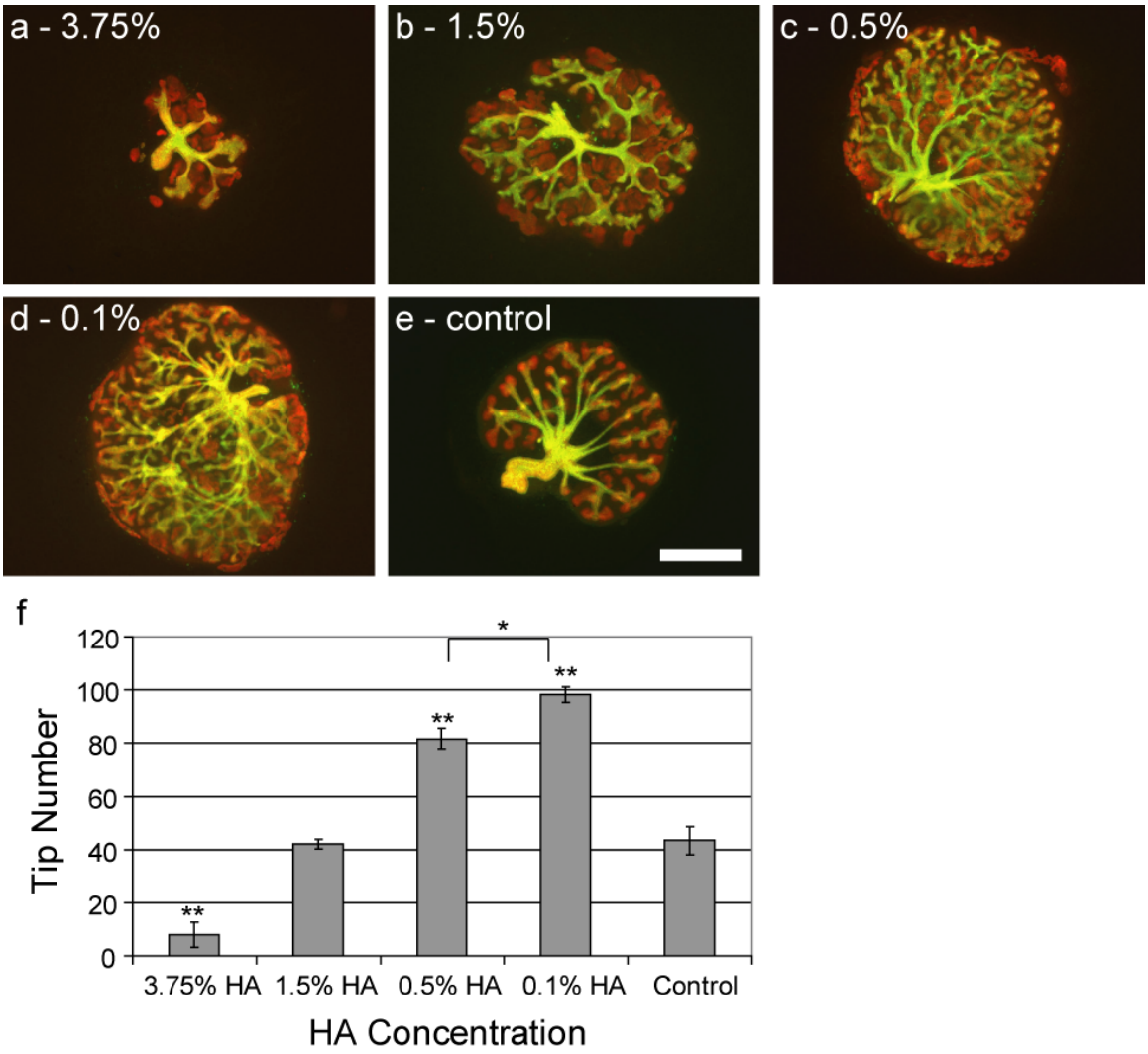

Figure 4.3: Effect of HA concentration on *in vitro* kidney growth and development. Whole embryonic kidneys (green = DB lectin, UB derived tissues; red = E-Cadherin, UB and MM derived epithelial tissues) after 7 days *in vitro* culture with HA, 234.4 kDa. (A) 3.75% (B) 1.5% (C) 0.5% (D) 0.1% (E) control. (F) Plot of tip number vs. HA concentration (ANOVA, $P \leq 0.00001$). * = $P \leq 0.05$, ** = $P \leq 0.001$. Scale bar corresponds to 500 μm.

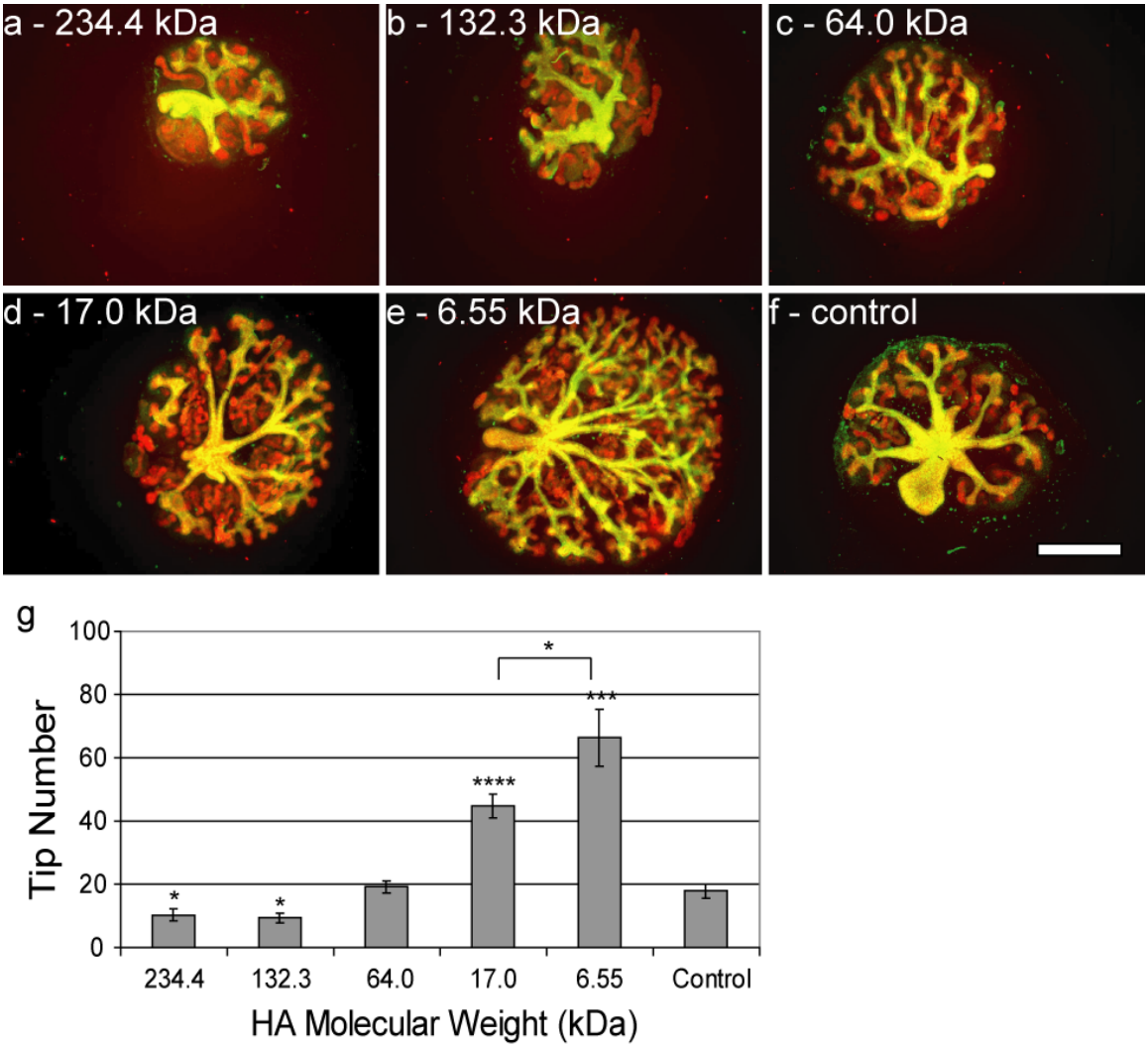

Figure 4.4: Effect of HA molecular weight on *in vitro* kidney growth and development. Whole embryonic kidneys (green = DB lectin, UB derived tissues; red = E-Cadherin, UB and MM derived epithelial tissues) after 7 days *in vitro* culture with 3.75% HA of the following molecular weights: (A) 234.4 kDa, (B) 132.3 kDa, (C) 64.0 kDa (D) MW 17.0 kDa, (E) 6.55kDa, (F) control. (G) Plot of tip number vs. HA molecular weight (ANOVA, $P \leq 0.00001$). * = $P \leq 0.05$, *** = $P \leq 0.0005$, **** = $P \leq 0.0001$. Scale bar corresponds to 500 μm.

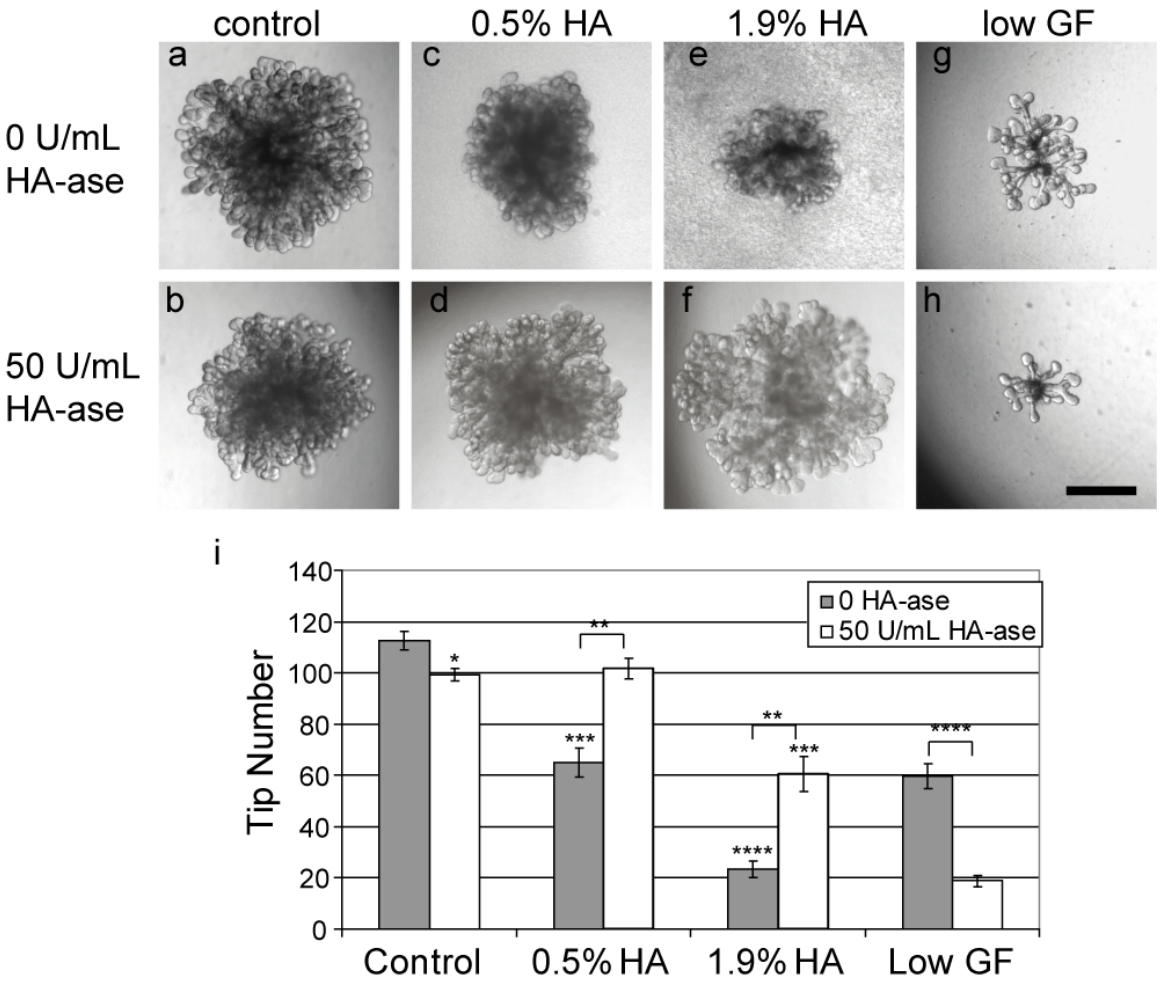

Figure 4.5: Isolated ureteric buds with HA and HA-ase. UB suspended in 50% Matrigel without (A) or with HA-ase (B), 0.5% HA/50% Matrigel without (C) or with HA-ase (D), and 1.9% HA/50% Matrigel without (E) or with HA-ase (F). A low growth factor condition (no HA) without (G) and with HA-ase (H) accentuates the HA-ase inhibition. Tip measurements (I) and pictures were taken after 7 days *in vitro* culture. * = $P \leq 0.05$, ** = $P \leq 0.005$, *** = $P \leq 0.0005$, **** = $P \leq 0.00005$. Scale bar corresponds to 500 μm.

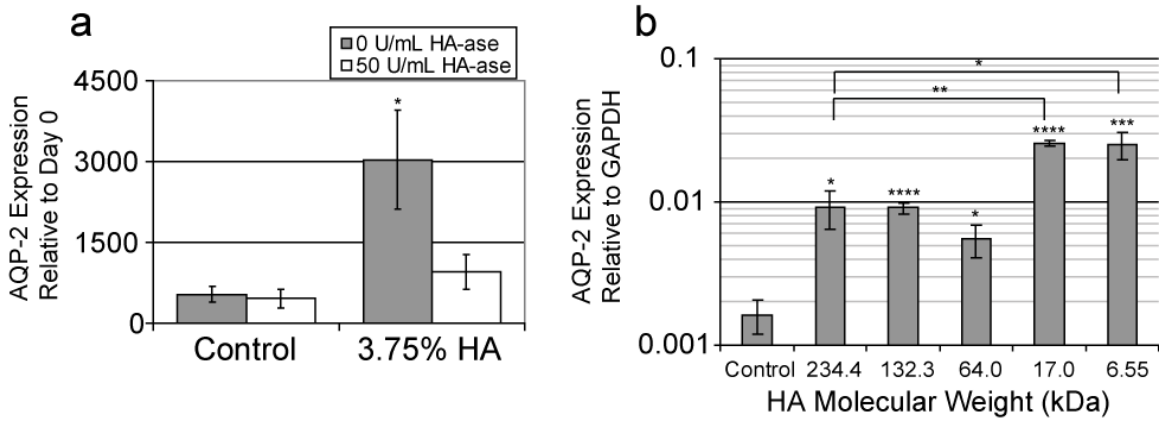

Figure 4.6: AQP-2 expression of embryonic kidney cultures. (A) AQP-2 expression in control kidneys and HA (3.75%, 235 kDa) cultured kidneys with and without HA-ase. (B) AQP-2 expression in kidneys cultured with various MW HA solutions (ANOVA, $P \leq 0.00001$). * = $P \leq 0.05$, ** = $P \leq 0.005$, *** = $P \leq 0.0005$, **** = $P \leq 0.00005$

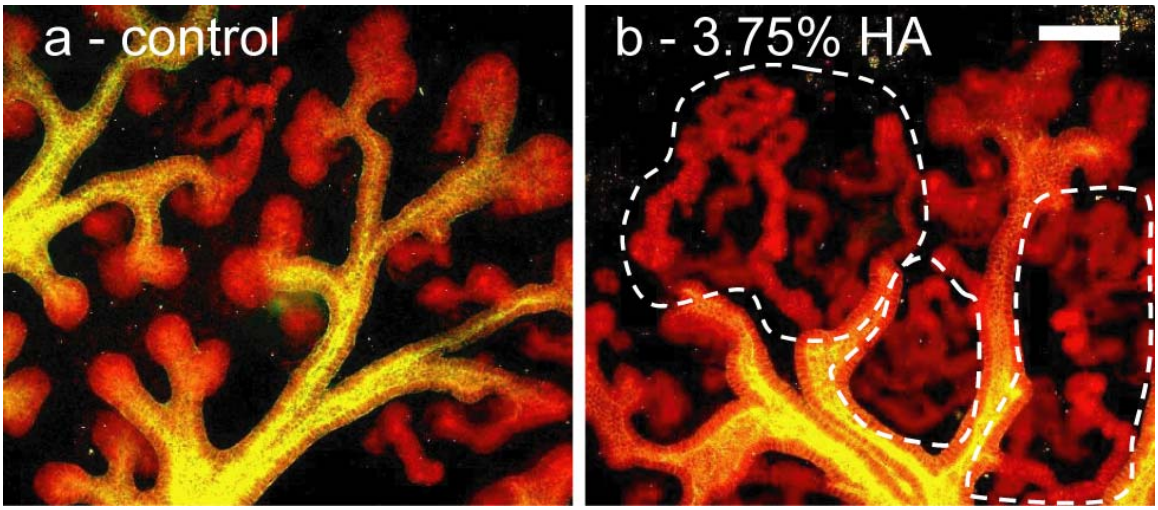

Figure 4.7: 2-photon microscopy images of HA-treated kidney cultures. (green = DB lectin, UB derived tissues; red = E-Cadherin, UB and MM derived epithelial tissues) A) Control B) in 3.75% HA. HA treated kidneys contain longer, more convoluted tubules (noted by the dotted lines). Scale bar corresponds to 100 μm.

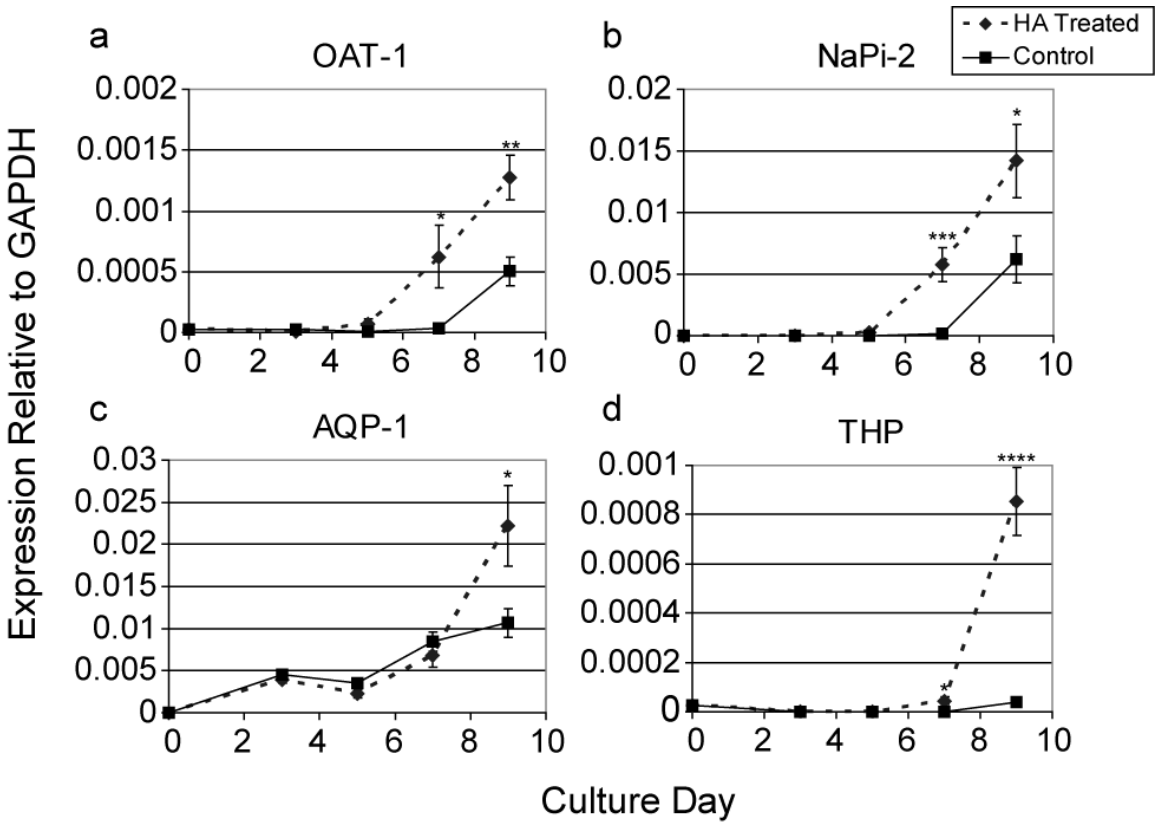

Figure 4.8: Temporal gene expression of nephron differentiation markers in kidneys grown on a filter and kidneys grown in HA. (A) OAT-1, (B) NaPi-2, (C) AQP-1, (D) THP. * = $P \leq 0.05$, ** = $P \leq 0.005$, *** = $P \leq 0.001$, **** = $P \leq 0.0001$

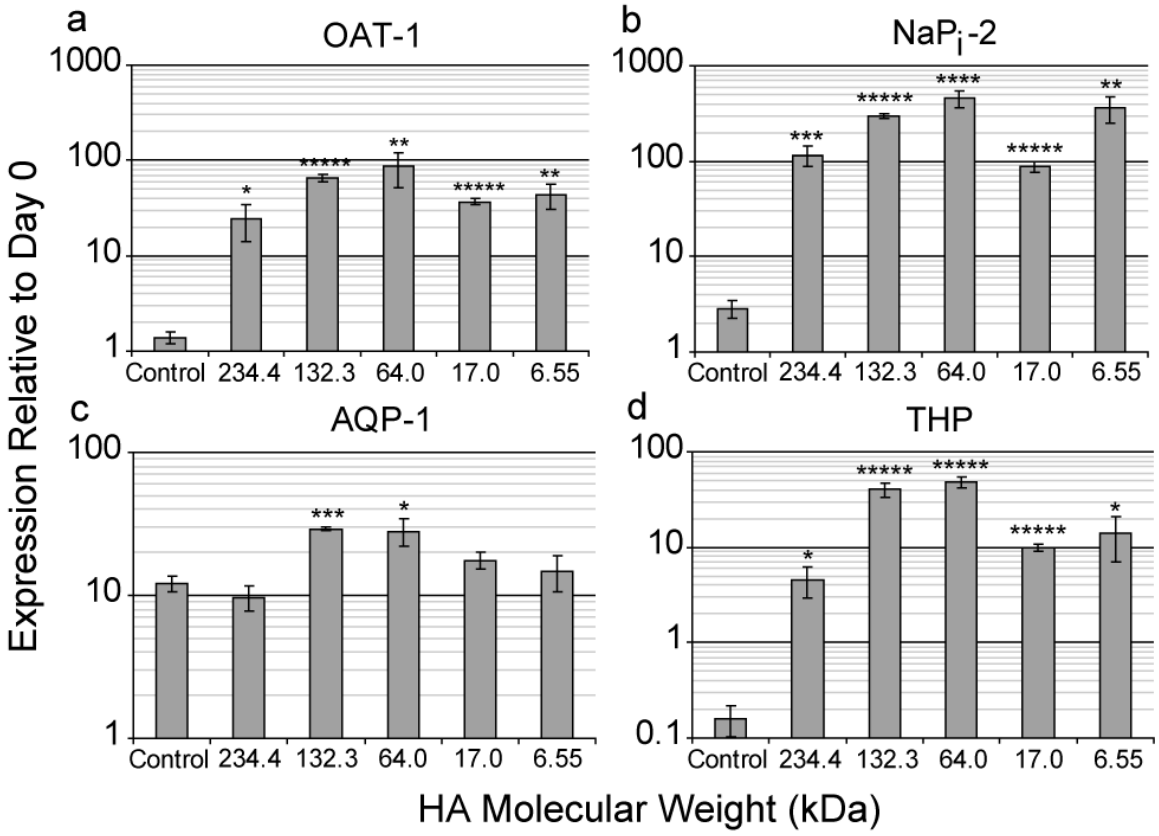

Figure 4.9: Gene expression of nephron differentiation markers after 7 days in culture for various molecular weights of HA. (A) OAT-1 (ANOVA, $P \leq 0.001$), (B) NaPi-2 (ANOVA, $P \leq 0.00001$), (C) AQP-1 (ANOVA, $P \leq 0.0005$), (D) THP (ANOVA, $P \leq 0.00001$). * = $P \leq 0.05$, ** = $P \leq 0.005$, *** = $P \leq 0.001$, **** = $P \leq 0.0001$, ***** = $P \leq 0.00001$

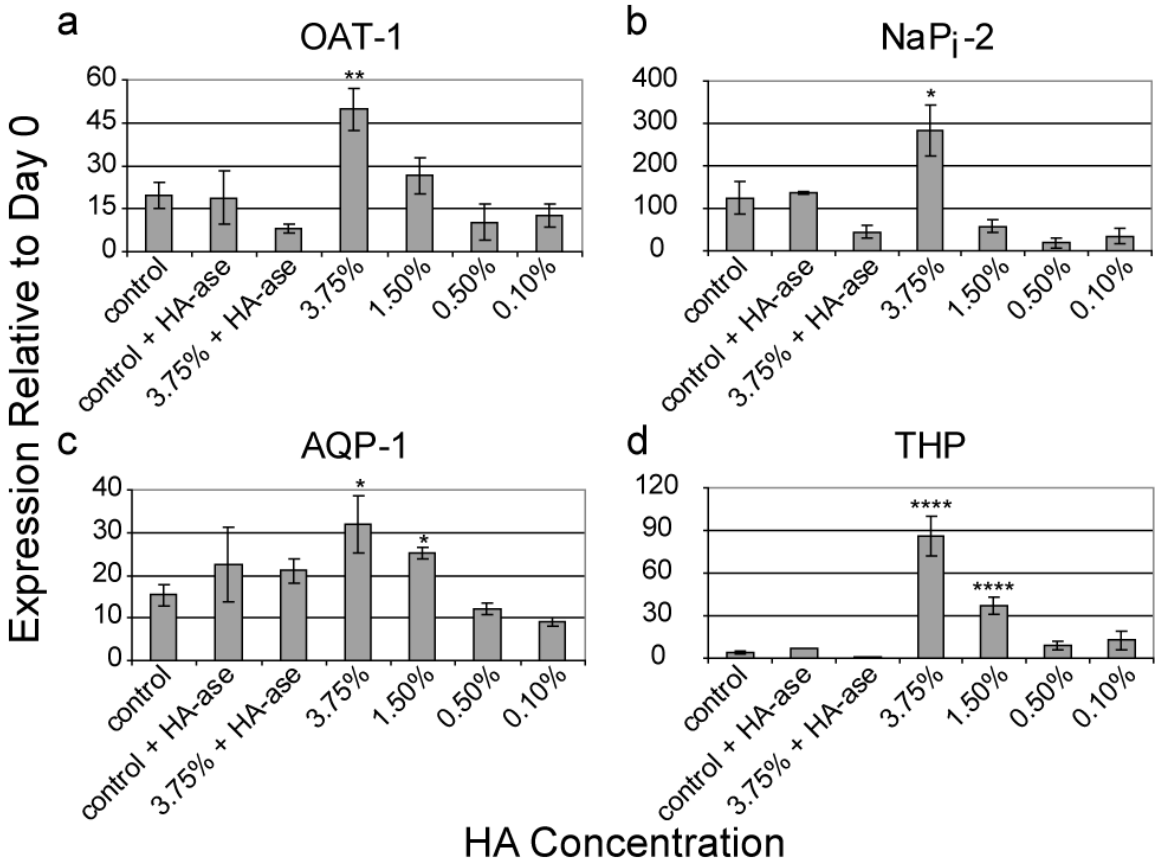

Figure 4.10: Effect of HA concentration on the expression of nephron differentiation markers after 9 days in culture. * = $P \leq 0.05$, ** = $P \leq 0.005$, *** = $P \leq 0.001$, **** = $P \leq 0.0001$

CHAPTER 5:

A MMP-Sensitive Crosslinker for Polymers with Free Hydroxyl Groups

5.1 Abstract

Artificial scaffolds and hydrogels designed for tissue engineering purposes are often designed to degrade over time or not at all. Newer strategies for tissue engineering may need to overcome the obstacle of three dimensional culture for tissue whose growth is of a larger scale than the scaffold pore sizes. A scaffold used for this purpose must be able to both provide support, yet also be remodeled by the suspended tissue as needed. To address this issue, a MMP-sensitive crosslinker molecule with potential to crosslink polymers with free hydroxyl groups has been designed and synthesized. A peptide containing a MMP recognition sequence flanked by cysteine residues was reacted with excess divinyl sulfone resulting in a peptide sequence with hydroxyl-reactive terminal vinyl groups. Reaction products were analyzed by MALDI-TOF-MS and HPLC to reveal a minimal presence of secondary byproducts, and a selectivity for the desired product greater than 9:1. While functionality of the crosslinker is suggested, detailed quality control and functional analysis were beyond the scope of this particular work.

5.2 Introduction

The general goal of tissue engineering is to use living cells to construct a viable tissue or organ that may ultimately be used for clinical purposes. Ideally, these cells would either contain the patients own DNA or be manipulated so that the final tissue engineered product elicits no immune response. In the case of kidney engineering, the goal is to create a kidney or kidney substitute that could be implanted for patients suffering from end stage renal disease. One strategy being pursued is to reconstruct renal progenitor tissues from cells and then culture those renal progenitor tissues *in vitro* to create an implantable kidney tissue [143, 144]. This method relies on obtaining a scaffold that is both biocompatible and can support 3D *in vitro* tissue growth.

Many of the scaffolds used for skin, cartilage, and bone tissue engineering are designed to degrade over time by hydrolysis while the seeded cells divide and migrate between the pores of the scaffold depositing their own extracellular matrix resulting in a final tissue [55, 61, 124]. This technique works for strategies that consist of cells acting individually in a fixed final volume to create a tissue. However, in the case of three dimensional organ culture, such as for the embryonic metanephric kidney, this strategy would not be suitable. The growth process occurs on a larger scale than the pore size of a scaffold and degradation would have to occur only as needed by the developing organ rather than uniformly throughout the scaffold.

To address this problem, scaffolds are being designed to be sensitive to matrix metalloproteases (MMPs) secreted by the suspended cells [94]. Hubbell and Lutolf

designed a MMP-sensitive scaffold using 4-arm polyethylene glycol (PEG) functionalized with divinyl sulfone [93]. This crosslinked biomaterial has been demonstrated to support the growth of various cell types [41, 129, 162]. However, PEG may not be the ideal scaffold for all cell and tissue types. The technique of divinyl sulfone functionalization used by Hubbell and Lutolf requires that the polymer being processed has a limited number of end hydroxyl groups, such as multi-arm PEG. This is so excess divinyl sulfone can be reacted with the polymer to achieve functionalization without immediate crosslinking. Additionally, a polymer with excessive hydroxyl groups, and therefore excessive functionalized divinyl sulfone ends, may yield cytotoxic, free vinyl sulfone groups following reaction with a crosslinker. This limitation excludes other desirable biopolymers, such as hyaluronic acid, which has been demonstrated to enhance *in vitro* growth and differentiation of embryonic kidneys [145]

In order to create MMP-sensitive scaffolds from polymers that may not fulfill the requirement of minimal hydroxyl groups, we have devised a method of using divinyl sulfone to synthesize a functionalized peptide crosslinker, rather than functionalized polymer. The functionalized peptide crosslinker could then potentially be used to crosslink any polymer with free hydroxyl groups, regardless of the number of hydroxyl groups.

5.3 Methods

5.3.1 Crosslinker Synthesis

The peptide sequence Ac-GCRD*GPQG+IWGQ*DRCG-NH_2 (the italicized letters indicate the MMP recognition sequence and the plus sign indicates the cleavage site [162]) was synthesized and obtained from either Global Peptide (Fort Collins, CO) or GL Biochem (Shanghai, China). The peptide was dissolved in molecular biology grade water (Hyclone, Logan, Utah) at a concentration of 1 mg/mL. The peptide was then reacted with divinyl sulfone (DVS) (Sigma, St. Louis, MO) at a molar ratio of either 200:1 or 1000:1 divinyl sulfone:peptide (or 100:1 DVS to -SH group and 500:1 DVS to -SH group). The reaction was left on a shaker for up to 72 hours at room temperature. After the reaction time, the sample was dialyzed against milli Q water using a 500 MWCO dialysis tubing from Spectrum Laboratories (Rancho Dominguez, CA). The dialysis occurred under constant mixing for 72 hours with water changes every 24 hours. After 72 hours, the dialysis tubing was removed from the water tank and then the sample was concentrated by applying 10 g of water absorbent (Spectrum Laboratories, Rancho Dominguez, CA) directly on the outside of the dialysis tubing. After ~90% of the water was absorbed, the sample was transferred to 15 mL culture tubes (2 mL sample/tube) and then lyophilized in the Labconco FreezeZone 4.5.

5.3.2 Synthesis Verification

The peptide synthesis was verified by matrix assisted laser desorption/ionization (MALDI) time of flight (TOF) mass spectrometry (MS) and high pressure liquid

chromatography (HPLC). For the MALDI-TOF-MS, 1 μL of sample (~1 mg/mL) was placed on a sample plate with 4 μL alpha-cyano-4-hydroxycinnamic acid (in 0.1% TFA and 50% acetonitrile) and analyzed with the Voyager DE STR from Applied Biosystems (Foster City, CA). For HPLC analysis, 50 μL of 1 mg/mL sample was submitted to the UCSD Glycotechnology Core Facility.

5.4 Results

5.4.1 Reaction of the Peptide with Divinyl Sulfone

In order to create a crosslinker capable of being used for a wide variety of polymers, the ability of divinyl sulfone to react with hydroxyl and sulfhydryl groups was exploited. First, an MMP-sensitive peptide sequence with cysteine residues on either side of the MMP recognition site was obtained (arginine and aspartate residues were present in the sequence as spacers between the recognition site and the cysteine residues). Then the peptide was reacted with excess divinyl sulfone at a molar ratio of 200:1 divinyl sulfone to peptide. The reaction and potential products are illustrated in Figure 5.1. A sample was collected at after 24, 48, and 72 hr of reaction time. A MALDI-TOF-MS analysis confirmed that there was little to no reactant present after 24 hours (there was no apparent difference between the 24, 48, and 72 hr reaction times) (Fig. 5.2).

5.4.2 Product Identification

The initial peak of the peptide at 1746 Da was absent after 24 hours of reaction time with the product containing one large peak at 1982 Da and one significantly smaller peak at 1864 Da (Fig. 5.2b). These products correspond to the peptide having reacted

with either two or one divinyl sulfone molecules (which has a molecular weight of ~118 Da), respectively. The 1864 Da peak also appeared to be the same size after 24 hr, 48 hr, and 72 hr of reaction time suggesting that the 1864 Da peak represents a terminal product and is not the result of having only one reacted cysteine; it is likely the result of both cysteine residues from one peptide reacting to different ends of the same divinyl sulfone molecule.

In order to eliminate the peak caused by the presence of the self crosslinked peptide, the molar ratio of divinyl sulfone to peptide was increased to from 200:1 to 1000:1. A MALDI-TOF-MS analysis showed that the increase in divinyl sulfone only marginally reduced the size of the peak at 1864 Da (Fig. 5.3). This suggests that the rate of self-crosslinking had already achieved its minimum.

There also existed the possibility that two cysteine residues from different peptides reacting to the same divinyl sulfone could lead to a peptide polymer. To test for this, the MALDI-TOF-MS was examined out to 4000 Da (Fig. 5.4). The lack of a peak at 3730 Da or 3850 Da, which would represent two peptides crosslinked in a closed manner or in an open manner, respectively, signifies that this did not occur.

5.4.3 Product Purity

While MALDI-TOF-MS can accurately give the molecular weight of the species in solution, it is only a qualitative measure of mass and cannot quantitatively provide purity of the desired product. Therefore, HPLC analyses were performed on the products from two independent runs of the peptide synthesis process. Both reaction runs yielded a molar ratio greater than 9:1 of functionalized peptide to self-crosslinked peptide (9.07

and 62.1) and overall purity greater than 90% (90.7% and 93.8%) (Table 1). These results suggest that there is little to no degradation of the peptide throughout the reaction, dialysis, and lyophilization processes and that the desired crosslinker product can be reproducibly attained with purity greater than 90%.

5.5 Discussion

Here we present a method of synthesizing a MMP-sensitive crosslinker that has the potential to be used with any polymer containing free hydroxyl or sulfhydryl groups. Divinyl sulfone is a molecule with two free vinyl groups that can react with hydroxyl and sulfhydryl groups by Michael-type addition resulting in a covalent bond. In the reaction presented here, excess divinyl sulfone was reacted with a peptide sequence containing cysteine residues on both ends surrounding a MMP recognition site. The result was a MMP-sensitive peptide sequence with cysteine residues on both ends functionalized to contain a free vinyl group. This vinyl groups are free to react with a polymer of interest trapping cells or tissue in a MMP-sensitive 3D scaffold (Fig. 5.5).

The particular MMP recognition sequence used in this reaction (GPQG+IWGQ) was selected for its broad MMP sensitivity and demonstrated use as crosslinker [95, 117]. The broad MMP sensitivity should render this crosslinker useful for many tissue types; however, this sequence may be especially useful for the goal of supporting *in vitro* kidney development. In particular, this sequence was demonstrated to respond to MMP-2 secreted by endothelial cells [162]. MMP-2, a protease that degrades type IV collagen, is also known to be an active protease during kidney development [82, 133]. Additionally, the MMP-2 substrate, type IV collagen, is the only purified extracellular matrix molecule

that has been demonstrated to support 3D *in vitro* isolated ureteric bud branching [144] and type IV collagen has also been demonstrated to support 3D whole embryonic kidney growth [143].

Previous studies involving divinyl sulfone functionalization performed a 72 hour reaction to allow for reaction completion [93]; therefore, the reaction performed in this study was allowed to proceed for 72 hour, with samples taken for analysis after 24 and 48 hours as well. MALDI-TOF-MS analysis revealed that all of the original peptide was reacted after the first 24 hours. Although all the peptide had reacted, there were two product sizes, 1864 Da (undesired) and 1982 Da (desired), detected by the MALDI-TOF-MS. Since the 1864 Da peak did not reduce in size over the 72 hour reaction period, that product is likely an irreversible product and not an intermediary towards the desired product. One explanation for this would be a self-crosslinked peptide as seen in Figure 1. Since the divinyl sulfone reaction is irreversible, it would not be possible for the self-crosslinked product to be an intermediary to a peptide with two divinyl sulfone groups. Because the cause of the self-crosslinked product is the result of a competition between a divinyl sulfone that has reacted with one of the cysteine groups versus a free divinyl sulfone group, an excess of divinyl sulfone to peptide ratio was employed to minimize the rate of self-crosslinking. However, the original reaction was already performed with a large excess of divinyl sulfone to peptide (200:1), so it was not surprising to find that increasing the ratio to 1000:1 did not eliminate the self-crosslinked product. The ratio of the desired product to the undesired product, or self-crosslinked peptide, was determined to be greater than 9:1, so, while the self crosslinking could not be further inhibited, the reaction still resulted in a greater than 9-fold selectivity towards the desired product.

Other reaction concerns that did not prove to be deleterious included multi-peptide chains and peptide degradation during processing. The MALDI-TOF-MS verified that multi-peptide chains did not occur, possibly because of the dilute concentration of peptide and the large excess of divinyl sulfone. The HPLC analysis of the reaction products following lyophilization and reconstitution showed only two peaks (that of the self crosslinked peptide and that of the desired product) and two small additional peaks in a second run. The two additional peaks from the second HPLC run did not show up on the MALDI-TOF-MS of the same sample suggesting the peaks were caused by contaminants introduced immediately prior to or during the HPLC procedure. The lack of significant peaks on the MALDI-TOF-MS between 500 and 1746 Da, as well as the absence of additional significant peaks in the HPLC analysis, suggest that degradation of the peptide did not occur significantly, if at all, during this process.

Most tissue engineering scaffolds used in the bone and cartilage tissue engineering fields are designed to degrade over time or not degrade at all. While this approach may work for cells that are migrating through a scaffold and slowly depositing their own extracellular matrix, it is not applicable for larger scale processes such as whole organ growth. For this purpose an MMP-sensitive scaffold that can be remodeled by the growing tissue may be necessary. Here we have synthesized a MMP-sensitive crosslinker with the potential to react with polymers containing free hydroxyl or sulfhydryl groups. The divinyl sulfone functionalized peptide represents a potential solution to the need for MMP-sensitive scaffolds. Should this crosslinker be capable of creating hyaluronic acid hydrogels, then it may be possible to create an instructive growth-enhancing scaffold for 3D *in vitro* kidney development.

5.6 Acknowledgements

I would like to acknowledge Miklos Gutman and Dr. Elizabeth Komives for allowing access and assisting with the MALDI-TOF-MS analyses. I would also like to acknowledge the UCSD Glycotechnology Core Facility for performing the HPLC analyses. E.R. was supported by the NSF graduate research fellowship.

Table 5.1: HPLC analysis of functionalized peptide

	Overall Product Purity	**Ratio of Desired Product to Self-crosslinked Product**
Run 1	90.7%	9.07
Run 2	93.8%	62.1

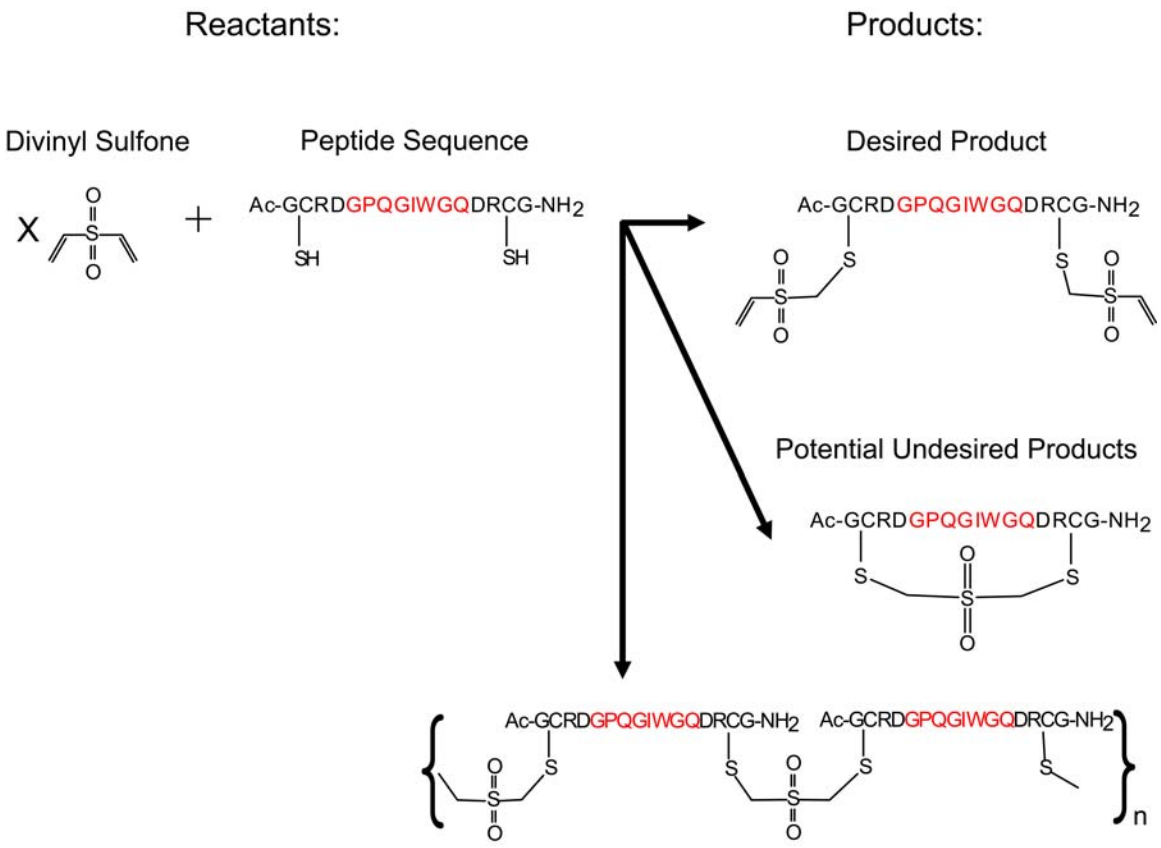

Figure 5.1: Reaction between peptide and divinyl sulfone and the potential products. The MMP recognition site is colored red.

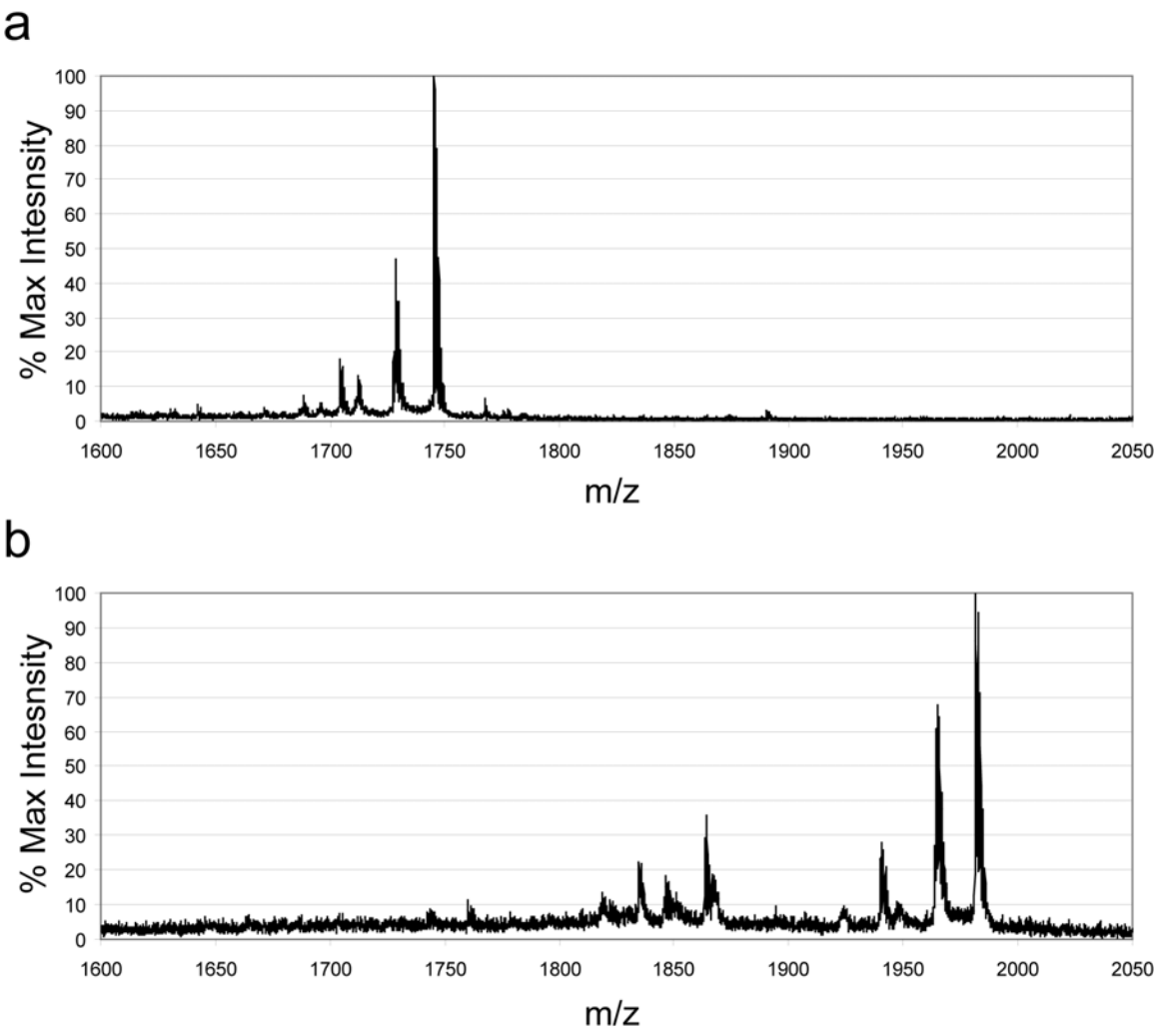

Figure 5.2: MALDI-TOF-MS spectra of the reactants and products using a divinyl sulfone to peptide ratio of 200:1. The peptide before the reaction had a molecular weight of 1746 Da (a), but after 72 hr the peak at 1746 Da was gone and two peaks at molecular weights of 1864 Da or 1982 Da appeared (b). The multiple peaks per product represent normal fragmentation that occurs during the MALDI-TOF-MS process.

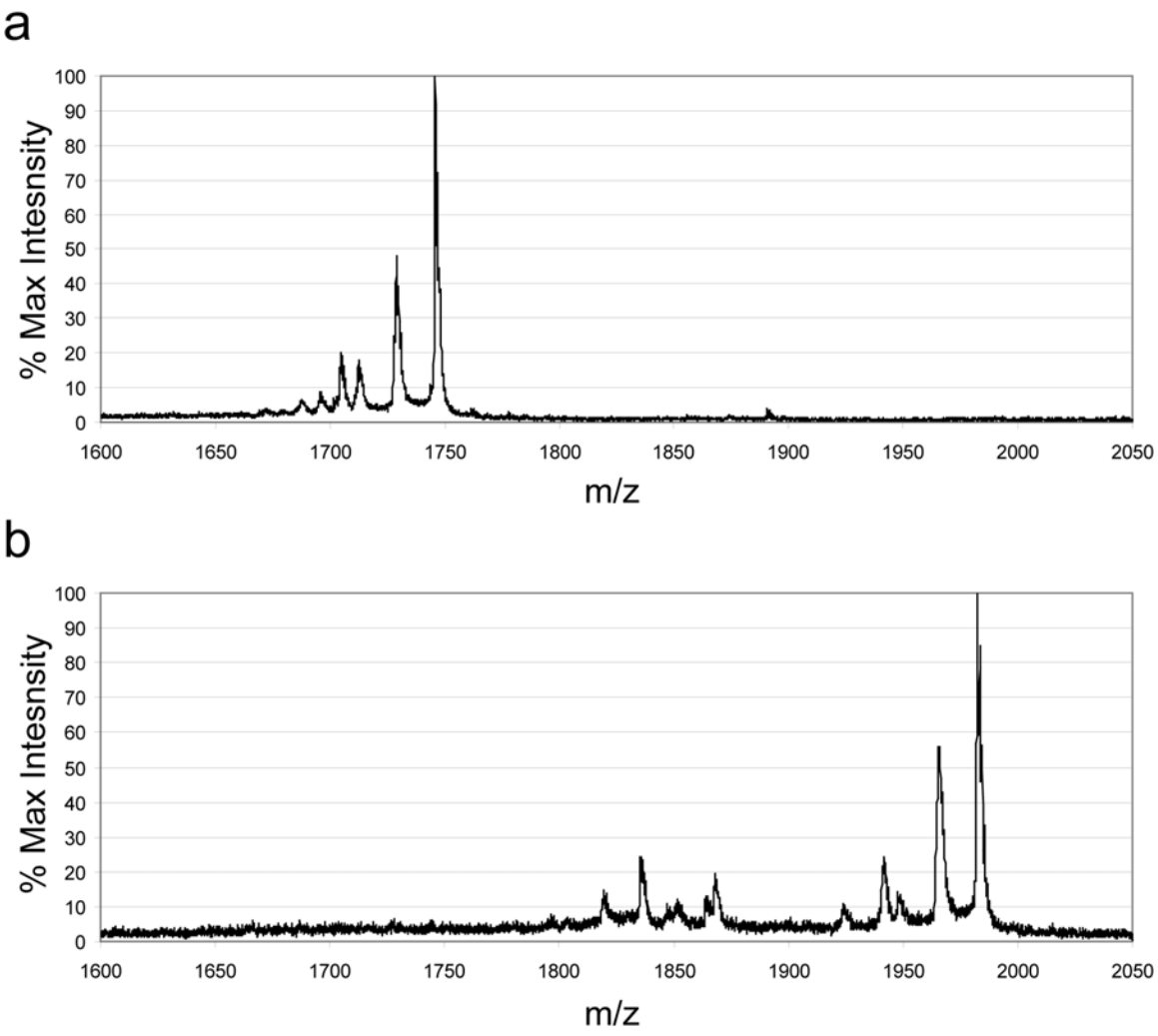

Figure 5.3: MALDI-TOF-MS spectra of the initial peptide and reaction products following a 24 hr reaction with a divinyl sulfone to peptide ratio of 1000:1. The initial peptide has a molecular weight of 1746 Da (a). Similar to the reaction with a 200:1 ratio, all the reactant had been utilized and two peaks were present in the products. The 1864 Da was marginally reduced compared to the reaction with a 200:1 divinyl sulfone to peptide ratio (b).

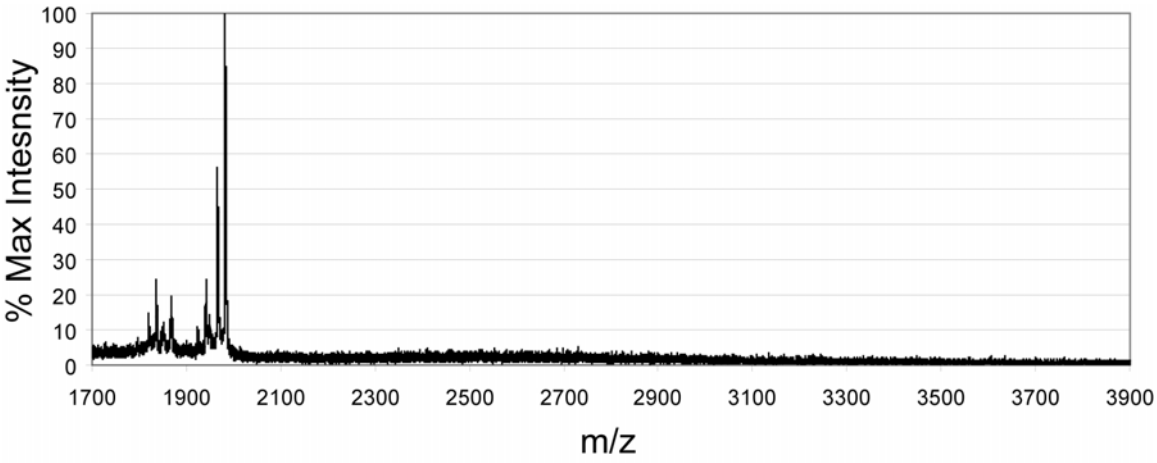

Figure 5.4: MALDI-TOF-MS spectrum of the reaction products after a 24 hr reaction and 1000:1 divinyl sulfone to peptide ratio. There were no peaks above 3500 Da suggesting no peptide multimers formed.

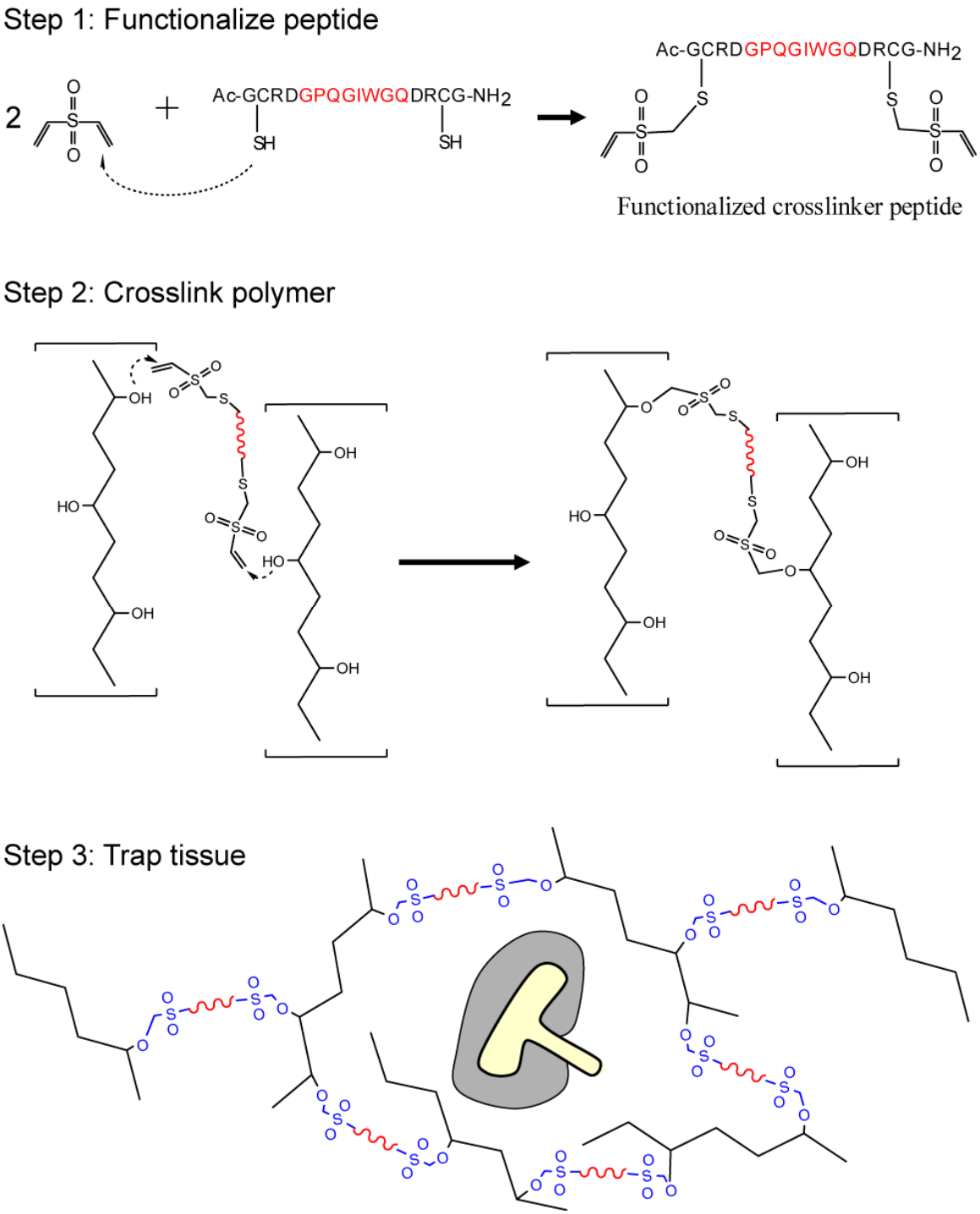

Figure 5.5: Potential application of the MMP-sensitive crosslinker to 3D kidney culture. First the peptide sequence is functionalized with divinyl sulfone. Then the functionalized peptide is reacted with a hydroxyl containing polymer. Finally, a tissue sample (an embryonic kidney is depicted here) is mixed in with the polymer as the reaction is taking place trapping the tissue within the hydrogel.

CHAPTER 6:

Conclusion

The work of this dissertation aims to demonstrate that a developmental approach to *in vitro* engineering of kidney tissues is both plausible and advantageous. While the ultimate goal of creating adult size kidneys as needed without requiring immunosuppression may be a distant prospect, the findings from this thesis as well as the tools and techniques presented in this thesis may represent important advances towards achieving that goal. The developmental approaches presented in this thesis aim to construct renal progenitor tissues from cells and to use those progenitor tissues to create 3D kidney tissues (Fig. 6.1). In one method, the renal progenitor tissues are induced *in vitro* to reproduce each stage of kidney development in a stepwise fashion while in a second method the renal progenitor tissues are directly assembled in to an embryonic kidney-like tissue that would then be cultured in a 3D whole kidney culture.

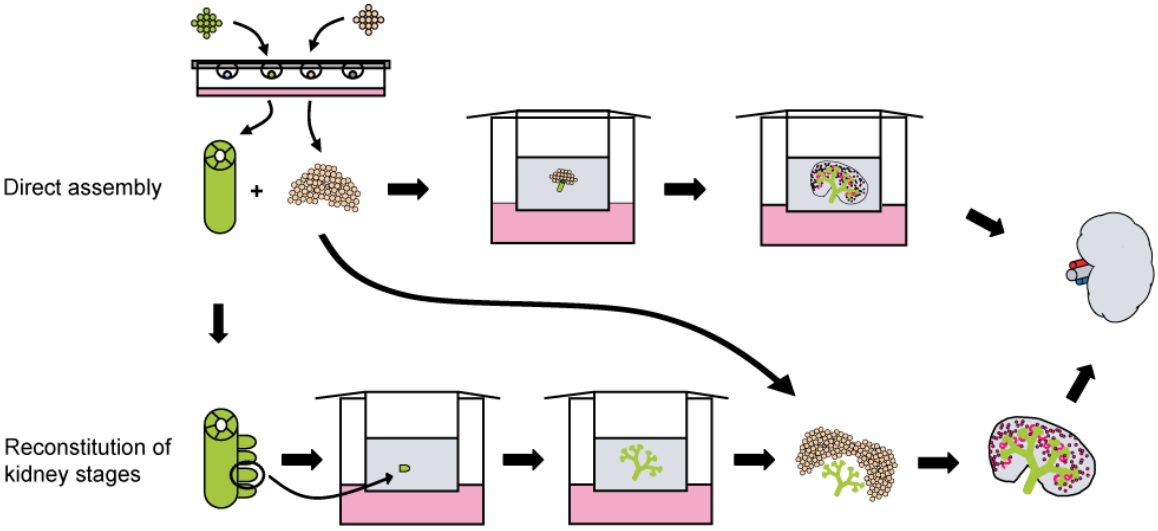

Figure 6.1: Developmental approaches to *in vitro* engineering of kidney-like tissues.

Other strategies currently aiming to provide fully functioning kidneys for organ transplantation include kidney reconstruction by cell sheet engineering [193], kidney reconstruction by seeding cells on decellularized kidney scaffolds [146], or implanting xenogenic partially developed embryonic kidneys [31, 142]. This thesis proposes that the developmental approaches described in this dissertation are more likely to succeed in the ultimate goal because they address problems not addressed by the alternative methods. While limitations exist that must be overcome for the proposed developmental kidney engineering strategies to achieve the ultimate goal, there are many advantages as well. First, the starting biological compoenent for these strategies is potentially only two cell types, an epithelial cell type and a mesenchymal cell type. Starting with cells allows for the potential to generate immunocompatible cells from either autologous adult stem cells, autologous stem cells created by nuclear transplantation, or introduction of immunomodulatory genes. Attaining only two embryonic cell types may represent an

easier goal than attempting to attain multiple adult cell types. Also, it may be easier to differentiate stem cells in to earlier developmental cell lineages rather than adult cell types. Additionally, the structures of an epithelial tube and mesenchymal tissue represent simpler tissues to reconstruct compared to an adult kidney. Similar to the other methods, the final tissue could potentially be a fully functional renal tissue.

The two developmental approaches to engineering tissues presented in this thesis also offer their own individual advantages over one another. *In vitro* reconstitution of kidney tissues in stages offers multiple points of propagation including at the point of cell line propagation, WD budding, and UB branching, whereas the direct assembly strategy offers propagation only at the level of the cells. The method of direct assembly offers the advantage of not requiring conditioned medium, growth factors, or Matrigel for optimal growth, all of which may increase the cost of the strategy and introduce additional potential proteins that may elicit immune responses. Also, the 3D culture of an assembled embryonic kidney may result in more natural 3D growth in which nephrogenesis occurs simultaneously with branching morphogenesis rather than as separate processes.

6.1 Summary of Findings

The findings of this thesis were focused on solving problems and addressing issues related to the developmental approaches for engineering kidney tissues. In Chapter 2, it was shown how *in vitro* models of kidney development could be used sequentially beginning with Wolffian duct (WD) and metanephric mesenchyme (MM) tissues and result in a kidney-like tissue with functional transporters and capable of recruiting an early vasculature when implanted in a host animal. Three different WD systems could be

utilized to induce budding (Fig. 2.1). It was determined that as more tissue surrounding the WD is removed, additional factors, either growth factors or extracellular matrix, had to be added to the culture to achieve budding (Table 2.1). One bud from a budded WD was excised and induced to undergo branching morphogenesis, thus demonstrating how a bud from an *in vitro* budded WD retains the ability to undergo branching morphogenesis and how one WD can produce multiple buds (Fig. 2.2). *In vitro* branching morphogenesis was determined to be type IV collagen dependent (Table 2.2). Recombination of the branched, *in vitro*-formed UB with metanephric mesenchyme resulted in mesenchymal to epithelial transformation (Fig. 2.3). Recombined tissue was demonstrated to regulate gene expression in a manner similar to that of the developing kidney (Table 2.4) and to contain functional organic anion transporters evidenced by cellular 6-carboxyfluorescein uptake (Fig. 2.4). Finally, recombined tissue was found to contain red blood cells and to express the endothelial cell marker, PECAM-1, when implanted under the renal capsule of a host rat (Fig. 2.5).

In Chapter 3, the potential for using homogenous cell lines for the construction of renal progenitor tissues was investigated. It was determined that a WD could replace the UB in embryonic kidney culture suggesting that the UB could be replaced by an epithelial tube of a homogenous cell composition (Fig. 3.1). UB cell aggregates were capable of inducing MM and connecting with MM-derived tubules, but not capable of undergoing branching morphogenesis (Fig. 3.2). Unfortunately, the findings of this research suggest that MM may not be modeled by the homogenous cell populations tested here, but it may be possible that an earlier mesenchymal cell type may be useful for the purpose of creating a mesenchymal renal progenitor tissue.

The strategy to create kidney-like tissues by assembling renal progenitor tissues (ideally constructed from cells) into an embryonic kidney-like structure may be most optimal with an *in vitro* 3D culture system that allows for development of the 3D structure known to be vital for kidney function. It was determined that an E13 rat embryonic metanephric kidney could be cultured *in vitro* to develop a 3D branching structure when suspended in a type I collagen or type IV collagen extracellular matrix molecules (Fig. 3.5). Type IV collagen was determined to allow for thicker tissue growth (600 ± 8 μm in type IV collagen versus 371 ± 7 μm in type I collagen and 79 ± 2 μm on a filter) and an umbrella-like branching pattern reminiscent of *in vivo* kidney development [21]. In addition, it was found that lower concentrations of extracellular matrix molecules allowed for increased kidney growth.

Hyaluronic acid is a biocompatible extracellular matrix molecule commonly used for tissue engineering purposes. Therefore, hyaluronic acid was applied to *in vitro* embryonic kidney culture to both determine if a role exists for HA in kidney development and to investigate the potential for HA as a scaffold material for the 3D *in vitro* kidney culture (Chapter 4). It was determined that HA can modulate branching morphogenesis of the *in vitro* kidney culture, thus stimulating branching morphogenesis at low concentrations (0.1%) and low MW (6.55 kDa) but inhibiting at high concentrations (3.75%) and high MW (234.4 kDa) (Fig. 4.3 and 4.4, respectively). Furthermore, all tested MWs of HA promoted collecting duct differentiation as measured by AQP-2 expression (Fig. 4.6). E-cadherin immunostaining (Fig. 4.7) and qPCR analysis of nephron differentiation markers (OAT-1, NaP_i-2, AQP-1, and THP) revealed that HA of a variety of MWs strongly promotes mesenchymal epithelialization and nephron

differentiation in a concentration-dependent manner (Fig. 4.10). These findings suggest that both the synthesis and size regulation of HA could act as part of a developmental mechanism that ends branching morphogenesis and promotes nephron formation. The ability of HA to promote increased branching morphogenesis and tubular differentiation of *in vitro* embryonic kidney development, together with the biocompatibility and prevalent use of HA as a biomaterial, suggest that HA may be an ideal molecule to pursue as a scaffold for engineering kidney tissues

While HA possesses many attractive qualities for use as a scaffold, there currently does not exist a method of creating an MMP-sensitive, crosslinked HA hydrogel. Therefore, a universal method of crosslinking polymers with hydroxyl groups was devised whereby polymers are crosslinked with an MMP-sensitive peptide sequence whose ends are functionalized with vinyl sulfone (Chapter 5). An MMP-sensitive peptide sequence flanked by cysteine residues was reacted with divinyl sulfone to yield a peptide sequence with vinyl sulfone end groups (Fig. 5.1). This reaction was determined to generate the desired product with a selectivity for the desired product greater than 9. Detailed quality control and functional analysis were beyond the scope of this thesis, but functionality is suggested.

6.2 Future Directions

The findings from this thesis suggest that future studies of the developmental approaches to engineering kidney tissues should focus on four areas – the source of cells for use in renal progenitor tissue construction, the method of progenitor tissue

construction, development of an immunocompatible scaffolding for 3D isolated UB culture and 3D embryonic kidney culture, and methods of *in vitro* vascularization.

Since this research suggested that renal progenitor tissues can be used to create functional renal tissues and that homogenous cells may be a sufficient starting point for the epithelial component of the embryonic kidney (Chapters 2 and 3), further research to identify cell sources would be reasonable. While it may be some time before an ideal autologous or completely immunocompatible source of cells is identified, future work can immediately continue on developing techniques to create an epithelial tubule from cells. Perhaps a novel micropatterning technique placing cells in a tubular orientation is required [119].

The work of this thesis demonstrated that a 3D *in vitro* embryonic kidney culture is in fact possible and suggested that type IV collagen may stimulate *in vivo*-like 3D growth and branching more so than other extracellular matrix molecules (Chapter 3). Additional research analyzing why type IV collagen has this particular effect could help in the design of non-antigenic scaffolds for use in 3D embryonic kidney culture as well as isolated UB branching culture. A potential scaffold polymer, hyaluronic acid, was demonstrated to enhance *in vitro* embryonic kidney development both in terms of branching morphogenesis and tubule differentiation (Chapter 4). A MMP-sensitive crosslinker designed to crosslink polymers such as hyaluronic acid was synthesized (Chapter 5), but preliminary studies were unable to determine the right reaction conditions to support crosslinking. Further work elucidating the conditions under which this crosslinker will work to crosslink polymers, including hyaluronic acid, could lead to the development of an ideal scaffold for *in vitro* kidney engineering.

The last issue that must be addressed is vascularization of the *in vitro* tissue. *In vitro* cultures of embryonic kidneys do not develop a vasculature, which poses a major problem since a kidney without a vasculature cannot be a functioning kidney. While it was demonstrated that a kidney-like tissue engineered in stages could recruit an early vasculature when implanted in to a host (Chapter 2), the implantable tissue was a relatively small mass of tissue. It is currently unknown how many *in vitro* engineered tissues would be necessary to provide adequate function. Also, while partially developed embryonic metanephroi can function when implanted, they have not been demonstrated to fully develop in to kidneys capable of sustaining function in the setting of injury to the native kidney [103]. However, the implantation does demonstrate the ability of these tissues to recruit a vasculature outside of the embryonic environment. To develop adult size kidneys via a developmental approach, a method of *in vitro* vascularization that allows for increased nutrient and oxygen supply as the *in vitro* kidney development occurs may be necessary. There are many ideas yet to be explored, and this limitation should not undermine the development or significance of other aspects of the process that are being investigated and resolved. Some other ideas for *in vitro* vascularization include turning this process into a three cell solution involving endothelial progenitor cells, creating scaffolds with inductive byproducts, or designing a scaffold containing angiogenic factors such as vascular endothelial growth factor, VEGF. Additionally, a micro pump or oxygenated nutrient solution may be necessary components of an *in vitro* vascularization system.

Further directions of this research may also include additional investigation of the role of hyaluronic acid as a switch molecule in kidney development. This thesis indicated

that kidney development is sensitive to both changes in HA concentration and HA molecular weight. A kidney-specific hyaluronic acid synthase-2 knockout mouse could verify whether hyaluronic acid is necessary for kidney development, and a knockout of the hyaluronidase-2 gene could help determine if HA molecular weight is a regulator of kidney development.

References

1. *USRDS 2005 Annual Data Report*. 2005, National Institute of Diabetes and Digestive and Kidney Diseases (NIDDK), National Institutes of Health (NIH), U.S. Department of Health and Human Services (DHHS): Bethesda, MD.

2. *United Network for Organ Sharing*. 2007 [cited 2007 December 1]; Available from: www.unos.org.

3. *USRDS 2006 Annual Data Report*. 2007, National Institute of Diabetes and Digestive and Kidney Diseases (NIDDK), National Institutes of Health (NIH), U.S. Department of Health and Human Services (DHHS): Bethesda, MD.

4. Abrahamson, D.R., P.L. St John, D.J. Pillion, and D.C. Tucker, *Glomerular development in intraocular and intrarenal grafts of fetal kidneys.* Lab Invest, 1991. **64**(5): p. 629-39.

5. Al-Awqati, Q. and M.R. Goldberg, *Architectural patterns in branching morphogenesis in the kidney.* Kidney Int, 1998. **54**(6): p. 1832-42.

6. Albrecht, D.R., G.H. Underhill, T.B. Wassermann, R.L. Sah, and S.N. Bhatia, *Probing the role of multicellular organization in three-dimensional microenvironments.* Nat Methods, 2006. **3**(5): p. 369-75.

7. Allison, D.D. and K.J. Grande-Allen, *Review. Hyaluronan: a powerful tissue engineering tool.* Tissue Eng, 2006. **12**(8): p. 2131-40.

8. Anderson, J.R., D.T. Chiu, R.J. Jackman, O. Cherniavskaya, J.C. McDonald, H. Wu, S.H. Whitesides, and G.M. Whitesides, *Fabrication of topologically complex three-dimensional microfluidic systems in PDMS by rapid prototyping.* Anal Chem, 2000. **72**(14): p. 3158-64.

9. Balazs, E.A., *Viscosupplementation for treatment of osteoarthritis: from initial discovery to current status and results.* Surg Technol Int, 2004. **12**: p. 278-89.

10. Balazs, E.A. and A. Leshchiner, *Crosslinked gels of hyaluronic acid and products containing such gels*. 1986: United States Patent #4,582,865.

11. Barasch, J., J. Yang, C.B. Ware, T. Taga, K. Yoshida, H. Erdjument-Bromage, P. Tempst, E. Parravicini, S. Malach, T. Aranoff, and J.A. Oliver, *Mesenchymal to epithelial conversion in rat metanephros is induced by LIF.* Cell, 1999. **99**(4): p. 377-86.

12. Baroli, B., *Hydrogels for tissue engineering and delivery of tissue-inducing substances.* J Pharm Sci, 2007. **96**(9): p. 2197-223.

13. Bellamy, N., J. Campbell, V. Robinson, T. Gee, R. Bourne, and G. Wells, *Viscosupplementation for the treatment of osteoarthritis of the knee.* Cochrane Database Syst Rev, 2006(2): p. CD005321.

14. Boateng, S.Y., S.S. Lateef, W. Mosley, T.J. Hartman, L. Hanley, and B. Russell, *RGD and YIGSR synthetic peptides facilitate cellular adhesion identical to that of laminin and fibronectin but alter the physiology of neonatal cardiac myocytes.* Am J Physiol Cell Physiol, 2005. **288**(1): p. C30-8.

15. Brenner, B.M. and F.C. Rector, *Brenner & Rector's the kidney*. 7th ed. 2004, Philadelphia: Saunders. 3-60.

16. Bullock, S.L., J.M. Fletcher, R.S. Beddington, and V.A. Wilson, *Renal agenesis in mice homozygous for a gene trap mutation in the gene encoding heparan sulfate 2-sulfotransferase.* Genes Dev, 1998. **12**(12): p. 1894-906.

17. Burdick, J.A., C. Chung, X. Jia, M.A. Randolph, and R. Langer, *Controlled degradation and mechanical behavior of photopolymerized hyaluronic acid networks.* Biomacromolecules, 2005. **6**(1): p. 386-91.

18. Bush, K.T., H. Sakurai, D.L. Steer, M.O. Leonard, R.V. Sampogna, T.N. Meyer, C. Schwesinger, J. Qiao, and S.K. Nigam, *TGF-beta superfamily members modulate growth, branching, shaping, and patterning of the ureteric bud.* Dev Biol, 2004. **266**(2): p. 285-98.

19. Bussolati, B., S. Bruno, C. Grange, S. Buttiglieri, M.C. Deregibus, D. Cantino, and G. Camussi, *Isolation of renal progenitor cells from adult human kidney.* Am J Pathol, 2005. **166**(2): p. 545-55.

20. Byrne, J.A., D.A. Pedersen, L.L. Clepper, M. Nelson, W.G. Sanger, S. Gokhale, D.P. Wolf, and S.M. Mitalipov, *Producing primate embryonic stem cells by somatic cell nuclear transfer.* Nature, 2007. **450**(7169): p. 497-502.

21. Cebrian, C., K. Borodo, N. Charles, and D.A. Herzlinger, *Morphometric index of the developing murine kidney.* Dev Dyn, 2004. **231**(3): p. 601-8.

22. Chen, D., R. Roberts, M. Pohl, S. Nigam, J. Kreidberg, Z. Wang, J. Heino, J. Ivaska, S. Coffa, R.C. Harris, A. Pozzi, and R. Zent, *Differential expression of collagen- and laminin-binding integrins mediates ureteric bud and inner medullary collecting duct cell tubulogenesis.* Am J Physiol Renal Physiol, 2004. **287**(4): p. F602-11.

23. Chia, S.H., B.L. Schumacher, T.J. Klein, E.J. Thonar, K. Masuda, R.L. Sah, and D. Watson, *Tissue-engineered human nasal septal cartilage using the alginate-recovered-chondrocyte method.* Laryngoscope, 2004. **114**(1): p. 38-45.

24. Cho, E.A., L.T. Patterson, W.T. Brookhiser, S. Mah, C. Kintner, and G.R. Dressler, *Differential expression and function of cadherin-6 during renal epithelium development.* Development, 1998. **125**(5): p. 803-12.

25. Coleman, P.J., D. Scott, R.M. Mason, and J.R. Levick, *Characterization of the effect of high molecular weight hyaluronan on trans-synovial flow in rabbit knees.* J Physiol, 1999. **514 (Pt 1)**: p. 265-82.

26. Csoka, A.B., G.I. Frost, and R. Stern, *The six hyaluronidase-like genes in the human and mouse genomes.* Matrix Biol, 2001. **20**(8): p. 499-508.

27. De Coppi, P., G. Bartsch, Jr., M.M. Siddiqui, T. Xu, C.C. Santos, L. Perin, G. Mostoslavsky, A.C. Serre, E.Y. Snyder, J.J. Yoo, M.E. Furth, S. Soker, and A. Atala, *Isolation of amniotic stem cell lines with potential for therapy.* Nat Biotechnol, 2007. **25**(1): p. 100-6.

28. Deed, R., P. Rooney, P. Kumar, J.D. Norton, J. Smith, A.J. Freemont, and S. Kumar, *Early-response gene signalling is induced by angiogenic oligosaccharides of hyaluronan in endothelial cells. Inhibition by non-angiogenic, high-molecular-weight hyaluronan.* Int J Cancer, 1997. **71**(2): p. 251-6.

29. DeGrendele, H.C., P. Estess, and M.H. Siegelman, *Requirement for CD44 in activated T cell extravasation into an inflammatory site.* Science, 1997. **278**(5338): p. 672-5.

30. Dekel, B., N. Amariglio, N. Kaminski, A. Schwartz, E. Goshen, F.D. Arditti, I. Tsarfaty, J.H. Passwell, Y. Reisner, and G. Rechavi, *Engraftment and differentiation of human metanephroi into functional mature nephrons after transplantation into mice is accompanied by a profile of gene expression similar to normal human kidney development.* J Am Soc Nephrol, 2002. **13**(4): p. 977-90.

31. Dekel, B., T. Burakova, F.D. Arditti, S. Reich-Zeliger, O. Milstein, S. Aviel-Ronen, G. Rechavi, N. Friedman, N. Kaminski, J.H. Passwell, and Y. Reisner, *Human and porcine early kidney precursors as a new source for transplantation.* Nat Med, 2003. **9**(1): p. 53-60.

32. Dekel, B., L. Zangi, E. Shezen, S. Reich-Zeliger, S. Eventov-Friedman, H. Katchman, J. Jacob-Hirsch, N. Amariglio, G. Rechavi, R. Margalit, and Y. Reisner, *Isolation and characterization of nontubular sca-1+lin- multipotent stem/progenitor cells from adult mouse kidney.* J Am Soc Nephrol, 2006. **17**(12): p. 3300-14.

33. Dent, C.E., *Rickets and osteomalacia from renal tubule defects.* J Bone Joint Surg Br, 1952. **34-B**(2): p. 266-74.

34. Ekblom, P., E. Lehtonen, L. Saxen, and R. Timpl, *Shift in collagen type as an early response to induction of the metanephric mesenchyme.* J Cell Biol, 1981. **89**(2): p. 276-83.

35. Evans, R.W., D.L. Manninen, L.P. Garrison, Jr., L.G. Hart, C.R. Blagg, R.A. Gutman, A.R. Hull, and E.G. Lowrie, *The quality of life of patients with end-stage renal disease.* N Engl J Med, 1985. **312**(9): p. 553-9.

36. Feinberg, R.N. and D.C. Beebe, *Hyaluronate in vasculogenesis.* Science, 1983. **220**(4602): p. 1177-9.

37. Ferreira, L.S., S. Gerecht, J. Fuller, H.F. Shieh, G. Vunjak-Novakovic, and R. Langer, *Bioactive hydrogel scaffolds for controllable vascular differentiation of human embryonic stem cells.* Biomaterials, 2007. **28**(17): p. 2706-17.

38. Fidkowski, C., M.R. Kaazempur-Mofrad, J. Borenstein, J.P. Vacanti, R. Langer, and Y. Wang, *Endothelialized microvasculature based on a biodegradable elastomer.* Tissue Eng, 2005. **11**(1-2): p. 302-9.

39. Fissell, W.H., D.B. Dyke, W.F. Weitzel, D.A. Buffington, A.J. Westover, S.M. MacKay, J.M. Gutierrez, and H.D. Humes, *Bioartificial kidney alters cytokine response and hemodynamics in endotoxin-challenged uremic animals.* Blood Purif, 2002. **20**(1): p. 55-60.

40. Fissell, W.H., S. Manley, A. Westover, H.D. Humes, A.J. Fleischman, and S. Roy, *Differentiated growth of human renal tubule cells on thin-film and nanostructured materials.* Asaio J, 2006. **52**(3): p. 221-7.

41. Fittkau, M.H., P. Zilla, D. Bezuidenhout, M.P. Lutolf, P. Human, J.A. Hubbell, and N. Davies, *The selective modulation of endothelial cell mobility on RGD peptide containing surfaces by YIGSR peptides.* Biomaterials, 2005. **26**(2): p. 167-74.

42. Foglia, R.P., J. DiPreta, M.B. Statter, and P.K. Donahoe, *Fetal allograft survival in immunocompetent recipients is age dependent and organ specific.* Ann Surg, 1986. **204**(4): p. 402-10.

43. Fraser, J.R., T.C. Laurent, and U.B. Laurent, *Hyaluronan: its nature, distribution, functions and turnover.* J Intern Med, 1997. **242**(1): p. 27-33.

44. Furnus, C.C., D.G. de Matos, and A.G. Martinez, *Effect of hyaluronic acid on development of in vitro produced bovine embryos.* Theriogenology, 1998. **49**(8): p. 1489-99.

45. Garreta, E., E. Genove, S. Borros, and C.E. Semino, *Osteogenic differentiation of mouse embryonic stem cells and mouse embryonic fibroblasts in a three-dimensional self-assembling peptide scaffold.* Tissue Eng, 2006. **12**(8): p. 2215-27.

46. Ghersetich, I., T. Lotti, G. Campanile, C. Grappone, and G. Dini, *Hyaluronic acid in cutaneous intrinsic aging.* Int J Dermatol, 1994. **33**(2): p. 119-22.

47. Gilbert, T.W., T.L. Sellaro, and S.F. Badylak, *Decellularization of tissues and organs.* Biomaterials, 2006. **27**(19): p. 3675-83.

48. Graf, J., R.C. Ogle, F.A. Robey, M. Sasaki, G.R. Martin, Y. Yamada, and H.K. Kleinman, *A pentapeptide from the laminin B1 chain mediates cell adhesion and binds the 67,000 laminin receptor.* Biochemistry, 1987. **26**(22): p. 6896-900.

49. Grobstein, C., *Trans-filter induction of tubules in mouse metanephrogenic mesenchyme.* Exp Cell Res, 1956. **10**(2): p. 424-40.

50. Gupta, S., C. Verfaillie, D. Chmielewski, S. Kren, K. Eidman, J. Connaire, Y. Heremans, T. Lund, M. Blackstad, Y. Jiang, A. Luttun, and M.E. Rosenberg, *Isolation and characterization of kidney-derived stem cells.* J Am Soc Nephrol, 2006. **17**(11): p. 3028-40.

51. Hall, C.L. and E.A. Turley, *Hyaluronan: RHAMM mediated cell locomotion and signaling in tumorigenesis.* J Neurooncol, 1995. **26**(3): p. 221-9.

52. Hammerman, M.R., *Transplantation of embryonic kidneys.* Clin Sci (Lond), 2002. **103**(6): p. 599-612.

53. Hardingham, T.E., *The role of link-protein in the structure of cartilage proteoglycan aggregates.* Biochem J, 1979. **177**(1): p. 237-47.

54. Hishikawa, K., T. Marumo, S. Miura, A. Nakanishi, Y. Matsuzaki, K. Shibata, T. Ichiyanagi, H. Kohike, T. Komori, I. Takahashi, O. Takase, N. Imai, M. Yoshikawa, T. Inowa, M. Hayashi, T. Nakaki, H. Nakauchi, H. Okano, and T. Fujita, *Musculin/MyoR is expressed in kidney side population cells and can regulate their function.* J Cell Biol, 2005. **169**(6): p. 921-8.

55. Hollister, S.J., *Porous scaffold design for tissue engineering.* Nat Mater, 2005. **4**(7): p. 518-24.

56. Homicz, M.R., S.H. Chia, B.L. Schumacher, K. Masuda, E.J. Thonar, R.L. Sah, and D. Watson, *Human septal chondrocyte redifferentiation in alginate, polyglycolic acid scaffold, and monolayer culture.* Laryngoscope, 2003. **113**(1): p. 25-32.

57. Humes, H.D., D.A. Buffington, S.M. MacKay, A.J. Funke, and W.F. Weitzel, *Replacement of renal function in uremic animals with a tissue-engineered kidney.* Nat Biotechnol, 1999. **17**(5): p. 451-5.

58. Humes, H.D., W.F. Weitzel, R.H. Bartlett, F.C. Swaniker, E.P. Paganini, J.R. Luderer, and J. Sobota, *Initial clinical results of the bioartificial kidney containing human cells in ICU patients with acute renal failure.* Kidney Int, 2004. **66**(4): p. 1578-88.

59. Humes, H.D., W.F. Weitzel, and W.H. Fissell, *Renal cell therapy in the treatment of patients with acute and chronic renal failure.* Blood Purif, 2004. **22**(1): p. 60-72.

60. Hutchings, H., N. Ortega, and J. Plouet, *Extracellular matrix-bound vascular endothelial growth factor promotes endothelial cell adhesion, migration, and survival through integrin ligation.* Faseb J, 2003. **17**(11): p. 1520-2.

61. Hutmacher, D.W. and S. Cool, *Concepts of scaffold-based tissue engineering--the rationale to use solid free-form fabrication techniques.* J Cell Mol Med, 2007. **11**(4): p. 654-69.

62. Itano, N., T. Sawai, M. Yoshida, P. Lenas, Y. Yamada, M. Imagawa, T. Shinomura, M. Hamaguchi, Y. Yoshida, Y. Ohnuki, S. Miyauchi, A.P. Spicer, J.A. McDonald, and K. Kimata, *Three isoforms of mammalian hyaluronan synthases have distinct enzymatic properties.* J Biol Chem, 1999. **274**(35): p. 25085-92.

63. Johkura, K., Y. Liang, R.F. Teng, N. Ogiwara, and K. Sasaki, *Nephrogenesis accompanied by vascularisation in the mouse embryonic metanephros transplanted into the adult kidney for the creation of additional nephrons.* Nephrology, 2002. **7**(2): p. 92-100.

64. Kaazempur-Mofrad, M.R., N.J. Krebs, J.P. Vacanti, and J.T. Borenstein. *A MEMS-based renal replacement system*. in *Proceedings of the 2004 Sensors and Actuators Conference*. 2004.

65. Kale, S., A. Karihaloo, P.R. Clark, M. Kashgarian, D.S. Krause, and L.G. Cantley, *Bone marrow stem cells contribute to repair of the ischemically injured renal tubule.* J Clin Invest, 2003. **112**(1): p. 42-9.

66. Kanwar, Y.S., J. Wada, S. Lin, F.R. Danesh, S.S. Chugh, Q. Yang, T. Banerjee, and J.W. Lomasney, *Update of extracellular matrix, its receptors, and cell adhesion molecules in mammalian nephrogenesis.* Am J Physiol Renal Physiol, 2004. **286**(2): p. F202-15.

67. Khetani, S.R. and S.N. Bhatia, *Engineering tissues for in vitro applications.* Curr Opin Biotechnol, 2006. **17**(5): p. 524-31.

68. Kielty, C.M., S.P. Whittaker, M.E. Grant, and C.A. Shuttleworth, *Type VI collagen microfibrils: evidence for a structural association with hyaluronan.* J Cell Biol, 1992. **118**(4): p. 979-90.

69. Kim, D. and G.R. Dressler, *Nephrogenic factors promote differentiation of mouse embryonic stem cells into renal epithelia.* J Am Soc Nephrol, 2005. **16**(12): p. 3527-34.

70. Kishore, B.K., J.M. Terris, and M.A. Knepper, *Quantitation of aquaporin-2 abundance in microdissected collecting ducts: axial distribution and control by AVP.* Am J Physiol, 1996. **271**(1 Pt 2): p. F62-70.

71. Kitamura, S., Y. Yamasaki, M. Kinomura, T. Sugaya, H. Sugiyama, Y. Maeshima, and H. Makino, *Establishment and characterization of renal progenitor like cells from S3 segment of nephron in rat adult kidney.* Faseb J, 2005. **19**(13): p. 1789-97.

72. Kleinman, H.K., M.L. McGarvey, L.A. Liotta, P.G. Robey, K. Tryggvason, and G.R. Martin, *Isolation and characterization of type IV procollagen, laminin, and heparan sulfate proteoglycan from the EHS sarcoma.* Biochemistry, 1982. **21**(24): p. 6188-93.

73. Kunter, U., S. Rong, Z. Djuric, P. Boor, G. Muller-Newen, D. Yu, and J. Floege, *Transplanted mesenchymal stem cells accelerate glomerular healing in experimental glomerulonephritis.* J Am Soc Nephrol, 2006. **17**(8): p. 2202-12.

74. Kushida, A., M. Yamato, Y. Isoi, A. Kikuchi, and T. Okano, *A noninvasive transfer system for polarized renal tubule epithelial cell sheets using temperature-responsive culture dishes.* Eur Cell Mater, 2005. **10**: p. 23-30; discussion 23-30.

75. Kushida, A., M. Yamato, C. Konno, A. Kikuchi, Y. Sakurai, and T. Okano, *Decrease in culture temperature releases monolayer endothelial cell sheets together with deposited fibronectin matrix from temperature-responsive culture surfaces.* J Biomed Mater Res, 1999. **45**(4): p. 355-62.

76. L'Heureux, N., S. Paquet, R. Labbe, L. Germain, and F.A. Auger, *A completely biological tissue-engineered human blood vessel.* Faseb J, 1998. **12**(1): p. 47-56.

77. Langer, R. and J.P. Vacanti, *Tissue engineering.* Science, 1993. **260**(5110): p. 920-6.

78. Lanza, R.P., H.Y. Chung, J.J. Yoo, P.J. Wettstein, C. Blackwell, N. Borson, E. Hofmeister, G. Schuch, S. Soker, C.T. Moraes, M.D. West, and A. Atala, *Generation of histocompatible tissues using nuclear transplantation.* Nat Biotechnol, 2002. **20**(7): p. 689-96.

79. Larsen, N.E., C.T. Pollak, K. Reiner, E. Leshchiner, and E.A. Balazs, *Hylan gel biomaterial: dermal and immunologic compatibility.* J Biomed Mater Res, 1993. **27**(9): p. 1129-34.

80. Laurent, T.C. and J.R. Fraser, *Hyaluronan.* Faseb J, 1992. **6**(7): p. 2397-404.

81. Lee, M., J.C. Dunn, and B.M. Wu, *Scaffold fabrication by indirect three-dimensional printing.* Biomaterials, 2005. **26**(20): p. 4281-9.

82. Legallicier, B., G. Trugnan, G. Murphy, B. Lelongt, and P. Ronco, *Expression of the type IV collagenase system during mouse kidney development and tubule segmentation.* J Am Soc Nephrol, 2001. **12**(11): p. 2358-69.

83. Lepperdinger, G., B. Strobl, and G. Kreil, *HYAL2, a human gene expressed in many cells, encodes a lysosomal hyaluronidase with a novel type of specificity.* J Biol Chem, 1998. **273**(35): p. 22466-70.

84. Levashova, Z.B., S.Y. Plisov, and A.O. Perantoni, *Conditionally immortalized cell line of inducible metanephric mesenchyme.* Kidney Int, 2003. **63**(6): p. 2075-87.

85. Levesque, L., P.L. Brubaker, and A.M. Sun, *Maintenance of long-term secretory function by microencapsulated islets of Langerhans.* Endocrinology, 1992. **130**(2): p. 644-50.

86. Lin-Gibson, S., S. Bencherif, J.A. Cooper, S.J. Wetzel, J.M. Antonucci, B.M. Vogel, F. Horkay, and N.R. Washburn, *Synthesis and characterization of PEG dimethacrylates and their hydrogels.* Biomacromolecules, 2004. **5**(4): p. 1280-7.

87. Lin, F., K. Cordes, L. Li, L. Hood, W.G. Couser, S.J. Shankland, and P. Igarashi, *Hematopoietic stem cells contribute to the regeneration of renal tubules after renal ischemia-reperfusion injury in mice.* J Am Soc Nephrol, 2003. **14**(5): p. 1188-99.

88. Liu Tsang, V., A.A. Chen, L.M. Cho, K.D. Jadin, R.L. Sah, S. DeLong, J.L. West, and S.N. Bhatia, *Fabrication of 3D hepatic tissues by additive photopatterning of cellular hydrogels.* Faseb J, 2007. **21**(3): p. 790-801.

89. Liu, Y., X. Zheng Shu, and G.D. Prestwich, *Biocompatibility and stability of disulfide-crosslinked hyaluronan films.* Biomaterials, 2005. **26**(23): p. 4737-46.

90. Lokeshwar, V.B. and M.G. Selzer, *Differences in hyaluronic acid-mediated functions and signaling in arterial, microvessel, and vein-derived human endothelial cells.* J Biol Chem, 2000. **275**(36): p. 27641-9.

91. Lowe, N.J. and R. Grover, *Injectable hyaluronic acid implant for malar and mental enhancement.* Dermatol Surg, 2006. **32**(7): p. 881-5; discussion 885.

92. Lupo, M.P., *Hyaluronic acid fillers in facial rejuvenation.* Semin Cutan Med Surg, 2006. **25**(3): p. 122-6.

93. Lutolf, M.P. and J.A. Hubbell, *Synthesis and physicochemical characterization of end-linked poly(ethylene glycol)-co-peptide hydrogels formed by Michael-type addition.* Biomacromolecules, 2003. **4**(3): p. 713-22.

94. Lutolf, M.P. and J.A. Hubbell, *Synthetic biomaterials as instructive extracellular microenvironments for morphogenesis in tissue engineering.* Nat Biotechnol, 2005. **23**(1): p. 47-55.

95. Lutolf, M.P., J.L. Lauer-Fields, H.G. Schmoekel, A.T. Metters, F.E. Weber, G.B. Fields, and J.A. Hubbell, *Synthetic matrix metalloproteinase-sensitive hydrogels for the conduction of tissue regeneration: engineering cell-invasion characteristics.* Proc Natl Acad Sci U S A, 2003. **100**(9): p. 5413-8.

96. Maathuis, M.H., H.G. Leuvenink, and R.J. Ploeg, *Perspectives in organ preservation.* Transplantation, 2007. **83**(10): p. 1289-98.

97. Maeshima, A., H. Sakurai, Y. Choi, S. Kitamura, D.A. Vaughn, J.B. Tee, and S.K. Nigam, *Glial cell-derived neurotrophic factor independent ureteric bud outgrowth from the Wolffian duct.* J Am Soc Nephrol, 2007. **18**(12): p. 3147-55.

98. Maeshima, A., H. Sakurai, and S.K. Nigam, *Adult kidney tubular cell population showing phenotypic plasticity, tubulogenic capacity, and integration capability into developing kidney.* J Am Soc Nephrol, 2006. **17**(1): p. 188-98.

99. Maeshima, A., D.A. Vaughn, Y. Choi, and S.K. Nigam, *Activin A is an endogenous inhibitor of ureteric bud outgrowth from the Wolffian duct.* Dev Biol, 2006. **295**(2): p. 473-85.

100. Maeshima, A., S. Yamashita, and Y. Nojima, *Identification of renal progenitor-like tubular cells that participate in the regeneration processes of the kidney.* J Am Soc Nephrol, 2003. **14**(12): p. 3138-46.

101. Mansbridge, J., K. Liu, R. Patch, K. Symons, and E. Pinney, *Three-dimensional fibroblast culture implant for the treatment of diabetic foot ulcers: metabolic activity and therapeutic range.* Tissue Eng, 1998. **4**(4): p. 403-14.

102. Marijnissen, W.J., G.J. van Osch, J. Aigner, S.W. van der Veen, A.P. Hollander, H.L. Verwoerd-Verhoef, and J.A. Verhaar, *Alginate as a chondrocyte-delivery substance in combination with a non-woven scaffold for cartilage tissue engineering.* Biomaterials, 2002. **23**(6): p. 1511-7.

103. Marshall, D., M.R. Dilworth, M. Clancy, C.A. Bravery, and N. Ashton, *Increasing renal mass improves survival in anephric rats following metanephros transplantation.* Exp Physiol, 2007. **92**(1): p. 263-71.

104. Masuda, S., T. Shimizu, M. Yamato, and T. Okano, *Cell sheet engineering for heart tissue repair.* Adv Drug Deliv Rev, 2008. **60**(2): p. 277-85.

105. McBride, W.H. and J.B. Bard, *Hyaluronidase-sensitive halos around adherent cells. Their role in blocking lymphocyte-mediated cytolysis.* J Exp Med, 1979. **149**(2): p. 507-15.

106. McDevitt, C.A., J. Marcelino, and L. Tucker, *Interaction of intact type VI collagen with hyaluronan.* FEBS Lett, 1991. **294**(3): p. 167-70.

107. McDonald, J.A. and T.D. Camenisch, *Hyaluronan: genetic insights into the complex biology of a simple polysaccharide.* Glycoconj J, 2002. **19**(4-5): p. 331-9.

108. Meyer, L.J. and R. Stern, *Age-dependent changes of hyaluronan in human skin.* J Invest Dermatol, 1994. **102**(3): p. 385-9.

109. Meyer, T.N., C. Schwesinger, K.T. Bush, R.O. Stuart, D.W. Rose, M.M. Shah, D.A. Vaughn, D.L. Steer, and S.K. Nigam, *Spatiotemporal regulation of morphogenetic molecules during in vitro branching of the isolated ureteric bud: toward a model of branching through budding in the developing kidney.* Dev Biol, 2004. **275**(1): p. 44-67.

110. Miyake, H., I. Hara, I. Okamoto, K. Gohji, K. Yamanaka, S. Arakawa, H. Saya, and S. Kamidono, *Interaction between CD44 and hyaluronic acid regulates human prostate cancer development.* J Urol, 1998. **160**(4): p. 1562-6.

111. Monheit, G.D. and K.M. Coleman, *Hyaluronic acid fillers.* Dermatol Ther, 2006. **19**(3): p. 141-50.

112. Monte, J.C., H. Sakurai, K.T. Bush, and S.K. Nigam, *The developmental nephrome: systems biology in the developing kidney.* Curr Opin Nephrol Hypertens, 2007. **16**(1): p. 3-9.

113. Montesano, R., K. Matsumoto, T. Nakamura, and L. Orci, *Identification of a fibroblast-derived epithelial morphogen as hepatocyte growth factor.* Cell, 1991. **67**(5): p. 901-8.

114. Morrison, H., L.S. Sherman, J. Legg, F. Banine, C. Isacke, C.A. Haipek, D.H. Gutmann, H. Ponta, and P. Herrlich, *The NF2 tumor suppressor gene product, merlin, mediates contact inhibition of growth through interactions with CD44.* Genes Dev, 2001. **15**(8): p. 968-80.

115. Muthny, F.A. and U. Koch, *Quality of life of patients with end-stage renal failure. A comparison of hemodialysis, CAPD, and transplantation.* Contrib Nephrol, 1991. **89**: p. 265-73.

116. Naets, J.P., *The kidney and erythropoiesis.* Nature, 1958. **182**(4648): p. 1516-7.

117. Nagase, H. and G.B. Fields, *Human matrix metalloproteinase specificity studies using collagen sequence-based synthetic peptides.* Biopolymers, 1996. **40**(4): p. 399-416.

118. Nakamura, M., H. Mishima, T. Nishida, and T. Otori, *Binding of hyaluronan to plasma fibronectin increases the attachment of corneal epithelial cells to a fibronectin matrix.* J Cell Physiol, 1994. **159**(3): p. 415-22.

119. Nelson, C.M., M.M. Vanduijn, J.L. Inman, D.A. Fletcher, and M.J. Bissell, *Tissue geometry determines sites of mammary branching morphogenesis in organotypic cultures.* Science, 2006. **314**(5797): p. 298-300.

120. Nishinakamura, R., Y. Matsumoto, K. Nakao, K. Nakamura, A. Sato, N.G. Copeland, D.J. Gilbert, N.A. Jenkins, S. Scully, D.L. Lacey, M. Katsuki, M. Asashima, and T. Yokota, *Murine homolog of SALL1 is essential for ureteric bud invasion in kidney development.* Development, 2001. **128**(16): p. 3105-15.

121. Nissenson, A.R., C. Ronco, G. Pergamit, M. Edelstein, and R. Watts, *Continuously functioning artificial nephron system: the promise of nanotechnology.* Hemodial Int, 2005. **9**(3): p. 210-7.

122. Nissenson, A.R., C. Ronco, G. Pergamit, M. Edelstein, and R. Watts, *The human nephron filter: toward a continuously functioning, implantable artificial nephron system.* Blood Purif, 2005. **23**(4): p. 269-74.

123. O'Brien, M.F., S. Goldstein, S. Walsh, K.S. Black, R. Elkins, and D. Clarke, *The SynerGraft valve: a new acellular (nonglutaraldehyde-fixed) tissue heart valve for autologous recellularization first experimental studies before clinical implantation.* Semin Thorac Cardiovasc Surg, 1999. **11**(4 Suppl 1): p. 194-200.

124. O'Halloran, D.M. and A.S. Pandit, *Tissue-engineering approach to regenerating the intervertebral disc.* Tissue Eng, 2007. **13**(8): p. 1927-54.

125. Oberpenning, F., J. Meng, J.J. Yoo, and A. Atala, *De novo reconstitution of a functional mammalian urinary bladder by tissue engineering.* Nat Biotechnol, 1999. **17**(2): p. 149-55.

126. Ohashi, K., T. Yokoyama, M. Yamato, H. Kuge, H. Kanehiro, M. Tsutsumi, T. Amanuma, H. Iwata, J. Yang, T. Okano, and Y. Nakajima, *Engineering functional two- and three-dimensional liver systems in vivo using hepatic tissue sheets.* Nat Med, 2007. **13**(7): p. 880-5.

127. Oliver, J.A., J. Barasch, J. Yang, D. Herzlinger, and Q. Al-Awqati, *Metanephric mesenchyme contains embryonic renal stem cells.* Am J Physiol Renal Physiol, 2002. **283**(4): p. F799-809.

128. Ott, H.C., T.S. Matthiesen, S.K. Goh, L.D. Black, S.M. Kren, T.I. Netoff, and D.A. Taylor, *Perfusion-decellularized matrix: using nature's platform to engineer a bioartificial heart.* Nat Med, 2008.

129. Park, Y., M.P. Lutolf, J.A. Hubbell, E.B. Hunziker, and M. Wong, *Bovine primary chondrocyte culture in synthetic matrix metalloproteinase-sensitive poly(ethylene glycol)-based hydrogels as a scaffold for cartilage repair.* Tissue Eng, 2004. **10**(3-4): p. 515-22.

130. Patel, P.N., A.S. Gobin, J.L. West, and C.W. Patrick, Jr., *Poly(ethylene glycol) hydrogel system supports preadipocyte viability, adhesion, and proliferation.* Tissue Eng, 2005. **11**(9-10): p. 1498-505.

131. Pavesio, A., G. Abatangelo, A. Borrione, D. Brocchetta, A.P. Hollander, E. Kon, F. Torasso, S. Zanasi, and M. Marcacci, *Hyaluronan-based scaffolds (Hyalograft C) in the treatment of knee cartilage defects: preliminary clinical findings.* Novartis Found Symp, 2003. **249**: p. 203-17; discussion 229-33, 234-8, 239-41.

132. Plisov, S.Y., K. Yoshino, L.F. Dove, K.G. Higinbotham, J.S. Rubin, and A.O. Perantoni, *TGF beta 2, LIF and FGF2 cooperate to induce nephrogenesis.* Development, 2001. **128**(7): p. 1045-57.

133. Pohl, M., H. Sakurai, K.T. Bush, and S.K. Nigam, *Matrix metalloproteinases and their inhibitors regulate in vitro ureteric bud branching morphogenesis.* Am J Physiol Renal Physiol, 2000. **279**(5): p. F891-900.

134. Pohl, M., H. Sakurai, R.O. Stuart, and S.K. Nigam, *Role of hyaluronan and CD44 in in vitro branching morphogenesis of ureteric bud cells.* Dev Biol, 2000. **224**(2): p. 312-25.

135. Qiao, J., K.T. Bush, D.L. Steer, R.O. Stuart, H. Sakurai, W. Wachsman, and S.K. Nigam, *Multiple fibroblast growth factors support growth of the ureteric bud but have different effects on branching morphogenesis.* Mech Dev, 2001. **109**(2): p. 123-35.

136. Qiao, J., H. Sakurai, and S.K. Nigam, *Branching morphogenesis independent of mesenchymal-epithelial contact in the developing kidney.* Proc Natl Acad Sci U S A, 1999. **96**(13): p. 7330-5.

137. Rai, S.K., F.M. Duh, V. Vigdorovich, A. Danilkovitch-Miagkova, M.I. Lerman, and A.D. Miller, *Candidate tumor suppressor HYAL2 is a glycosylphosphatidylinositol (GPI)-anchored cell-surface receptor for jaagsiekte sheep retrovirus, the envelope protein of which mediates oncogenic transformation.* Proc Natl Acad Sci U S A, 2001. **98**(8): p. 4443-8.

138. Richter, A.W., E.M. Ryde, and E.O. Zetterstrom, *Non-immunogenicity of a purified sodium hyaluronate preparation in man.* Int Arch Allergy Appl Immunol, 1979. **59**(1): p. 45-8.

139. Richter, W., *Non-immunogenicity of purified hyaluronic acid preparations tested by passive cutaneous anaphylaxis.* Int Arch Allergy Appl Immunol, 1974. **47**(2): p. 211-7.

140. Ringeisen, B.R., C.M. Othon, J.A. Barron, D. Young, and B.J. Spargo, *Jet-based methods to print living cells.* Biotechnol J, 2006. **1**(9): p. 930-48.

141. Rogers, S.A., H. Liapis, and M.R. Hammerman, *Normalization of glucose post-transplantation of pig pancreatic anlagen into non-immunosuppressed diabetic rats depends on obtaining anlagen prior to embryonic day 35.* Transpl Immunol, 2005. **14**(2): p. 67-75.

142. Rogers, S.A., J.A. Lowell, N.A. Hammerman, and M.R. Hammerman, *Transplantation of developing metanephroi into adult rats.* Kidney Int, 1998. **54**(1): p. 27-37.

143. Rosines, E., K. Johkura, and S.K. Nigam, *Creating renal progenitor tissues from cells and three-dimensional in vitro kidney culture: towards in vitro engineering of kidney tissues.* In preparation, 2007.

144. Rosines, E., R.V. Sampogna, K. Johkura, D.A. Vaughn, Y. Choi, H. Sakurai, M.M. Shah, and S.K. Nigam, *Staged in vitro reconstitution and implantation of engineered rat kidney tissue.* Proc Natl Acad Sci U S A, 2007. **104**(52): p. 20938-43.

145. Rosines, E., H.J. Schmidt, and S.K. Nigam, *The effect of hyaluronic acid size and concentration on branching morphogenesis and tubule differentiation in developing kidney culture systems: Potential applications to engineering of renal tissues.* Biomaterials, 2007. **28**(32): p. 4806-17.

146. Ross, E.A., M.J. Williams, T. Hamazaki, M. Jorgensen, W.L. Clapp, G.W. Ellison, N. Terada, and C.D. Batich. *Tissue engineering: differentiation of murine pluripotential embryonic stem cells seeded in whole organ decellularized rat kidney scaffolds*. in *American Society of Nephrology National Meeting*. 2006. San Diego, CA.

147. Rowley, J.A., G. Madlambayan, and D.J. Mooney, *Alginate hydrogels as synthetic extracellular matrix materials.* Biomaterials, 1999. **20**(1): p. 45-53.

148. Ruoslahti, E. and M.D. Pierschbacher, *Arg-Gly-Asp: a versatile cell recognition signal.* Cell, 1986. **44**(4): p. 517-8.

149. Sagrinati, C., G.S. Netti, B. Mazzinghi, E. Lazzeri, F. Liotta, F. Frosali, E. Ronconi, C. Meini, M. Gacci, R. Squecco, M. Carini, L. Gesualdo, F. Francini, E. Maggi, F. Annunziato, L. Lasagni, M. Serio, S. Romagnani, and P. Romagnani, *Isolation and characterization of multipotent progenitor cells from the Bowman's capsule of adult human kidneys.* J Am Soc Nephrol, 2006. **17**(9): p. 2443-56.

150. Sakurai, H., E.J. Barros, T. Tsukamoto, J. Barasch, and S.K. Nigam, *An in vitro tubulogenesis system using cell lines derived from the embryonic kidney shows dependence on multiple soluble growth factors.* Proc Natl Acad Sci U S A, 1997. **94**(12): p. 6279-84.

151. Sakurai, H., K.T. Bush, and S.K. Nigam, *Identification of pleiotrophin as a mesenchymal factor involved in ureteric bud branching morphogenesis.* Development, 2001. **128**(17): p. 3283-93.

152. Sakurai, H., K.T. Bush, and S.K. Nigam, *Heregulin induces glial cell line-derived neurotrophic growth factor-independent, non-branching growth and differentiation of ureteric bud epithelia.* J Biol Chem, 2005. **280**(51): p. 42181-7.

153. Sampogna, R.V. and S.K. Nigam, *Implications of gene networks for understanding resilience and vulnerability in the kidney branching program.* Physiology (Bethesda), 2004. **19**: p. 339-47.

154. Santos, O.F. and S.K. Nigam, *HGF-induced tubulogenesis and branching of epithelial cells is modulated by extracellular matrix and TGF-beta.* Dev Biol, 1993. **160**(2): p. 293-302.

155. Sariola, H., P. Ekblom, E. Lehtonen, and L. Saxen, *Differentiation and vascularization of the metanephric kidney grafted on the chorioallantoic membrane.* Dev Biol, 1983. **96**(2): p. 427-35.

156. Sariola, H., B. Peault, N. LeDouarin, C. Buck, F. Dieterlen-Lievre, and L. Saxen, *Extracellular matrix and capillary ingrowth in interspecies chimeric kidneys.* Cell Differ, 1984. **15**(1): p. 43-51.

157. Savani, R.C., G. Cao, P.M. Pooler, A. Zaman, Z. Zhou, and H.M. DeLisser, *Differential involvement of the hyaluronan (HA) receptors CD44 and receptor for HA-mediated motility in endothelial cell function and angiogenesis.* J Biol Chem, 2001. **276**(39): p. 36770-8.

158. Saxen, L. and E. Lehtonen, *Embryonic kidney in organ culture.* Differentiation, 1987. **36**(1): p. 2-11.

159. Saxen, L. and H. Sariola, *Early organogenesis of the kidney.* Pediatr Nephrol, 1987. **1**(3): p. 385-92.

160. Schittny, J.C., H. Kresse, and P.H. Burri, *Immunostaining of a heterodimeric dermatan sulphate proteoglycan is correlated with smooth muscles and some basement membranes.* Histochem Cell Biol, 1995. **103**(4): p. 271-9.

161. Schmits, R., J. Filmus, N. Gerwin, G. Senaldi, F. Kiefer, T. Kundig, A. Wakeham, A. Shahinian, C. Catzavelos, J. Rak, C. Furlonger, A. Zakarian, J.J. Simard, P.S. Ohashi, C.J. Paige, J.C. Gutierrez-Ramos, and T.W. Mak, *CD44 regulates hematopoietic progenitor distribution, granuloma formation, and tumorigenicity.* Blood, 1997. **90**(6): p. 2217-33.

162. Seliktar, D., A.H. Zisch, M.P. Lutolf, J.L. Wrana, and J.A. Hubbell, *MMP-2 sensitive, VEGF-bearing bioactive hydrogels for promotion of vascular healing.* J Biomed Mater Res A, 2004. **68**(4): p. 704-16.

163. Semino, C.E., J. Kasahara, Y. Hayashi, and S. Zhang, *Entrapment of migrating hippocampal neural cells in three-dimensional peptide nanofiber scaffold.* Tissue Eng, 2004. **10**(3-4): p. 643-55.

164. Sikri, K.L., C.L. Foster, N. MacHugh, and R.D. Marshall, *Localization of Tamm-Horsfall glycoprotein in the human kidney using immuno-fluorescence and immuno-electron microscopical techniques.* J Anat, 1981. **132**(Pt 4): p. 597-605.

165. Simmons, R.G. and L. Abress, *Quality-of-life issues for end-stage renal disease patients.* Am J Kidney Dis, 1990. **15**(3): p. 201-8.

166. Song, H.-K., W.-Y. Kim, H.-W. Lee, E.-Y. Park, and J. Kim. *Developmental Expression of Hyaluronan in Rat Kidney.* in *American Society of Nephrology National Meeting*. 2006. San Diego, CA.

167. Statter, M.B., K.J. Fahrner, E.M. Barksdale, Jr., D.E. Parks, R.A. Flavell, and P.K. Donahoe, *Correlation of fetal kidney and testis congenic graft survival with reduced major histocompatibility complex burden.* Transplantation, 1989. **47**(4): p. 651-60.

168. Steer, D.L., K.T. Bush, T.N. Meyer, C. Schwesinger, and S.K. Nigam, *A strategy for in vitro propagation of rat nephrons.* Kidney Int, 2002. **62**(6): p. 1958-65.

169. Steer, D.L. and S.K. Nigam, *Developmental approaches to kidney tissue engineering.* Am J Physiol Renal Physiol, 2004. **286**(1): p. F1-7.

170. Steer, D.L., M.M. Shah, K.T. Bush, R.O. Stuart, R.V. Sampogna, T.N. Meyer, C. Schwesinger, X. Bai, J.D. Esko, and S.K. Nigam, *Regulation of ureteric bud branching morphogenesis by sulfated proteoglycans in the developing kidney.* Dev Biol, 2004. **272**(2): p. 310-27.

171. Stuart, R.O., K.T. Bush, and S.K. Nigam, *Changes in global gene expression patterns during development and maturation of the rat kidney.* Proc Natl Acad Sci U S A, 2001. **98**(10): p. 5649-54.

172. Stuart, R.O., K.T. Bush, and S.K. Nigam, *Changes in gene expression patterns in the ureteric bud and metanephric mesenchyme in models of kidney development.* Kidney Int, 2003. **64**(6): p. 1997-2008.

173. Sweet, D.H., S.A. Eraly, D.A. Vaughn, K.T. Bush, and S.K. Nigam, *Organic anion and cation transporter expression and function during embryonic kidney development and in organ culture models.* Kidney Int, 2006. **69**(5): p. 837-45.

174. Tang, M.D., A.P. Golden, and J. Tien, *Molding of three-dimensional microstructures of gels.* J Am Chem Soc, 2003. **125**(43): p. 12988-9.

175. Thibodeau, G.A. and K.T. Patton, *Structure & function of the body*. 12th ed. 2004, St. Louis: Mosby. xxii, 528, [56].

176. Thomas, L., H.R. Byers, J. Vink, and I. Stamenkovic, *CD44H regulates tumor cell migration on hyaluronate-coated substrate.* J Cell Biol, 1992. **118**(4): p. 971-7.

177. Tiranathanagul, K., V. Dhawan, I.F. Lytle, W. Zhang, G.H. Borschel, D.A. Buffington, E. Tziampazis, D.L. Brown, and H.D. Humes, *Tissue engineering of an implantable bioartificial hemofilter.* Asaio J, 2007. **53**(2): p. 176-86.

178. Tolg, C., R. Poon, R. Fodde, E.A. Turley, and B.A. Alman, *Genetic deletion of receptor for hyaluronan-mediated motility (Rhamm) attenuates the formation of aggressive fibromatosis (desmoid tumor).* Oncogene, 2003. **22**(44): p. 6873-82.

179. Tomihata, K. and Y. Ikada, *Crosslinking of hyaluronic acid with water-soluble carbodiimide.* J Biomed Mater Res, 1997. **37**(2): p. 243-51.

180. Toyokawa, K., H. Harayama, and M. Miyake, *Exogenous hyaluronic acid enhances porcine parthenogenetic embryo development in vitro possibly mediated by CD44.* Theriogenology, 2005. **64**(2): p. 378-92.

181. Trochon, V., C. Mabilat, P. Bertrand, Y. Legrand, F. Smadja-Joffe, C. Soria, B. Delpech, and H. Lu, *Evidence of involvement of CD44 in endothelial cell proliferation, migration and angiogenesis in vitro.* Int J Cancer, 1996. **66**(5): p. 664-8.

182. Turley, E.A., C.A. Erickson, and R.P. Tucker, *The retention and ultrastructural appearances of various extracellular matrix molecules incorporated into three-dimensional hydrated collagen lattices.* Dev Biol, 1985. **109**(2): p. 347-69.

183. Unger, M.A., H.P. Chou, T. Thorsen, A. Scherer, and S.R. Quake, *Monolithic microfabricated valves and pumps by multilayer soft lithography.* Science, 2000. **288**(5463): p. 113-6.

184. Valderrabano, F., R. Jofre, and J.M. Lopez-Gomez, *Quality of life in end-stage renal disease patients.* Am J Kidney Dis, 2001. **38**(3): p. 443-64.

185. Velasco, A.L. and O.D. Hegre, *Decreased immunogenicity of fetal kidneys: the role of passenger leukocytes.* J Pediatr Surg, 1989. **24**(1): p. 59-63; discussion 63.

186. Vercruysse, K.P., D.M. Marecak, J.F. Marecek, and G.D. Prestwich, *Synthesis and in vitro degradation of new polyvalent hydrazide cross-linked hydrogels of hyaluronic acid.* Bioconjug Chem, 1997. **8**(5): p. 686-94.

187. Wang, P.C. and T. Takezawa, *Reconstruction of renal glomerular tissue using collagen vitrigel scaffold.* J Biosci Bioeng, 2005. **99**(6): p. 529-40.

188. Wei, C., M. Larsen, M.P. Hoffman, and K.M. Yamada, *Self-organization and branching morphogenesis of primary salivary epithelial cells.* Tissue Eng, 2007. **13**(4): p. 721-35.

189. Wintour, E.M., L. Earnest, D. Alcorn, A. Butkus, L. Shandley, and K. Jeyaseelan, *Ovine AQP1: cDNA cloning, ontogeny, and control of renal gene expression.* Pediatr Nephrol, 1998. **12**(7): p. 545-53.

190. Xu, T., C.A. Gregory, P. Molnar, X. Cui, S. Jalota, S.B. Bhaduri, and T. Boland, *Viability and electrophysiology of neural cell structures generated by the inkjet printing method.* Biomaterials, 2006. **27**(19): p. 3580-8.

191. Yamaguchi, Y., *Lecticans: organizers of the brain extracellular matrix.* Cell Mol Life Sci, 2000. **57**(2): p. 276-89.

192. Yamamoto, M., L. Cui, K. Johkura, K. Asanuma, Y. Okouchi, N. Ogiwara, and K. Sasaki, *Branching ducts similar to mesonephric ducts or ureteric buds in teratomas originating from mouse embryonic stem cells.* Am J Physiol Renal Physiol, 2006. **290**(1): p. F52-60.

193. Yang, J., M. Yamato, C. Kohno, A. Nishimoto, H. Sekine, F. Fukai, and T. Okano, *Cell sheet engineering: recreating tissues without biodegradable scaffolds.* Biomaterials, 2005. **26**(33): p. 6415-22.

194. Yang, S., K.F. Leong, Z. Du, and C.K. Chua, *The design of scaffolds for use in tissue engineering. Part I. Traditional factors.* Tissue Eng, 2001. **7**(6): p. 679-89.

195. Yeh, J., Y. Ling, J.M. Karp, J. Gantz, A. Chandawarkar, G. Eng, J. Blumling, 3rd, R. Langer, and A. Khademhosseini, *Micromolding of shape-controlled, harvestable cell-laden hydrogels.* Biomaterials, 2006. **27**(31): p. 5391-8.

196. Zand, M.S., *Immunosuppression and immune monitoring after renal transplantation.* Semin Dial, 2005. **18**(6): p. 511-9.

197. Zent, R., K.T. Bush, M.L. Pohl, V. Quaranta, N. Koshikawa, Z. Wang, J.A. Kreidberg, H. Sakurai, R.O. Stuart, and S.K. Nigam, *Involvement of laminin binding integrins and laminin-5 in branching morphogenesis of the ureteric bud during kidney development.* Dev Biol, 2001. **238**(2): p. 289-302.

198. Zhai, X.Y., J.S. Thomsen, H. Birn, I.B. Kristoffersen, A. Andreasen, and E.I. Christensen, *Three-dimensional reconstruction of the mouse nephron.* J Am Soc Nephrol, 2006. **17**(1): p. 77-88.

199. Zisch, A.H., U. Schenk, J.C. Schense, S.E. Sakiyama-Elbert, and J.A. Hubbell, *Covalently conjugated VEGF--fibrin matrices for endothelialization.* J Control Release, 2001. **72**(1-3): p. 101-13.

Appendix

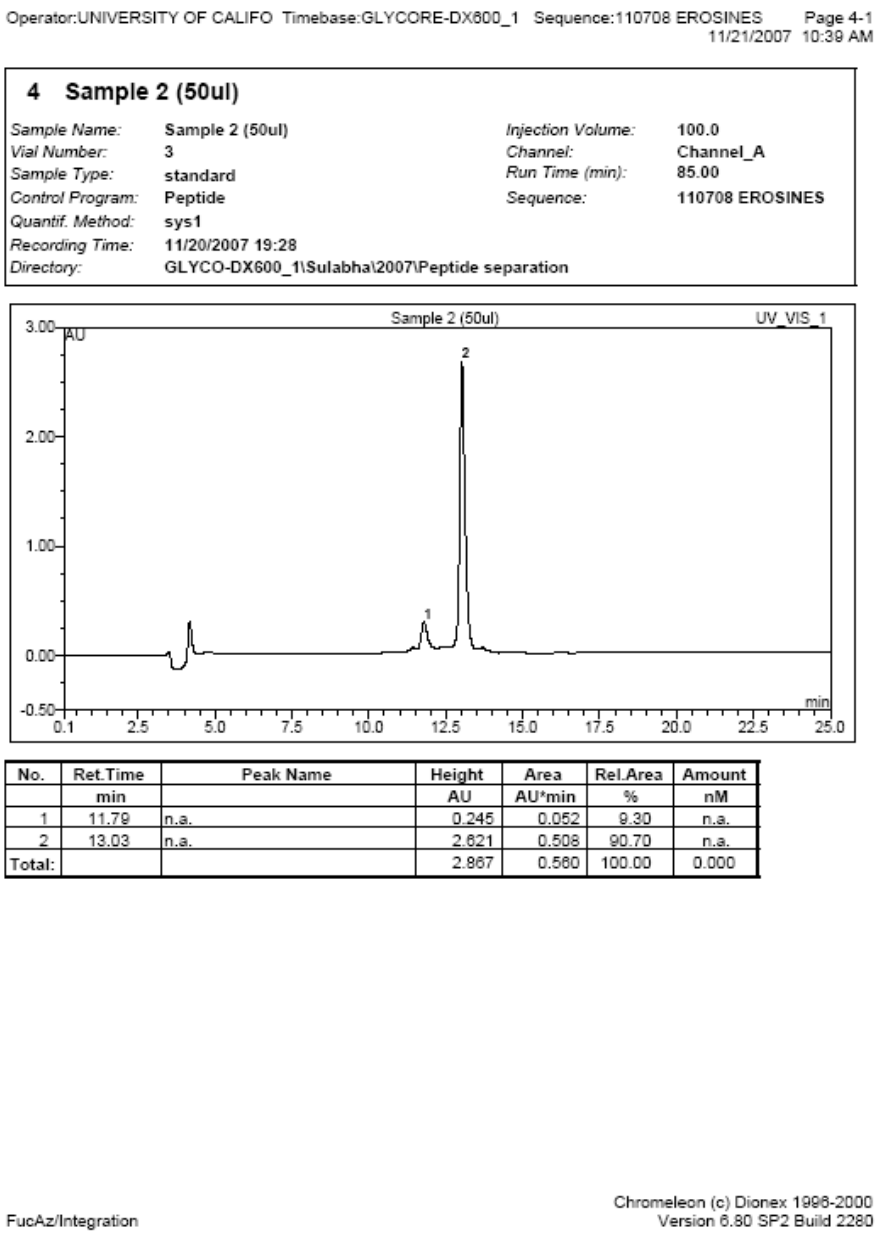

Figure A.1: HPLC chromatogram from first run functionalized peptide synthesis.

2 ER peptide 2 (50ul)

Sample Name:	ER peptide 2 (50ul)	*Injection Volume:*	100.0
Vial Number:	2	*Channel:*	Channel_A
Sample Type:	unknown	*Run Time (min):*	85.00
Control Program:	Peptide	*Sequence:*	110710 EROSINES
Quantif. Method:	sys1		
Recording Time:	11/26/2007 16:16		
Directory:	GLYCO-DX600_1\Sulabha\2007\Peptide separation		

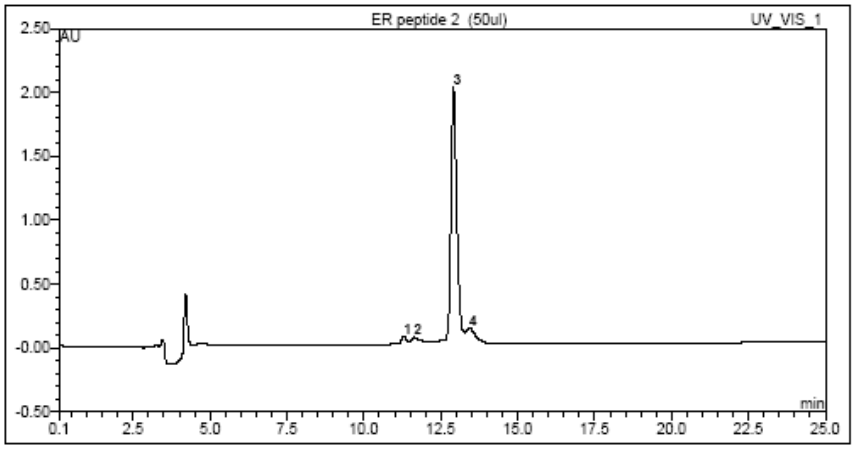

No.	Ret.Time	Peak Name	Height	Area	Rel.Area	Amount
	min		AU	AU*min	%	nM
1	11.30	n.a.	0.048	0.008	1.80	n.a.
2	11.64	n.a.	0.031	0.006	1.51	n.a.
3	12.91	n.a.	1.942	0.400	93.81	n.a.
4	13.43	n.a.	0.053	0.012	2.88	n.a.
Total:			2.074	0.426	100.00	0.000

Chromeleon (c) Dionex 1998-2000
Version 6.80 SP2 Build 2280

Figure A.2: HPLC chromatogram from second run functionalized peptide synthesis.